

AccuTOFLC series

DART (Direct Analysis in Real Time)
Applications Notebook

Edition April 2016

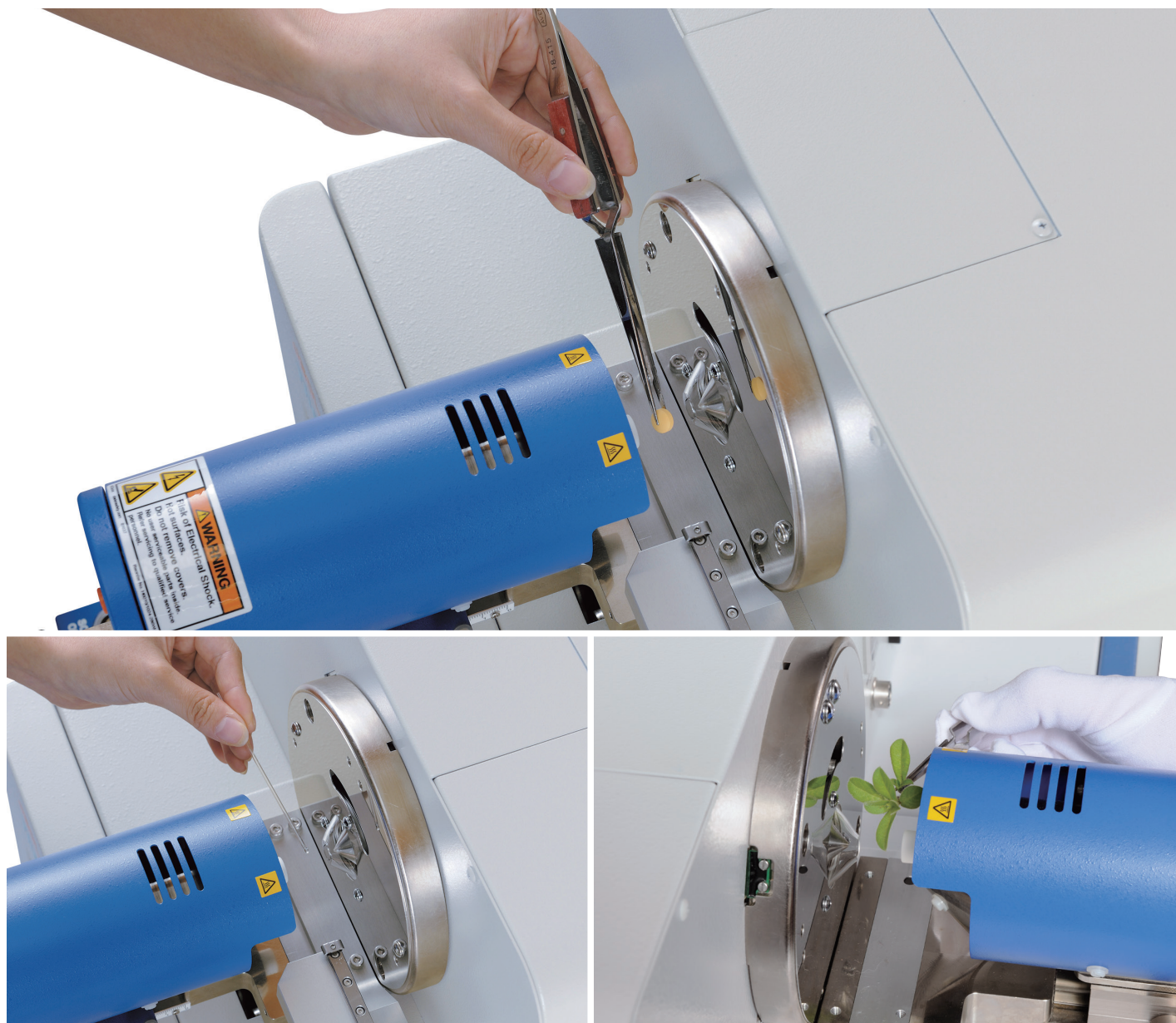


Table of Contents

Introduction and fundamentals.....	1
Direct Analysis in Real Time (DART) Mass Spectrometry	1
The AccuTOF Atmospheric Pressure Interface	7
Drug Analysis.....	13
Instantaneous Screening for Counterfeit Drugs with No Sample Preparation	13
Direct Analysis of Drugs in Pills and Capsules with No Sample Preparation.....	14
See also: Instantaneous Detection of Illicit Drugs on Currency	41
See also: Instantaneous Detection of the “Date-Rape” Drug – GHB.....	42
Food, Flavors, and Fragrances	15
Rapid Detection of Melamine in Dry Milk Using AccuTOF-DART	15
Detection of Lycopene in Tomato Skin	16
Instantaneous Detection of Opiates in Single Poppy Seeds	17
Distribution of Capsaicin in Chili Peppers	18
Detection of Unstable Compound Released by Chopped Chives	19
Rapid Detection of Fungicide in Orange Peel.....	20
Detection of Oleocanthal in Freshly Pressed Extra-Virgin Olive Oil	21
“No-prep” Analysis of Lipids in Cooking Oils and Detection of Adulterated Olive Oil.....	23
Flavones and Flavor Components in Two Basil Leaf Chemotypes	27
Direct analysis of caffeine in soft drinks and coffee and tea infusions.....	29
Rapid screening of stobilurins in crude solid materials (wheat grains) using DART-TOFMS.....	31
Analysis of stobilurins in wheat grains using DART-TOFMS	33
Analysis of deoxynivalenol in beer.....	35
Using Solid Phase Microextraction with AccuTOF-DART for Fragrance Analysis.....	37
Forensics.....	39
Chemical Analysis of Fingerprints	39
Instantaneous Detection of Illicit Drugs on Currency	41
Instantaneous Detection of the “Date-Rape” Drug – GHB	42
“Laundry Detective”: Identification of a Stain	43
Analysis of Biological Fluids	45
Clandestine Methamphetamine Labs: Rapid Impurity Profiling by AccuTOF-DART.....	49
X-Ray Fluorescence Helps Identify Peaks in DART Mass Spectrum of Electrical Tape - ElementEye JSX-1000S and AccuTOF-DART	51

Homeland Security	54
Detection of the Peroxide Explosives TATP and HMTD	54
Instantaneous Detection of Explosives on Clothing	55
Detection of Explosives in Muddy Water	56
Rapid Detection and Exact Mass Measurements of Trace Components in an Herbicide	57
Industrial Materials	58
Rapid Analysis of p-Phenylenediamine Antioxidants in Rubber	58
Direct Analysis of Adhesives	59
Identification of Polymers	63
Rapid Analysis of Glues, Cements, and Resins.....	65
Analysis of Organic Contaminant on Metal Surface.....	67
Analysis of low polar compound by DART ~ analysis of organic electroluminescence materials ~	68
Organic Chemistry.....	69
Chemical Reaction Monitoring with the AccuTOF-DART Mass Spectrometer	69
Direct Analysis of Organometallic Compounds.....	71
Analysis of highly polar compound by DART ~ analysis of ionic liquid ~.....	74
Miscellaneous	75
Elemental Compositions from Exact Mass Measurements and Accurate Isotopic Abundances...	75
Identifying “Buried” Information in LC/MS Data.....	77
DART Contamination Resistance: Analysis of Compounds in Saturated Salt and Buffer Solutions	78
AccuTOF LC series with DART bibliography (August 2015)	79

Direct Analysis in Real Time (DART™) Mass Spectrometry

Robert B. Cody[†], James A. Laramée^{††},
J. Michael Nilles^{†††}, and H. Dupont Durst^{††††}

[†]JEOL USA, Inc.

^{††}EAI Corporation

^{†††}Geo-Centers Inc.

^{††††}Edgewood Chemical Biological Center

Introduction

Mass Spectrometry (MS) is one of the fastest-growing areas in analytical instrumentation. The use of mass spectrometry in support of synthetic, organic, and pharmaceutical chemistry is well established. Mass spectrometry is also used in materials science, environmental research, and forensic chemistry. It has also evolved into one of the core methods used in biotechnology. However, currently available ion sources place extreme restrictions on the speed and convenience of sample analysis by mass spectrometry. Here we report a method for using mass spectrometry to instantaneously analyze gases, liquids, and solids in open air at ground potential under ambient conditions.

Traditional ion sources used in mass spectrometry require the introduction of samples into a high vacuum system. Traditional ion sources operated in vacuum include electron ionization (EI)[1], chemical ionization (CI)[2], fast atom bombardment (FAB)[3], and field desorption/field ionization (FD/FI)[4]. These techniques have been used successfully for decades. However, the requirement that samples be introduced into a high vacuum for analysis is a severe limitation. Gas or liquid samples must be introduced through a gas chromatograph or a specially designed inlet system. Solid samples must be introduced by using a direct insertion probe and a vacuum lock system. Direct insertion probes can result in vacuum failure and/or contamination of the

ion source if too much sample is introduced.

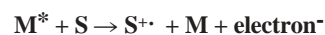
Atmospheric pressure ion sources such as atmospheric pressure chemical ionization (APCI)[5], electrospray ionization (ESI)[6-8], matrix-assisted laser desorption ionization (MALDI)[9-10] and atmospheric pressure photoionization (APPI)[11] have broadened the range of compounds that can be analyzed by mass spectrometry. However, these ion sources require that samples be exposed to elevated temperatures and electrical potentials, ultraviolet irradiation, laser radiation, or a high-velocity gas stream. Safety considerations require that the ion source be fully enclosed to protect the operator from harm.

The new ion source reported herein overcomes these limitations. The new technique, referred to as Direct Analysis in Real Time (DART™), has been coupled to the AccuTOF-LC™ atmospheric pressure ionization mass spectrometer to permit high-resolution, exact mass measurements of gases, liquids, and solids[12,13]. DART successfully sampled hundreds of chemicals, including chemical agents and their signatures, pharmaceuticals, metabolites, pesticides and environmentally significant compounds, peptides and oligosaccharides, synthetic organics, organometallics, drugs of abuse, explosives, and toxic industrial chemicals. These chemicals were detected on a variety of surfaces such as concrete, human skin, currency, airline boarding passes, fruits and vegetables, body fluids, cocktail glasses, and clothing. The composition of drug capsules and tablets was directly analyzed.

sources used in hand-held detectors for chemical weapons agents (CWAs), drugs, and explosives. The discovery that DART could be used for positive-ion and negative-ion non-contact detection of materials on surfaces, as well as for detection of gases and liquids, led to the development of a commercial product.

DART is based on the atmospheric pressure interactions of long-lived electronic excited-state atoms or vibronic excited-state molecules with the sample and atmospheric gases. The DART ion source is shown in **Figure 1**. A gas (typically helium or nitrogen) flows through a chamber where an electrical discharge produces ions, electrons, and excited-state (metastable) atoms and molecules. Most of the charged particles are removed as the gas passes through perforated lenses or grids and only the neutral gas molecules, including metastable species, remain. A perforated lens or grid at the exit of the DART provides several functions: it prevents ion-ion and ion-electron recombination, it acts as a source of electrons by surface Penning ionization, and it acts as an electrode to promote ion drift toward the orifice of the mass spectrometer's atmospheric pressure interface.

Several ionization mechanisms are possible, depending on the polarity and reaction gas, the proton affinity and ionization potential of the analyte, and the presence of additives or dopants. The simplest process is Penning ionization [14] involving transfer of energy from the excited gas M^* to an analyte S having an ionization potential lower than the energy of M^* . This produces a radical molecular cation $S^{+\cdot}$ and an electron (e^-).



Penning ionization is a dominant reaction mechanism when nitrogen or neon is used in the DART source. Nitrogen or neon ions are effectively removed by the electrostatic lenses and are never observed in the DART back-

Background and Principle of Operation

DART grew out of discussions at JEOL USA, Inc. between two of the authors (Laramée and Cody) about the possibility of developing an atmospheric pressure thermal electron source to replace the radioactive

[†]11 Dearborn Road, Peabody, Massachusetts, USA.

^{††}1308 Continental Drive, Suite J, Abingdon, MD 21009

^{†††}Box 68 Gunpowder Branch, APG, MD 21010

^{††††}Aberdeen Proving Grounds, Maryland USA

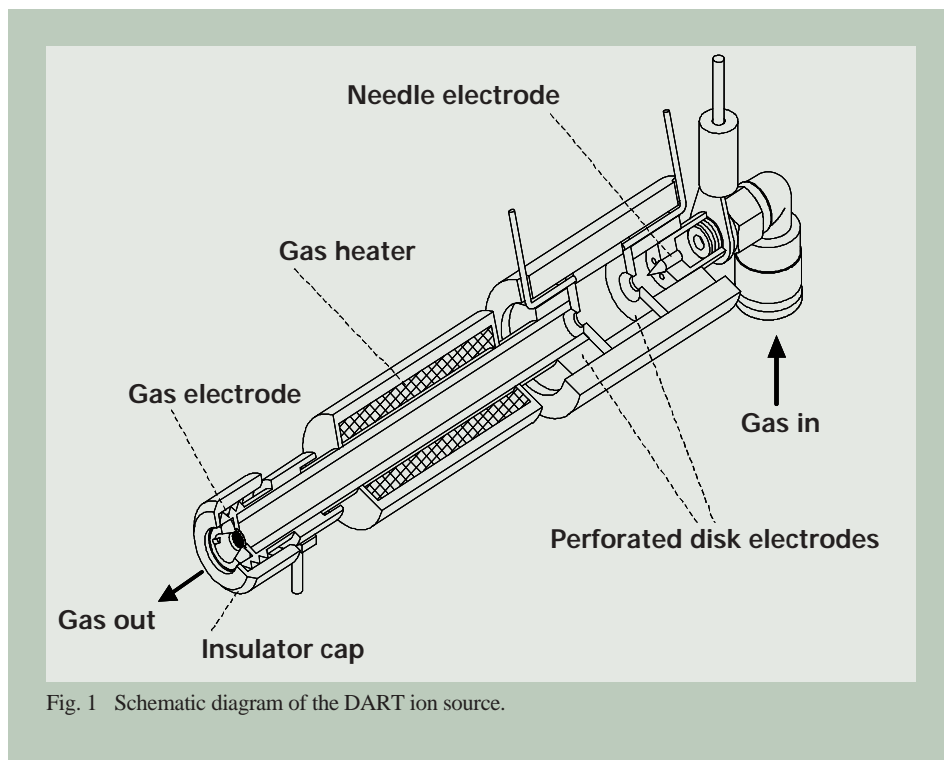
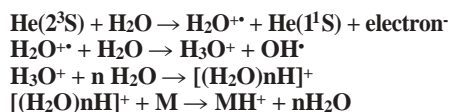


Fig. 1 Schematic diagram of the DART ion source.

ground mass spectrum.

When helium is used, the dominant positive-ion formation mechanism involves the formation of ionized water clusters followed by proton transfer reactions:



The helium 2^3S state has an energy of 19.8 eV. Its reaction with water is extremely efficient [15] with the reaction cross section estimated at 100 \AA^2 . Because of this extraordinarily high cross section, DART performance is not affected by humidity.

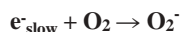
Negative-ion formation occurs by a different mechanism. Electrons (e^-) are produced by Penning ionization or by surface Penning ionization:



These electrons are rapidly thermalized by collisions with atmospheric pressure gas



Thermal electrons undergo electron capture by atmospheric oxygen



to produce O_2^- , which reacts with the analyte to produce anions. The DART negative-ion reagent mass spectra are virtually identical for nitrogen, neon, and helium. However, negative-ion sensitivity increases for DART gases in the following order:



This is due to the increased efficiency in forming electrons by Penning ionization and

surface Penning ionization as the internal energy of the metastable species increases.

The polarity of the DART ion source is switched between positive-ion mode and negative-ion mode by changing the polarity of the disk electrode and grid. The polarity of the discharge needle is not changed, so the plasma is not interrupted. This permits rapid switching between positive and negative modes.

Other reactions are possible. The presence of traces of dopants such as ammonium (e.g. from ammonium hydroxide headspace vapor) or chloride (e.g. from methylene chloride vapor) can modify the chemistry allowing the chemist to tailor the experiment for specific analyses.

DART produces relatively simple mass spectra characterized by M^+ ; and/or $[\text{M}+\text{H}]^+$ in positive-ion mode, and M^- or $[\text{M}-\text{H}]^-$ in negative-ion mode. Fragment ions are observed for some compounds. The degree of fragmentation can be influenced by the choice of gas, the temperature, and the AccuTOF orifice 1 potential. Alkali metal cation attachment and double-charge ions are not observed.

The mechanism involved in desorption of materials from surfaces by DART is less well characterized. Thermal desorption plays a role if the gas stream is heated. However, the analysis by DART of inorganic materials such as sodium perchlorate or organic salts having little or no vapor pressure is evidence of other processes. It is postulated that the transfer energy to the surface by metastable atoms and molecules facilitates desorption and ionization.

In contrast with other ion sources that use metastable species [16-23], the DART ion source does not operate under reduced pressure, apply a high electrical potential to the analyte, or expose the analyte directly to the discharge plasma. Argon, used in many of these ion sources, is not well suited for use with DART because argon metastables are rapidly quenched in the presence of water vapor [20] by a reaction involving homolytic

cleavage of the water bond without concomitant ion formation. None of these ion sources are designed for direct analysis of gases, liquids, and solids in open air under ambient conditions.

Experimental

A DARTtm source [24] was installed on a JEOL AccuTOF LCtm time-of-flight mass spectrometer. The DART source replaces the standard electrospray ionization (ESI) source supplied with the AccuTOF. No vacuum vent is required. The ion sources can be exchanged and made operational within minutes.

The mass spectrometer operates at a constant resolving power of approximately 6000 (FWHM definition). Typical atmospheric pressure interface conditions are: orifice 1 = 30V, and both orifice 2 and ring lens are set to 5V. The AccuTOF ion guide voltage is varied as needed depending on the lowest m/z to be measured. Orifice 1 temperature is typically kept warm (80 degrees C) to prevent contamination. Although there is some electrical potential on the exposed orifice 1, the voltage and current are so low that there is absolutely no danger to the operator, even with prolonged direct contact.

The DART source is operated with typical gas flows between 1.5 and 3 liters per minute. Gas temperature is programmable from ambient temperature up to approximately 350 degrees C (gas heater temperature from OFF to a maximum of 550 degrees C). Typical potentials are: discharge needle 2 kV to 4 kV, electrode 1: 100V, grid: 250 V. Gas, liquid, or solid samples positioned in the gap between the DART source and mass spectrometer orifice 1 are ionized.

Because the mass spectrometer orifice is continually bathed in hot inert gas, the DART source is remarkably resistant to contamination and sample carryover. Mass scale calibration is easily accomplished by placing neat poly-

ethylene glycol average molecular weight 600 (PEG 600) on a glass rod or a piece of absorbent paper in front of the DART source. In positive-ion mode, this produces a series of $[M+H]^+$ and $[M+H-H_2O]^+$ peaks from m/z 45 up to beyond m/z 1000. By including background peaks, the calibrated mass range can be extended down to m/z 18 or 19. Negative-ion spectra of PEG are characterized by $[M+O_2-H]^-$ and $[(C_2H_4O)_n+O_2-H]^-$ ion series.

The reference spectrum can be acquired within seconds. There is no memory effect or carryover of the reference compound -- the PEG peaks do not persist after the reference standard is removed. For these reasons, a full reference mass spectrum can be quickly and easily included in each data file, and accurate mass measurements are routinely acquired for all samples.

Applications

The DART ion source has been used to analyze an extremely wide range of analytes, including drugs (prescription, over-the-counter, veterinary, illicit, and counterfeit) in dose form or in body fluids or tissues, explosives and arson accelerants, chemical weapons agents and their signatures, synthetic organic or organometallics compounds, environmentally important compounds, inks and dyes, foods, spices and beverages. An important benefit of DART is that materials can be analyzed directly on surfaces such as glass, TLC plates, concrete, paper, or currency without requiring wipes or solvent extraction.

Drugs can be detected in pill form by placing the pill in front of the DART source for a few minutes. An example is shown below (Figure 2) for the rapid detection of illicit drugs in pills confiscated by a law-enforcement agency. The intact pills were simply placed in front of the DART source and analyte ions were observed within seconds. Exact mass and isotopic measurements confirmed the elemental compositions of the labeled components. All labeled assignments in the following examples were confirmed by exact mass measurements.

Drug counterfeiting is becoming a serious and widespread public health problem. Counterfeit drugs are not only illegal, but dangerous; they may contain little or no actual drug content, or they may contain completely different drugs with potentially toxic consequences.

DART can be used to rapidly screen for counterfeit drugs. An example is shown below in Figure 3 where DART was used to analyze a sample of a real drug containing the anti-malarial dihydroartemisinin, and a counterfeit drug containing no active ingredients.

DART has been applied to the direct detection of drugs and metabolites in raw, unprocessed body fluids, including blood, urine, perspiration, and saliva. An example is shown below in Figure 4 for the negative-ion analysis of the urine of a subject taking prescription ranitidine. No extraction or other processing was used: a glass rod was dipped in raw urine and placed in front of the DART source.

For easy viewing, only abundant components are labeled in this figure. A more complete list of assignments is given in Table 1. Assignments are made for compounds com-

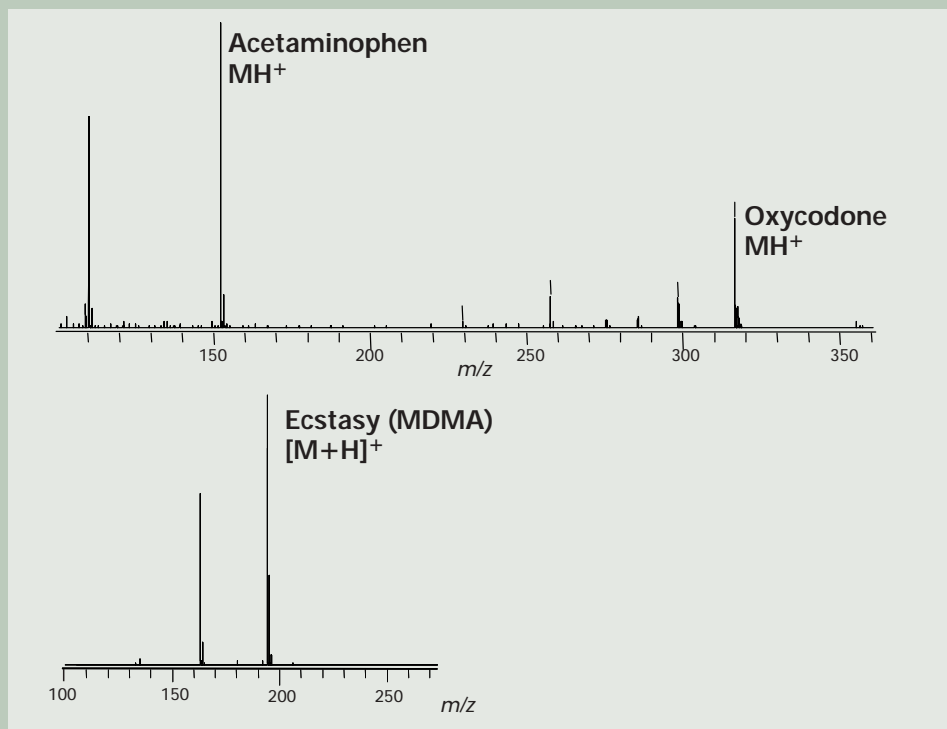


Fig. 2 DART mass spectra of two pills: An analgesic containing acetaminophen plus oxycodone (top) and methylenedioxyamphetamine ("ecstasy", bottom).

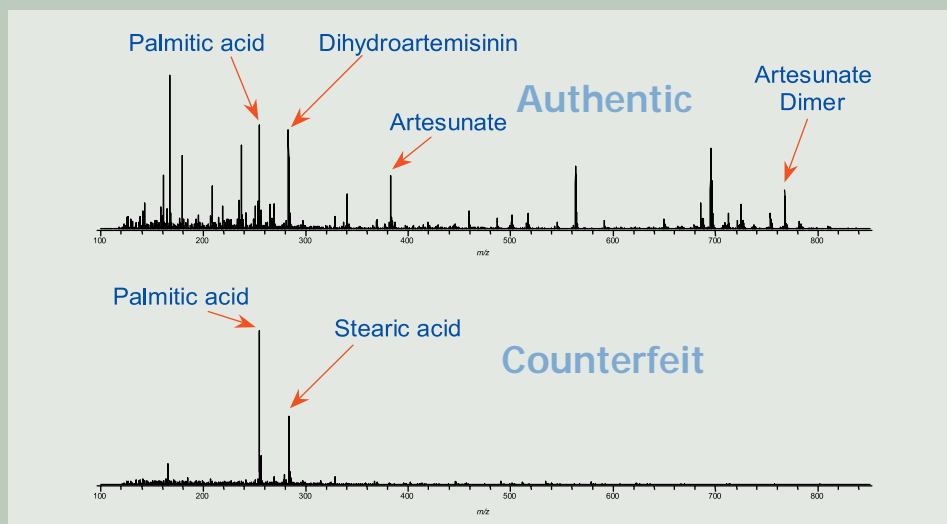


Fig. 3 Rapid detection of counterfeit drug. The top mass spectrum shows the authentic drug and the bottom mass spectrum shows the counterfeit drug.

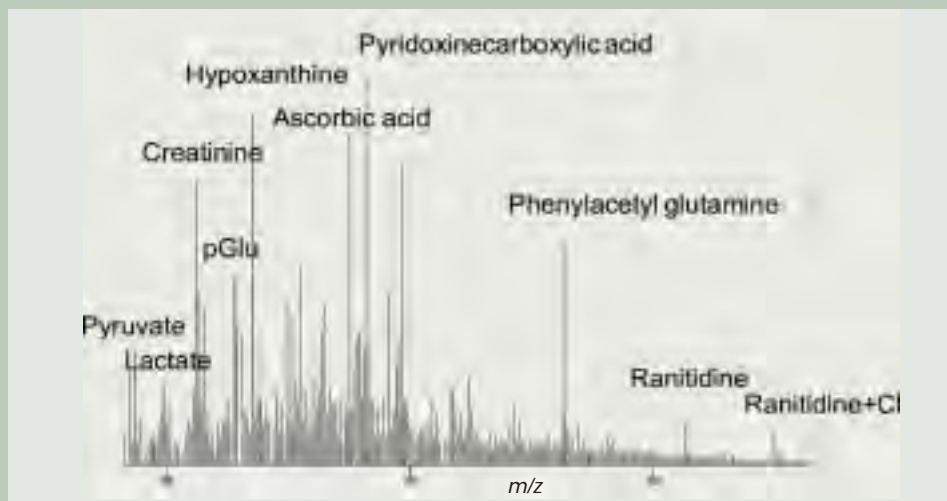


Fig. 4 Negative-ion DART analysis of the urine of a subject taking prescription ranitidine.

Table 1 Assignments for Compounds Detected in Negative-Ion DART Mass Spectrum of Raw Urine.

Name	Meas.	Calc.	Diff(u)	Abund.
GBL	85.0295	85.0290	0.0006	11.0317
Pyruvic_acid	87.0084	87.0082	0.0002	7.1700
Lactic_acid	89.0236	89.0239	-0.0002	8.3658
Cresol	107.0492	107.0497	-0.0004	.9294
Uracil	111.0153	111.0195	-0.0041	14.3328
Creatinine	112.0513	112.0511	0.0002	81.6851
Purine	119.0354	119.0358	-0.0004	31.9510
Niacin	122.0277	122.0242	0.0035	3.1489
Dihydro_methyluracil	127.0486	127.0508	-0.0021	23.3773
pGlu	128.0353	128.0348	0.0006	59.2337
Methylmaleic_acid	129.0212	129.0188	0.0024	37.1191
Me_succinate/diMe_malonate	131.0368	131.0358	0.0010	19.3593
Deoxyribose	133.0489	133.0501	-0.0012	28.3521
Hypoxanthine	135.0306	135.0307	-0.0001	100.0000
Adipic_acid	145.0469	145.0501	-0.0032	11.7389
Methyl_hypoxanthine	149.0454	149.0463	-0.0009	37.5243
Hydroxymethyl_methyl_uracil	155.0453	155.0457	-0.0003	55.5832
a-aminoadipic_acid	160.0568	160.0610	-0.0042	9.5885
Methionine_sulfoxide	164.0419	164.0381	0.0037	11.7609
Methylxanthine	165.0408	165.0412	-0.0004	32.4341
Formiminoglutamic_acid	173.0536	173.0562	-0.0027	12.3531
Ascorbic_acid	175.0285	175.0243	0.0042	23.1998
Hippuric_acid	178.0513	178.0504	0.0009	66.4487
Glucose	179.0552	179.0556	-0.0004	39.7499
Dimethylxanthine	179.0552	179.0569	-0.0017	39.7499
Pyridoxinecarboxylic_acid	182.0479	182.0453	0.0026	34.7913
Hydroxyindoleacetic_acid	190.0542	190.0504	0.0037	5.4133
Dimethyluric_acid	195.0527	195.0518	0.0009	23.7577
AAMU (caffeine metabolite)	197.0667	197.0675	-0.0007	79.6617
Cinnamalidinemalonic_acid	217.0483	217.0501	-0.0017	60.5399
AFMU (caffeine metabolite)	225.0643	225.0624	0.0019	21.9092
Cytidine	242.0801	242.0777	0.0024	3.4545
Uridine	243.0641	243.0617	0.0024	21.1156
Phenylacetyl_glutamine	263.1033	263.1032	0.0001	48.9665
Adenosine	266.0861	266.0889	-0.0028	1.4869
Ranitidine	313.1321	313.1334	-0.0013	8.7459
Ranitidine+Cl	349.1113	349.1101	0.0011	11.7296

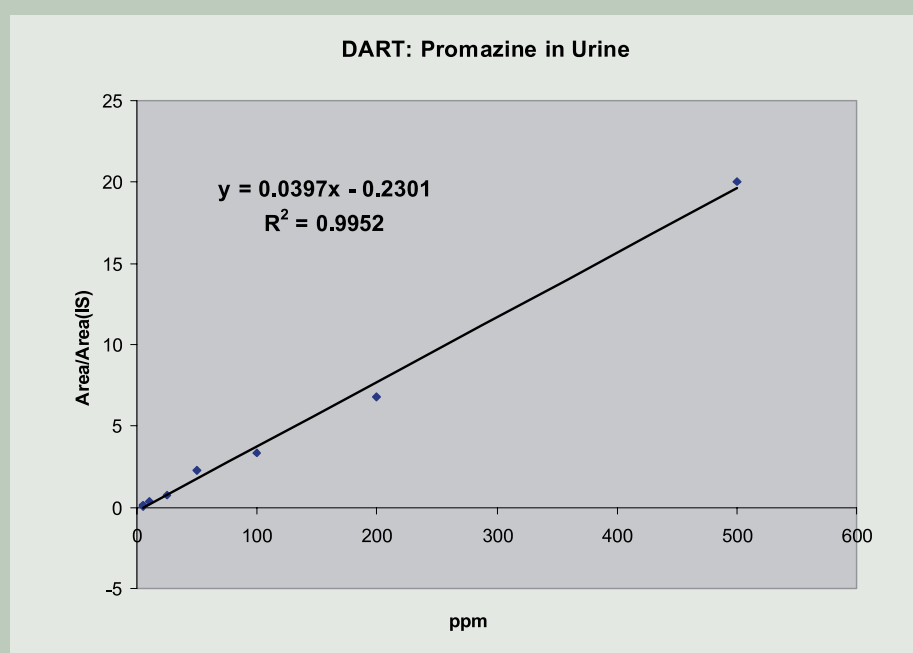


Fig. 5 Rapid quantitative analysis by DART of promazine in urine. Chlorpromazine was added as an internal standard.

monly encountered in urine that have elemental compositions that match the measured m/z values. It is interesting to note that the basic drug, ranitidine, is observed as an $[M-H]^-$ species in the negative-ion mass spectrum as well as an abundant $[M+H]^+$ species in the positive-ion mass spectrum. Ranitidine metabolites are also observed [11] in the positive-ion mass spectrum (not shown).

DART can be used for quantitative analysis. The absolute abundance of ions produced by DART depends on the positioning of the target in the gas stream. However, the use of an internal standard permits rapid quantitative analysis of drugs in urine, plasma, or other body fluids. Figure 5 shows a working curve obtained for urine samples spiked with promazine at the 1 to 500 ppm level. Chlorpromazine (50 ppm) was added as an internal standard. Undiluted urine samples were applied to a glass rod. Each analysis was complete within seconds of placing the rod in front of the DART source. This approach has also been used to screen for the “date rape” drug gamma hydroxy butyrate (GHB) in urine [24] and for the rapid quantitative analysis of developmental drugs in plasma.

The detection of explosives is important for forensics and security. DART has been applied to the detection of nitro explosives such as nitroglycerine, TNT, and HMX, inorganic explosives such as ammonium nitrate, perchlorate and azide, and peroxide explosives such as TATP and HMTD. Examples are shown in Figures 6 and 7.

The high dynamic range of the DART-AccuTOF combination can permit the identification of trace-level impurities for quality control and similar applications. An example is shown in Figure 8 and Table 2 for the exact-mass analysis of 1% propazine and 0.2% simazine in a sample of the herbicide atrazine.

Conclusion

A new ion source has been developed that permits the analysis of gases, liquids, and solids in open air under ambient conditions. No solvents or high-pressure gases are used. The sample is not directly exposed to high voltages, laser beams or radiation or plasma. The combination of this source with a high-resolution time-of-flight mass spectrometer permits rapid qualitative and quantitative analysis of a wide variety of materials.

Acknowledgment

Technical assistance and keen scientific insight were unselfishly provided by (in alphabetical order) Daniel Banquer, Ted Boileau, William Creasy, Daniel Evans, Drew McCrady, Michael McKie, Michael Nilles, Edward Owen, Gary Samuelson, Philip Smith, John Stuff, and Dean Tipple. The authors would like to thank Prof. Facundo Fernandez of Georgia Tech University for the dihydroartemisinin and counterfeit drug sample.

Additional Information

Additional applications and digital videos showing DART analysis are available on the internet at <http://www.jeolusa.com/ms/msprod->

References

- [1] Dempster, A. J. *Phys. Rev.*, **11**, 316-324, (1918).
- [2] Munson, M. S. B.; Franklin, F. H. *J. Am. Chem. Soc.*, **88**, 2621, (1966).
- [3] Barber, M.; Bordoli, R. S.; Elliott, G. J.; Sedgwick, R. D.; Tyler, A. N. *J. Chem. Soc. Chem. Commun.*, **325**, (1981).
- [4] Beckey H. D. *Research/Development*, **20**(11), 26-29, (1969).
- [5] Horning, E. C.; Horning, M. E.; Carroll, D. I.; Dzidic, I.; Stilwell, R. N.; *Anal. Chem.*, **45**, 936-943, (1973).
- [6] Dole, M. Mack, L. L. Hines, R. L.; Mobley, R. C.; Ferguson, L. D. Alice, M. *J. Chem. Phys.*, **49**, 2240, (1968).
- [7] Aleksandrov, M. L.; Gall, L. N. Krasnov, N. V. Nikolaev, V. I. Pavlenko, V. A.; Shkurov, V. A. *Dokl. Akad. Nauk. SSSR*, **277**, 379-383, (1984).
- [8] Fenn, J. B.; Mann, M.; Meng, C. K.; Wong, S. F. *Science*, **246**, 64-71, (1989).
- [9] Tanaka, K.; Waki, H.; Ido, Y.; Akita, S.; Yoshida, Y. *Rapid. Commun. Mass Spectrom.*, **2**, 151-153, (1988).
- [10] Karas, M.; Hillenkamp, F. *Anal. Chem.*, **60**, 2299-2301, (1988).
- [11] Robb, D. B.; Covey, T. R.; Bruins, A. P. *Anal. Chem.*, **72**, 3653-3659, (2000).
- [12] Cody, R. B.; Laramee, J. A.; Durst, H. D. *Anal. Chem.*, **77**(8), 2297 - 2302, (2005).
- [13] Patents pending.
- [14] Penning, F. M. *Naturwissenschaften*, **15**, 818, (1927).
- [15] Mastwijk, H. C. Cold Collisions of Metastable Helium Atoms, Ph.D. Thesis, University of Utrecht, Netherlands, (1997).
- [16] Faubert, D.; Paul, G.J.C., Giroux, J.; Bertrand, M. J. *Int. J. Mass Spectrom. Ion Proc.*, **124**, 69, (1993).
- [17] Faubert, D.; L'Heureux, A.; Peraldi, O.; Mousselmal, M.; Sanchez, G.; Bertrand, M. J.; "Metastable Atom Bombardment (MAB) Ionization Source: Design, Optimization and Analytical Performances" in *Adv. Mass Spectrom.: 15th International Mass Spectrometry Conference*, Wiley: Chichester, UK, 431-432, (2001).
- [18] http://www.jeol.com/ms/docs/map_note.pdf.
- [19] Tsuchiya, M. Kuwabara, H.; *Anal. Chem.*, **56**, 14, (1984).
- [20] Tsuchiya, M. *Mass Spectrom. Rev.*, **17**, 51, (1998).
- [21] Tsuchiya, M. *Analytical Sciences.*, **14**, 661-676, (1998).
- [22] Hiraoka, K.; Fujimaki, S.; Kambara, S.; Furuya, H.; Okazaki, S. *Rapid Commun. Mass Spectrom.*, **18**, 2323-2330, (2004).
- [23] McLuckey, S. A.; Glish, G. L.; Asano, K. G.; Grant, B. C., *Anal. Chem.*, **60**, 2220, (1988).
- [24] Guzowski, J. P., Jr.; Broekaert, J. A. C.; Ray, S. J.; Hieftje, G. M. J. *Anal. At. Spectrom.*, **14**, 1121-1127, (1999).
- [25] IonSense, Inc., 11 Dearborn Road, Peabody, MA USA 01960.
- [26] Jagerdeo, E.; Cody, R. B. unpublished results.

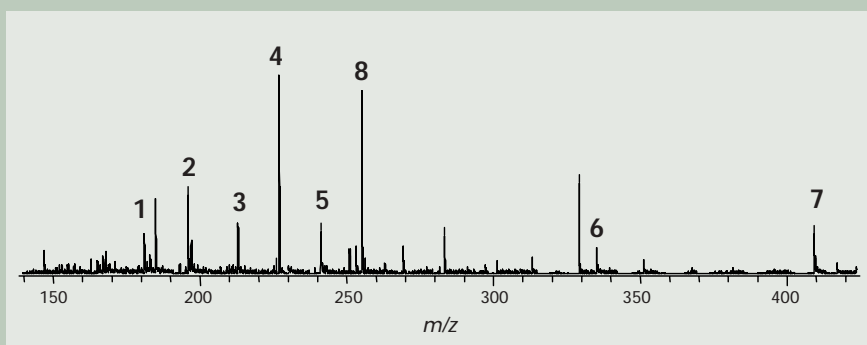


Fig. 6 3 ppm explosives spiked into muddy water. 1=DNT, 2=amino-DNT, 3=trinitrobenzene, 4=TNT, 5=RDY+TFA, 6=Tetryl, 7=HMX+TFA, 8=palmitate in the water background (used as lock mass). Headspace vapor from a 0.1% aqueous solution of trifluoroacetic acid was used to produce TFA adducts.

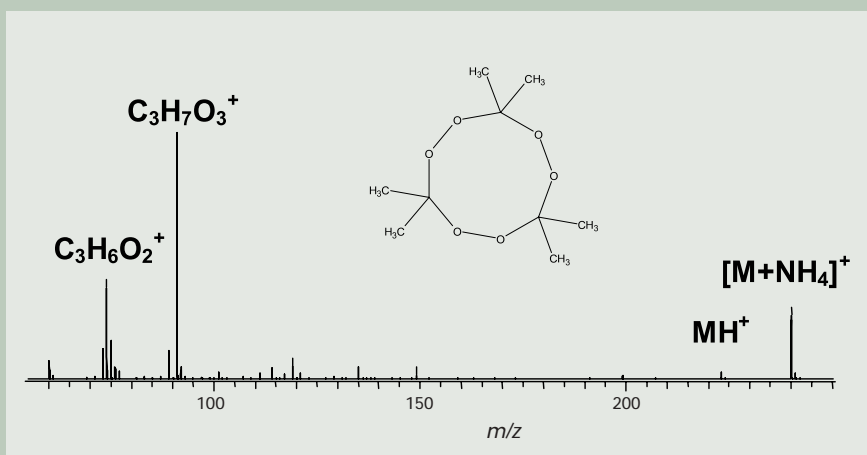


Fig. 7 Positive-ion DART mass spectrum of triacetone triperoxide (TATP). Ammonium hydroxide headspace vapor provided a source of NH_4^+ .

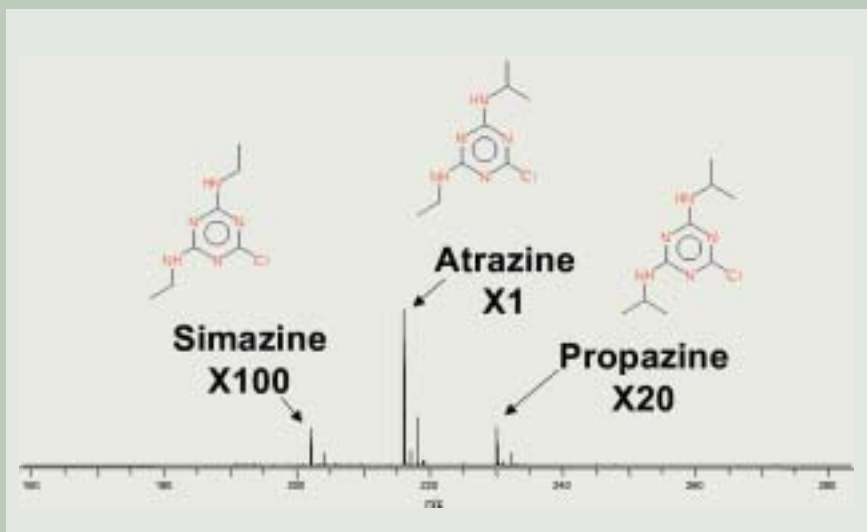
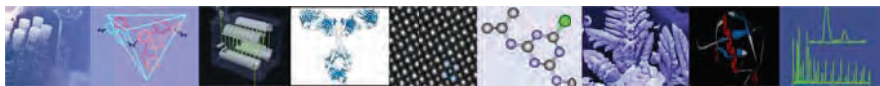


Fig. 8 Exact-mass analysis of trace simazine and propazine in a sample of the herbicide atrazine.

Table 2 DART measured masses for $[\text{M}+\text{H}]^+$ from atrazine and trace impurities.

Compound	Composition	Measured	Calculated	Diff. (mmu)
Atrazine	$\text{C}_8\text{H}_{15}\text{N}_5\text{Cl}$	216.10159	216.10160	-0.01
Propazine	$\text{C}_9\text{H}_{17}\text{N}_5\text{C}$	230.11760	230.11725	+0.35
Simazine	$\text{C}_7\text{H}_{13}\text{N}_5\text{Cl}$	202.08440	202.08595	+1.60

This page intentionally left blank for layout purpose.



The AccuTOF® Atmospheric Pressure Interface: an Ideal Configuration for DART® and Ambient Ionization

Introduction

The DART ion source was developed on the JEOL AccuTOF time-of-flight mass spectrometer which allows the exit of the DART source to be positioned within millimeters of the sampling orifice (orifice 1) of the mass spectrometer atmospheric pressure interface (API). The AccuTOF vacuum system is robust, highly resistant to contamination, and capable of pumping helium DART gas without assistance.

The AccuTOF API

Figure 1 shows a schematic diagram of the AccuTOF atmospheric pressure interface. The API consists of two off-axis skimmers (designated “orifice 1” and “orifice 2”) with an intermediate ring lens, followed by a bent RF ion guide. The off-axis skimmer design traps contamination -- ions are electrostatically guided upward toward orifice 2 whereas neutral molecules are pumped downward. Any contamination that enters the API is either pumped away into the rough pump (RP) or trapped on the lower part of orifice 2. The bent RF ion guide provides an additional level of protection. This makes the AccuTOF an ideal mass spectrometer for DART analysis of dirty “real-world” samples such as mud, biological fluids, melted chocolate, polymers, and even crude oil. In addition, orifice 1 is easily accessible and is operated at low voltage and current, making it a convenient platform for ambient ionization sources.

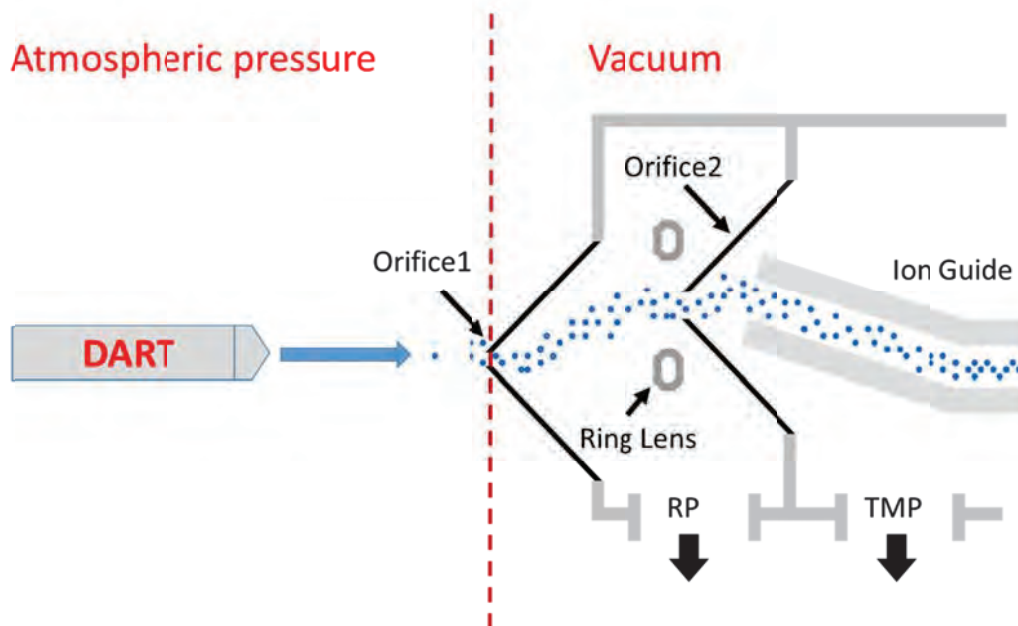


Figure 1. Schematic diagram of the AccuTOF atmospheric pressure interface (API)

AccuTOF® is a registered trademark of JEOL Ltd. (Akishima Japan)

DART® is a registered trademark of JEOL USA, Inc. (Peabody, MA USA)

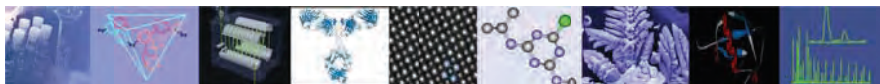


Figure 2 shows the DART source mounted on the AccuTOF with the exit of the ceramic insulator positioned approximately 1 cm from the apex of orifice 1. This is the optimal positioning of the DART source for normal operation.

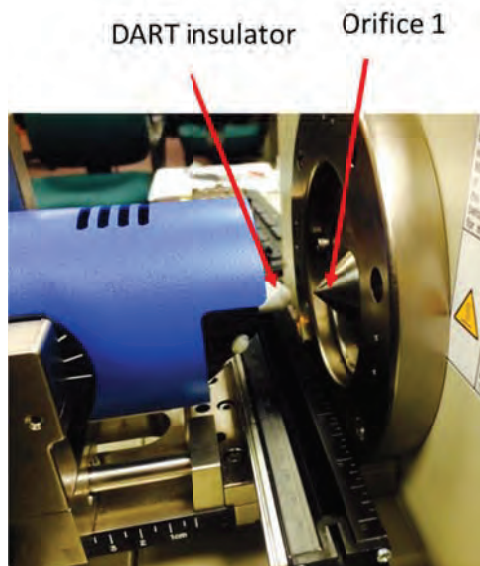


Figure 2. The white DART ceramic insulator cap is positioned approximately 1 cm from the apex of orifice 1 (the silver cone on the right).

The Vapur® Interface

Description

The vacuum systems of other mass spectrometer systems are not capable of handling the additional pumping burden and may shut down if the DART is operated with helium. The Vapur® interface allows the DART source to be used with non-JEOL mass spectrometers. It consists of a ceramic tube mounted on a custom flange and an auxiliary pumping station (Figure 3 and Figure 4) that is used as an interface for mounting the DART on ALL non-JEOL mass spectrometers and for mounting certain DART accessories that require additional clearance.

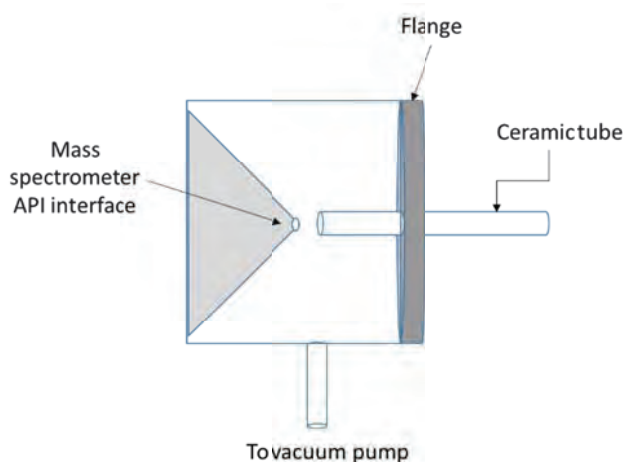


Figure 3. Schematic diagram of Vapur interface. On the AccuTOF, the gap between orifice 1 and the exit of the Vapur ceramic tube should be 2 mm for optimal performance.

Vapur® is a registered trademark of IonSense LLC (Saugus, MA USA)

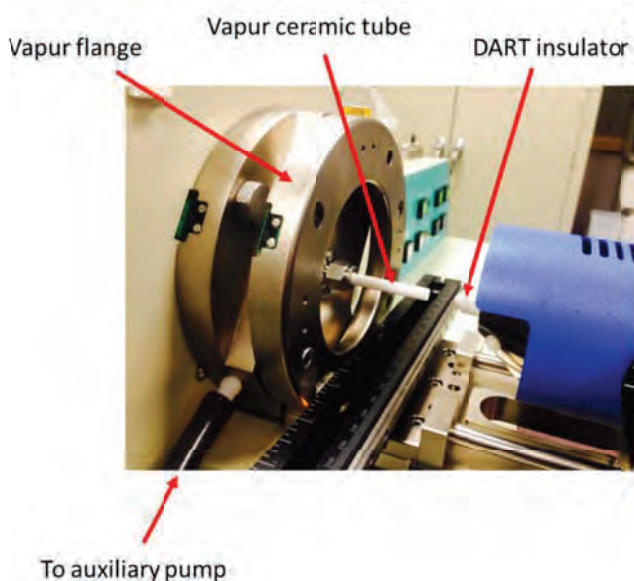


Figure 4. The Vapur interface mounted on the AccuTOF DART.

Loss of signal

The large diameter of the Vapur interface's ceramic tube improves reproducibility for some analyses by reducing gas turbulence and it provides space for mounting some accessories such as the IonSense 3+D Scanner. However, increasing the gas flow path increases the likelihood of ion-molecule reactions occurring, which can cause a loss of signal for samples that do not have a high proton affinity. Figure 5a shows the normal DART positive-ion low-mass background without the Vapur installed. The dominant reagent ions are protonated water and proton-bound water dimer. Figure 5b shows the background measured with the Vapur installed. Protonated water is barely visible, even at a magnification of 25X. The other peaks are trace impurities in the gas line and in the background that have a higher proton affinity than water.

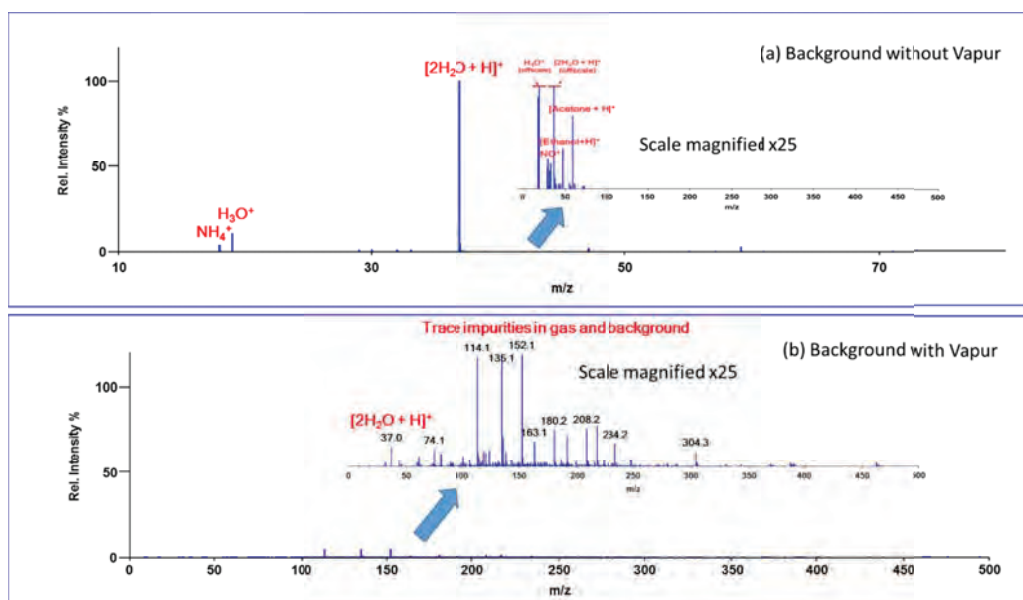


Figure 5. (a) positive-ion low-mass DART background without the Vapur installed, showing the dominant reagent ions with trace laboratory solvent peaks and (b) the low-mass background observed with the Vapur installed.



Nonpolar compounds are particularly susceptible to signal loss due to ion-molecule reactions at atmospheric pressure. Figure 6 illustrates the signal loss for a roughly equimolar mixture of epitestosterone and quinine with trace levels of methyl stearate as the Vapur is installed. The methyl stearate signal is completely lost, epitestosterone's signal reduced by a factor of 6, and even the relatively polar quinine is attenuated by a factor of 2.

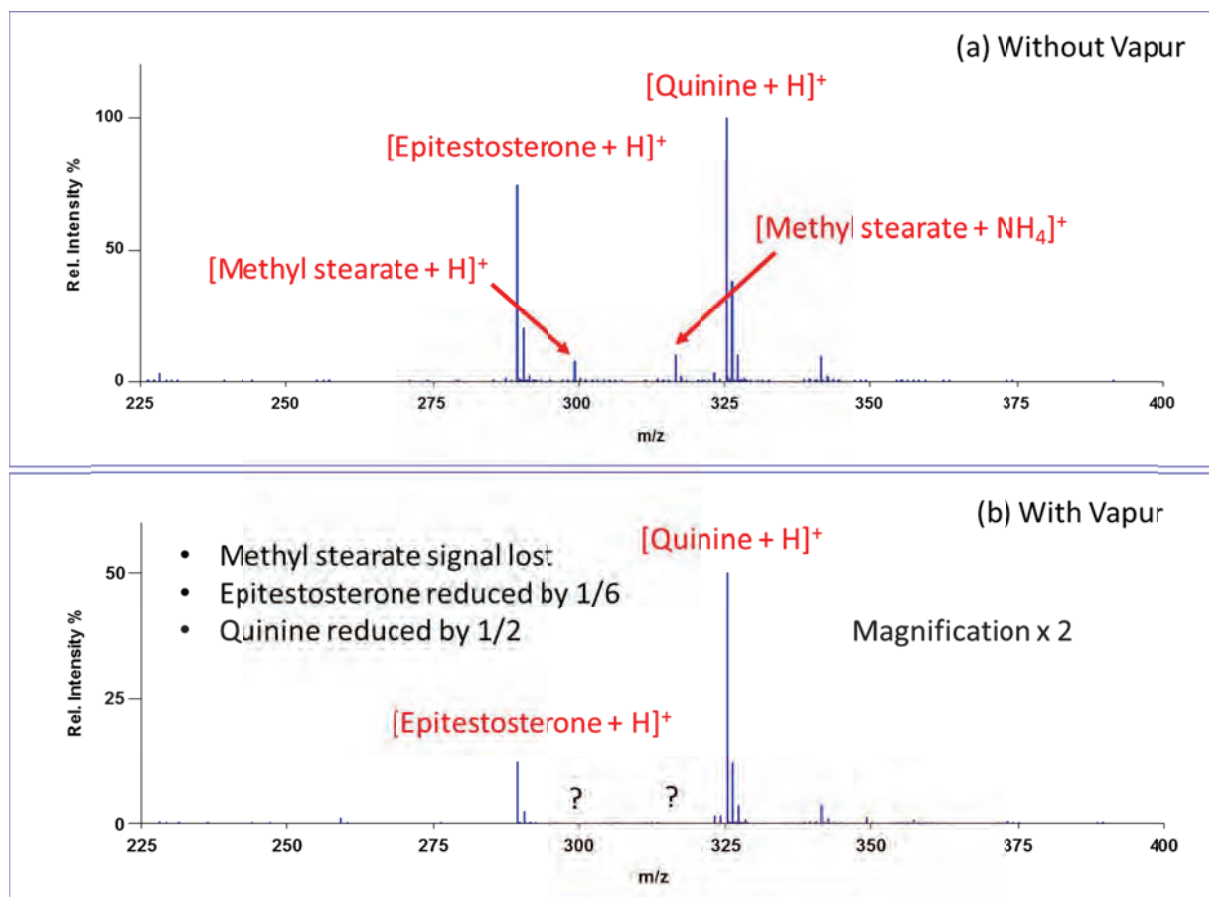


Figure 6. Comparison of signal for quinine, epitestosterone, and methyl stearate (a) without the Vapur interface and (b) with the Vapur interface.

Differences in ionization chemistry

Samples such as ethers and carbonyls measured with the Vapur interface installed tend to form ammonium adducts preferentially. This results from ion-molecule reactions occurring during sample transport through the Vapur, which favor ammonium over hydronium due to the high proton affinity of trace atmospheric ammonia. Samples without a strongly basic site that normally produce proton adducts with DART without the Vapur may be observed as ammonium adducts if the Vapur is installed. Figure 7 shows the comparison of the DART mass spectra measured for a polyethylene glycol (PEG) sample measured without the Vapur (Figure 7a) and with the Vapur (Figure 7b). Proton and ammonium adducts are observed in both spectra, but the proton adducts dominate in Figure 7a, whereas ammonium adducts dominate in Figure 7b.

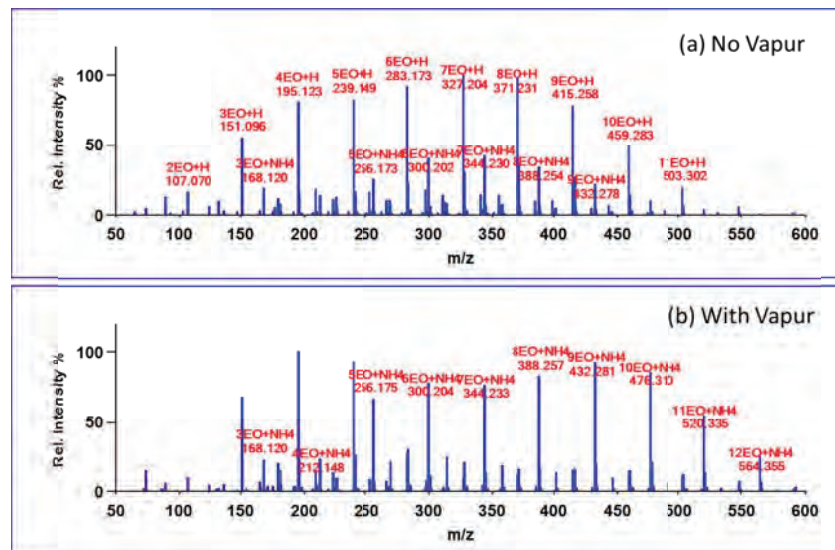
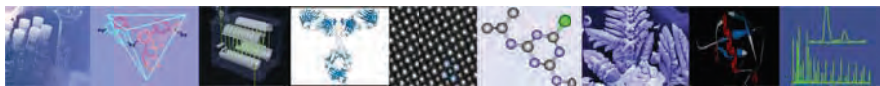


Figure 7. Positive-ion DART mass spectra of a PEG sample measured (a) with no Vapur and (b) with the Vapur installed.

Sample Carryover

Sample carryover in the Vapur is a problem for some samples. Therefore it is important to limit sample quantity when using the Vapur and to check for cross-contamination between samples. Figure 8 shows an example for the analysis of a sample containing 1% diisobutyl phthalate in isopropanol. Samples were introduced by depositing them onto the sealed end of a melting point tube and positioning the tube in the DART gas stream for several seconds. Three replicate measurements were made for the sample, followed by a mass reference standard (Jeffamine® M-600, Huntsman Corporation). Figure 8a shows the results of the sample measurement without the Vapur installed, and Figure 8b shows the results of the same measurements with the Vapur installed. The red arrows indicate the time at which each sample was introduced into the DART gas stream. Note that the total ion current and reconstructed ion current chromatogram (RIC) for diisobutyl phthalate show increasing contamination in Figure 7b as the DIBP is adsorbed onto the ceramic tube. The results obtained without the Vapur do not show any sample carryover and it is easy to determine when each sample was measured.

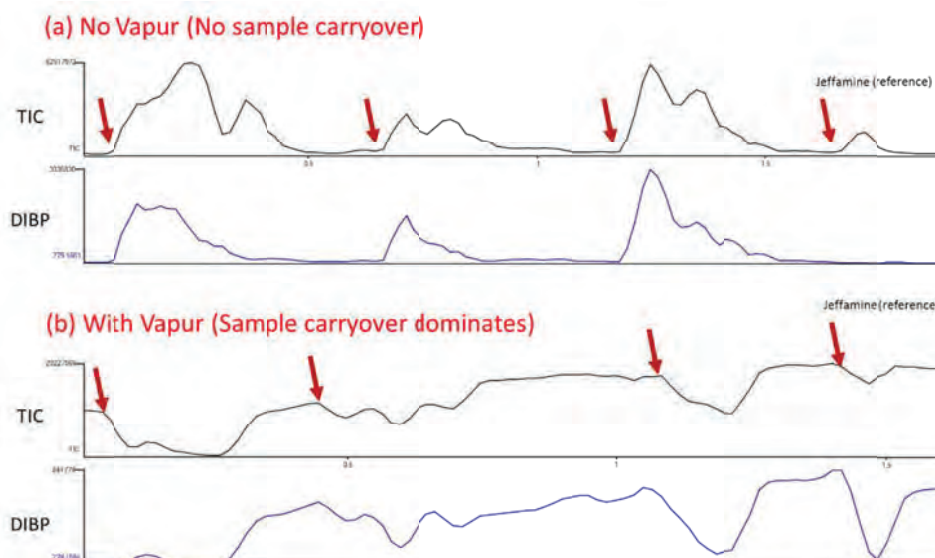
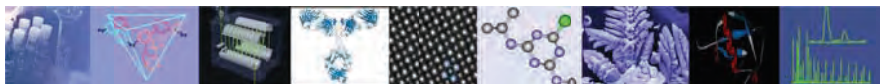


Figure 8. Chromatograms for three replicate measurements of a sample containing diisobutyl phthalate (DIBP) (a) with no Vapur and (b) with the Vapur installed.



Vapur Summary

- Features
 - Assists weaker vacuum systems to pump helium.
 - Improves reproducibility by reducing effects of turbulence
 - Provides a universal DART interface.
- Problems
 - Required for DART on ALL mass spectrometers EXCEPT THE JEOL AccuTOF.
 - Ion-molecule reactions occur as ions are transported over a longer distance
 - Loss of non-polar and reactive compounds including the air peaks
 - Ammonium adducts dominate over MH^+
 - Increased oxidation
 - Problems with sample carryover if compounds stick to the Vapur ceramic tube.
 - Requires an extra vacuum pump

Conclusion

The AccuTOF mass spectrometer atmospheric pressure interface is an ideal platform for use with the DART and ambient ionization sources. It permits the use of the DART without additional pumps, interfaces, or hardware that can cause sample carryover, loss of signal, or changes in the DART ionization chemistry.

Instantaneous Screening for Counterfeit Drugs with No Sample Preparation

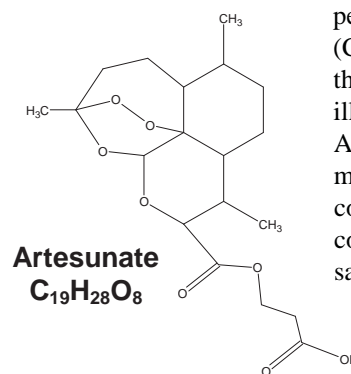
Drug counterfeiting is becoming a serious and widespread public health problem. The number of FDA open investigations into drug counterfeiting rose sharply from 2000 to 2001 and has remained high in recent years¹. Counterfeit drugs are not only illegal, but dangerous; they may contain little or no actual drug content, or they may contain completely different drugs with potentially toxic consequences. The problem is worldwide; it has been reported that nearly 50% of all anti-malarial drugs in Africa are thought to be counterfeit¹.

Direct Analysis in Real Time (DART™) offers a simple solution to screening for counterfeit drugs. DART can detect the presence or absence of drugs in medicines within seconds by simply placing the pill or medicine in front of the mass spectrometer. In combination with the AccuTOF, DART provides exact masses and accurate isotopic patterns that provide elemental compositions for known and unknown substances.

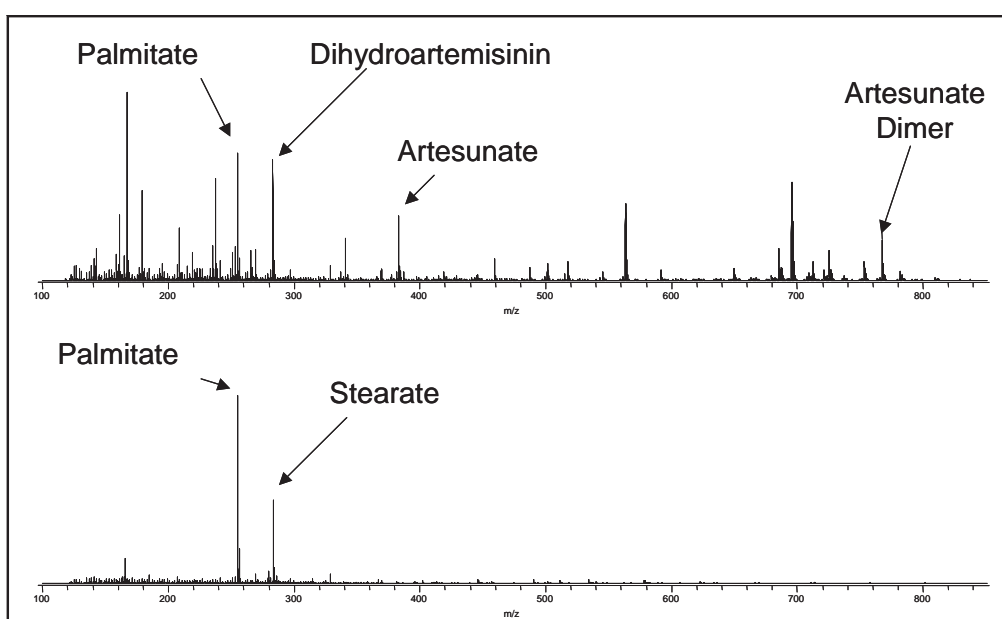
The top spectrum (below left) shows a sample of a genuine drug containing the anti-malarial compound "Guilin B" containing artesunate (structure below right), and the bottom spectrum shows a counterfeit drug containing only binders (stearate and palmitate) and no

active ingredient². The samples were placed in front of the DART with no sample preparation and the mass spectra were obtained within seconds.

It is noteworthy that the peak at m/z 283.15476 in the genuine drug is assigned the composition $C_{15}H_{23}O_5^-$ (dihydroartemisinin or a fragment from artesunate). The measured m/z differs from the calculated m/z by only 0.2 millimass units and is easily distinguished by its exact mass measurement from the



peak at m/z 283.26405 ($C_{18}H_{35}O_2^-$ or stearate) in the phony drug. This illustrates the value of AccuTOF's exact mass measurements in making correct assignments for compounds having the same integer mass.



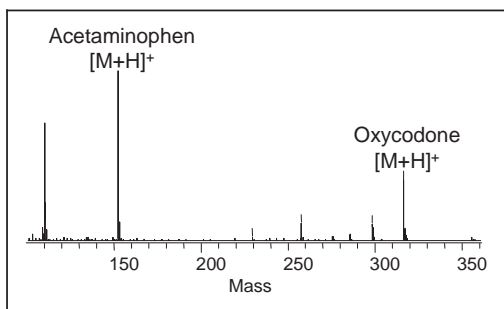
¹ http://www.fda.gov/oc/initiatives/counterfeit/report02_04.html#scope

² Samples were provided courtesy of Prof. Facundo Fernandez, Georgia Institute of Technology

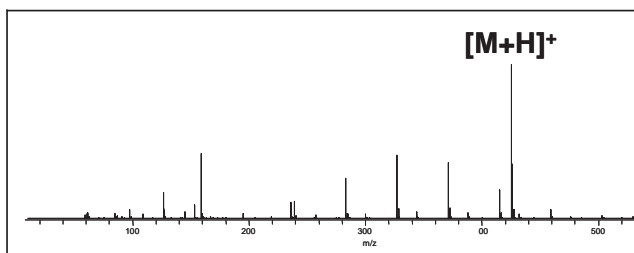
Direct Analysis of Drugs in Pills and Capsules with No Sample Preparation

The AccuTOF™ equipped with Direct Analysis in Real Time (DART™) is capable of analyzing drugs in pills and capsules with no sample preparation. In most cases, the pill can simply be placed in front of the DART and the active ingredients can be detected within seconds. This application note shows a wide variety of pills that have been analyzed by using DART. The examples include

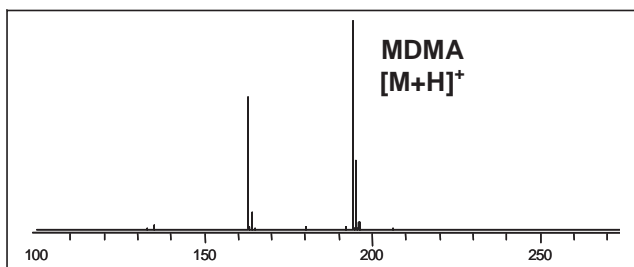
prescription drugs, over-the-counter medicines, and illicit drugs that were confiscated by a law-enforcement agency.



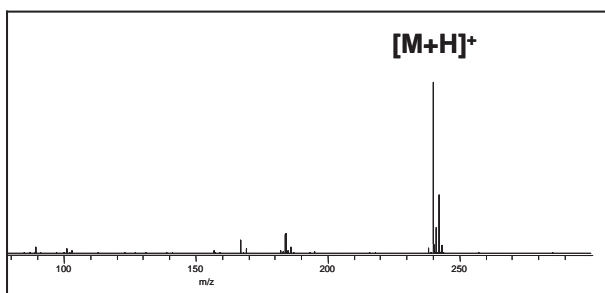
Endocet tablet (oxycodone: narcotic)



Lotensin Tablet (Benazepril: Antihypertensive)



"Ecstasy" (MDMA: illegal drug)



Generic Wellbutrin (Bupropion antidepressant)

Examples of Pills and Medicines that Have Been Analyzed Directly by DART

OTC Medicines

- Ibuprofen (anti-inflammatory)
- Naproxen sodium (anti-inflammatory)
- Aspirin (anti-inflammatory)
- Acetaminophen ("Tylenol" painkiller)
- Sudafed® (pseudoephedrine decongestant)
- Melatonin (sleep aid)
- Chlortrimeton (antihistamine)
- Cough syrup (guaiafenesin and dextromethorphan)
- Codeine with Tylenol® (painkiller)

Prescription Drugs

- Generic Wellbutrin® (Bupropion antidepressant)
- Zantac® (ranitidine: histamine H₂-receptor antagonist) Sealed capsule.
- Lipitor® (atorvastatin: treatment of hypercholesterolemia)
- Endocet® (oxycodone plus acetaminophen)
- Levsin® sublingual tablet (Hyoscyamine anticholinergic)

Dietary Supplements and Herbal Medicines

- Coenzyme Q10 with Vitamin E and Di- and Triglycerides
- Magnolia Bark (Chinese herbal medicine)
- Conjugated Linoleic Acid ("CLA" weight-loss formulation)

Confiscated Illicit Drugs

- Dimethoxyamphetamine plus methamphetamine
- Methylenedioxymethamphetamine ("Ecstasy" or MDMA)
- OxyContin®

All brand names are registered trademarks of their respective manufacturers.

Rapid Detection of Melamine in Dry Milk Using AccuTOF-DART

Introduction

Recent events have led to the recall of both pet food and dairy food products from international consumer markets. In both cases, melamine was added to these products to show a higher chemical signature for proteins, which in turn would increase the reported quality of the food. Unfortunately, the effect of this melamine addition caused the death of both pets and babies that consumed these tainted products. As a result, there is growing government and consumer concern towards the presence of melamine in food products.^{1, 2} Because of this concern, there is a need for a rapid and accurate test to quickly determine the presence of melamine in these food products. Previously, the JEOL AccuTOF-DART was shown to be an effective technique for determining the presence of melamine in pet food.³ In this work, we extend the application of AccuTOF-DART to show that melamine can be rapidly detected when it is present in dry nonfat milk.

Experimental

Solid melamine granules were artificially spiked into commercially available dry nonfat milk at levels between 1000ppm and 500 ppb. These samples were then pulverized with a mortar and pestle to homogenize the mixtures. For analysis, the AccuTOF-DART system was set to the following parameters: needle voltage 3500V, discharge

electrode 150V, grid electrode 40V, Helium temperature 150 degrees C, and He flowrate 2.3 L/min. A melting point tube was dipped and swirled through the melamine/milk mixture and then placed in the Helium stream between the DART and the AccuTOF atmospheric pressure interface. The data was collected in a matter of seconds from the moment the samples were introduced into the DART stream. A representative mass spectrum is shown in Figure 1 that shows the high resolution and isotopic data for the melamine [M+H]⁺. Additionally, a semi-quantitative calibration curve was constructed to show the ability of the AccuTOF-DART to measure melamine in dry milk over a dynamic range of concentrations (Figure 2). Furthermore, using this methodology, the AccuTOF-DART was able to detect 1 ppm of melamine in dry milk, which is below the United States Food and Drug Administration's maximum allowable concentration of 2.5 ppm.¹

Conclusion

Unlike other analytical techniques, the AccuTOF-DART methodology described above does not require time consuming extractions or chromatographic methods to detect melamine in dry milk. Additionally, within seconds of sampling the tainted milk, the AccuTOF-DART provides high resolution and isotopic data to identify melamine.

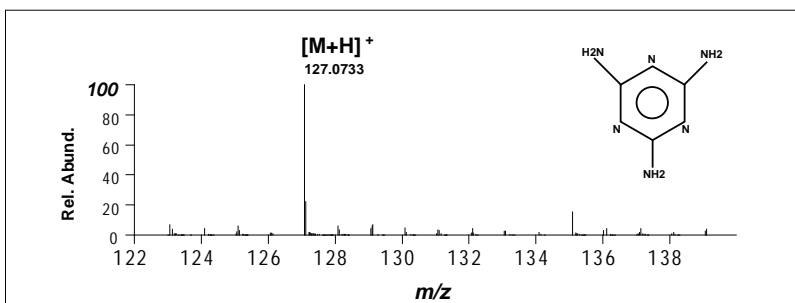


Figure 1. Mass spectrum of melamine in dry nonfat milk.

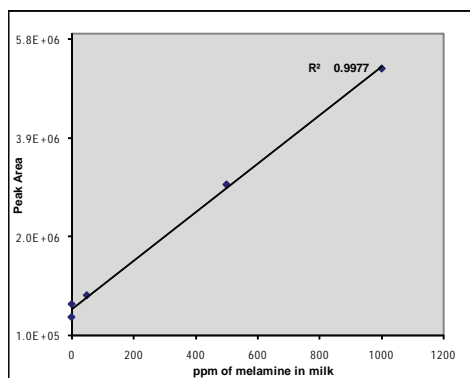


Figure 2. Semi quantitative calibration curve for melamine in dry nonfat milk.

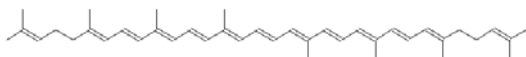
References

- 1 Kwisnek, S. FDA Issues Interim Safety and Risk Assessment of Melamine and Melamine-related Compounds in Food. *FDA News* **2008**, [cited 2008 October 21]; Available from: <http://www.fda.gov/bbs/topics/NEWS/2008/NEW01895.html>.
- 2 Statement of EFSA on risks for public health due to the presences of melamine in infant milk and other milk products in China. *The EFSA Journal* **2008**, 807: p. 1-10.
- 3 Vail, T., P.R. Jones, and O.D. Sparkman. Rapid and unambiguous identification of melamine in contaminated pet food based on mass spectrometry with four degrees of confirmation. *J Anal Toxicol.* **2007**, 31(6): p. 304-12.

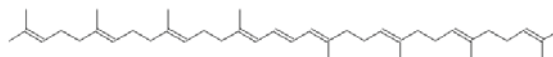
Detection of Lycopene in Tomato Skin

Tomatoes are rich in lycopene, a hydrocarbon antioxidant that is the source of the red coloring in ripe tomatoes. The potential benefits of nutritional antioxidants such as lycopene have received a great deal of attention in the popular media.

A piece of tomato skin was placed in front of the DART and the positive-ion mass spectrum was recorded. Peaks were quickly observed at the expected exact masses for lycopene and $[M+H]^+$ ($C_{40}H_{57}^+$, m/z 537.4460) and phytoene $[M+H]^+$ ($C_{40}H_{65}^+$, m/z 545.5086).



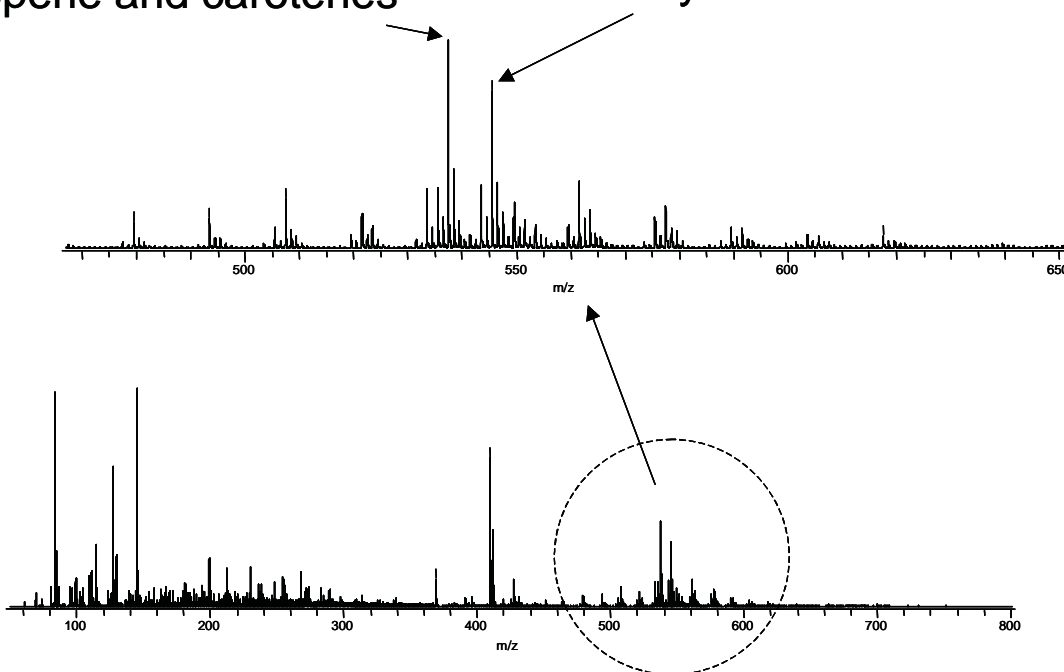
Lycopene



Phytoene

Lycopene and carotenes

Phytoene



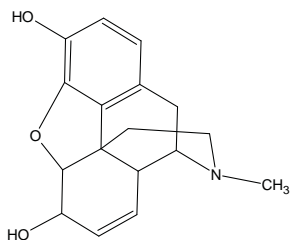
Instantaneous Detection of Opiates in Single Poppy Seeds

Poppy seed is a common flavoring ingredient that is known to contain small amounts of opiates. Maximum morphine and codeine concentrations are estimated to be about 33 and 14 micrograms respectively per gram of seed¹. Consumption of typical amounts of baked goods containing poppy seeds has not been shown to cause any ill effects. However, ingestion of poppy seeds may result in false positives from drug tests.

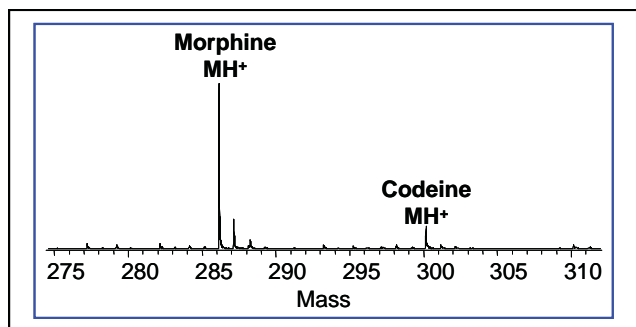
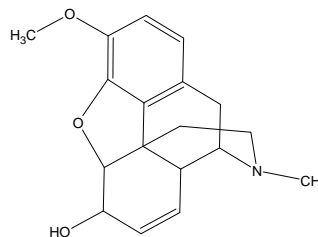
Single poppy seeds from different sources were analyzed independently in two different laboratories by using the DART™/AccuTOF™ combination. The resulting mass spectra were nearly identical.



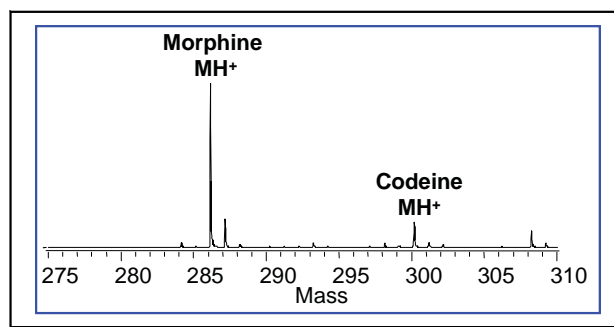
Morphine C₁₇H₁₉NO₃



Codeine C₁₈H₂₁NO₃



Poppy seed # 1 (DART in Maryland)



Poppy seed # 2 (DART in Massachusetts)

Measured Mass

286.1443 Da
300.1611 Da

Mass Error (mmu)

<0.001
0.001

Elemental Composition

C₁₇H₂₀N₁O₃ (Morphine)
C₁₈H₂₂N₁O₃ (Codeine)

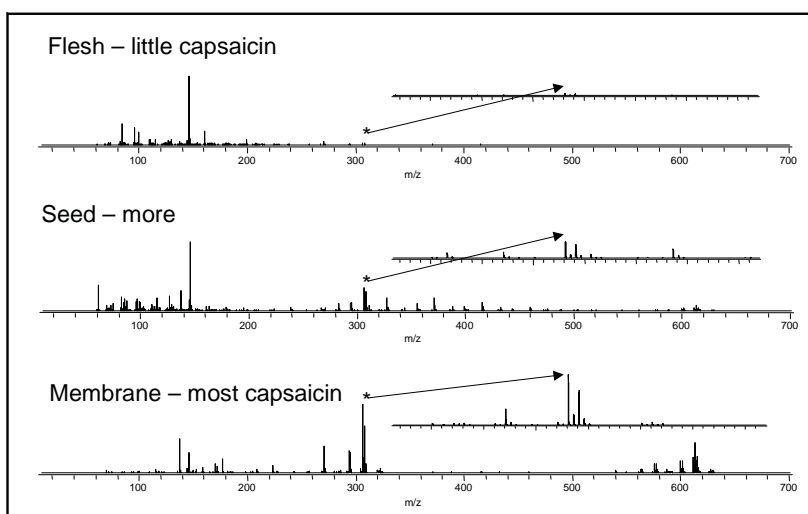
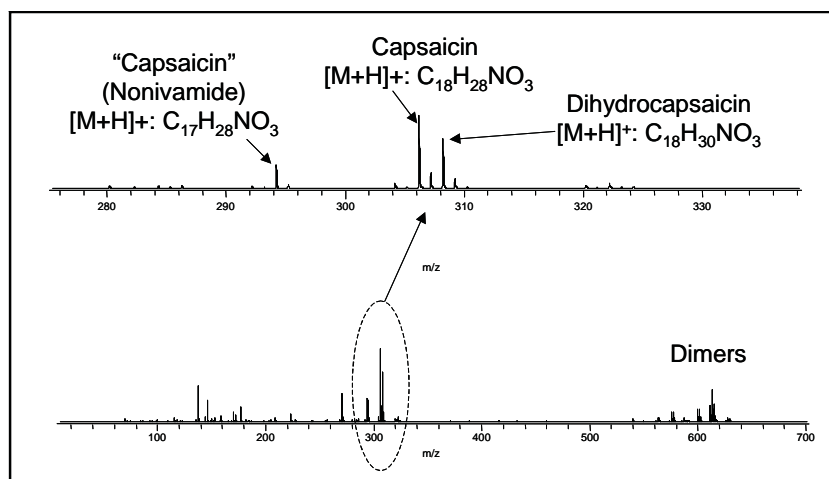
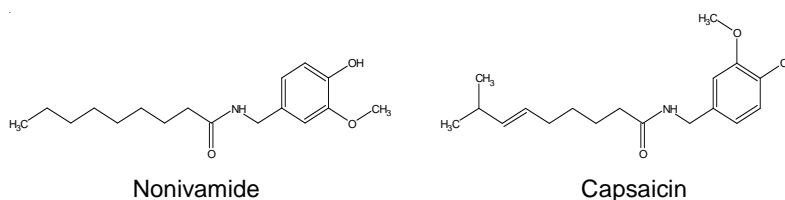
¹Opiate concentrations following the ingestion of poppy seed products – evidence for the poppy seed defense. Medway, C.; George, S.; Braithwaite, R. *Forensic Sci. Int.* vol. 96 (1998), pp. 29-38.

Distribution of Capsaicin in Chili Peppers

Capsaicin ($C_{18}H_{27}NO_3$) is the molecule that causes the hot, burning sensation when you eat chili peppers. Capsaicin, dihydrocapsaicin ($C_{18}H_{29}NO_3$), and a related compound, nonivamide ($C_{17}H_{27}NO_3$) are found in different concentrations in different parts of the pepper pod.

We examined different parts of a hot pepper to determine which part of the pepper contains the highest

concentration of capsaicin. Different sections of the pepper were placed between the DART and the AccuTOF orifice. Little capsaicin was found in the fleshy part of the pepper; higher concentrations were found in the pepper seeds. The highest concentration of capsaicin was found in the membrane inside the pepper pod onto which the seeds are attached.

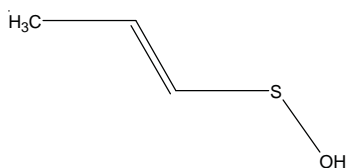


Detection of Unstable Compound Released by Chopped Chives

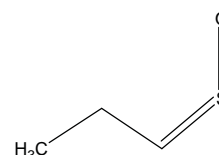
Every cook knows that chopping onions releases chemicals that cause eye irritation. The lachrymator released by chopped onions and related plants is formed by the action of a pair of enzymes on a cysteine derivative to ultimately form propanethial S-oxide (C_3H_6SO), the compound that causes eye irritation.

This compound is reactive and unstable and is therefore difficult to analyze by conventional mass spectrometry techniques.

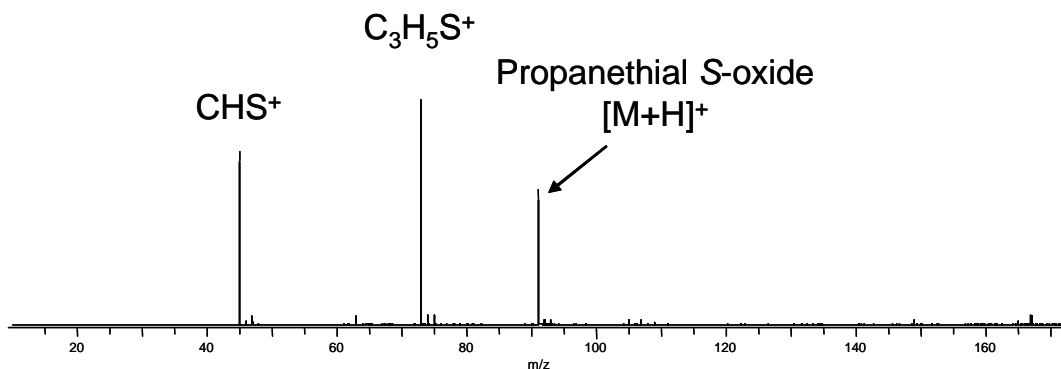
However, DART was easily able to detect propanethial S-oxide when a freshly cut chive bulb was placed in front of the mass spectrometer. The sample was analyzed at atmospheric pressure under ambient conditions and no sample preparation was required, other than cutting into the chive bulb. The compound was detected as $[M+H]^+$ ($C_3H_7SO^+$, m/z 91.0139).



Sulfenic acid released by enzymatic reactions when an onion is cut



Propanethial S-oxide lachrymator in onion



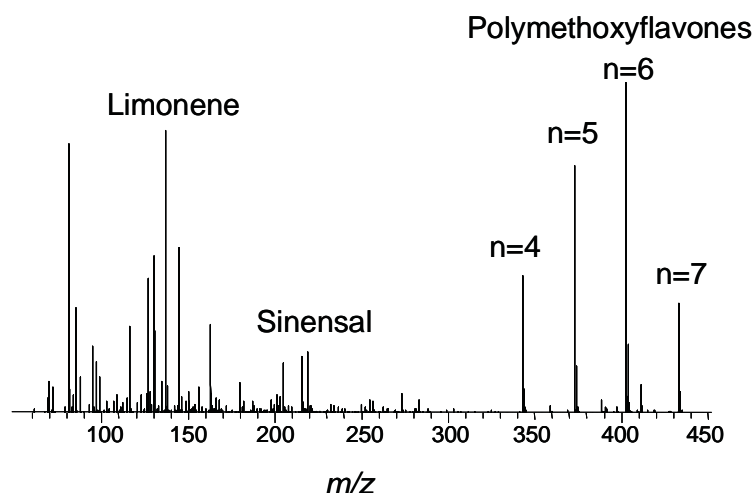
Lachrymator detected from freshly chopped chive bulbs placed in front of the mass spectrometer.

Rapid Detection of Fungicide in Orange Peel

Thiabendazole is an anthelmintic and a highly persistent systematic benzimidazole fungicide that is widely used for controlling spoilage in citrus fruit. It is considered a General Use Pesticide (GUP) in EPA Toxicity Class III – Slight Toxicity.

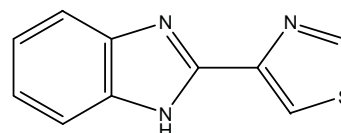
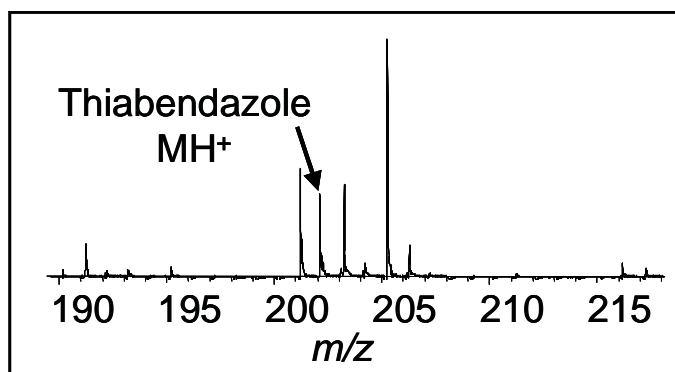
A small piece of orange peel (a few square millimeters in size) from a Florida orange was placed in

the DART sampling region. Compounds present in the peel were detected within seconds. Among these were the familiar orange-oil flavor components such as limonene and sinensal as well as polymethoxylated flavones that are attributed with antioxidant and cholesterol-reducing properties.



An enlarged view of the region near m/z 202 is shown below. The large peak at m/z 205.1949 has the elemental composition $C_{15}H_{24}$, assigned as the $[M+H]^+$

for farnesene. Residual thiabendazole was detected as $[M+H]^+$ at m/z 202.0444, which differs by only 0.0005 from the theoretical m/z of 202.0439.



Thiabendazole

$C_{10}H_7N_3S$

Measured: 202.0444 Da

Calculated: 202.0439 Da

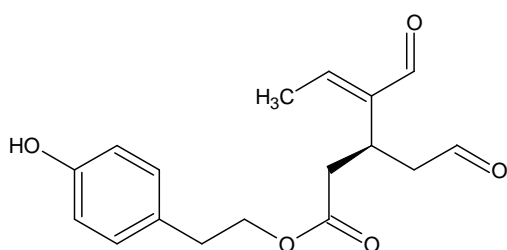
Difference: 0.0005 Da

Conclusion: DART was used for the rapid detection of trace pesticides on fruit.

Detection of Oleocanthal in Freshly Pressed Extra-Virgin Olive Oil

According to a recent report in *Nature*¹, freshly pressed extra-virgin olive oil contains a compound, oleocanthal, that has properties similar to the common anti-inflammatory drug, ibuprofen.

We used DART to rapidly examine cooking oils for the presence of this compound. Fresh-pressed extra-virgin olive oil from a specialty food store was compared with a medium-quality grocery-store brand. Sesame oil and a low-quality spray-on cooking oil were also examined. No sample preparation was required. Glass melting point tubes were dipped into the oil samples and then placed in front of the DART source for analysis. The DART source was operated with helium in positive-ion mode at a gas heater temperature of 350°C. A cotton swab dipped in dilute aqueous ammonium hydroxide was placed nearby to permit the formation of $[M+NH_4]^+$ for triglycerides and other oil components. A mass spectrum of neat PEG 600 on a glass rod was acquired and stored in the same data file to provide an external calibrant for exact mass measurements.



Oleocanthal

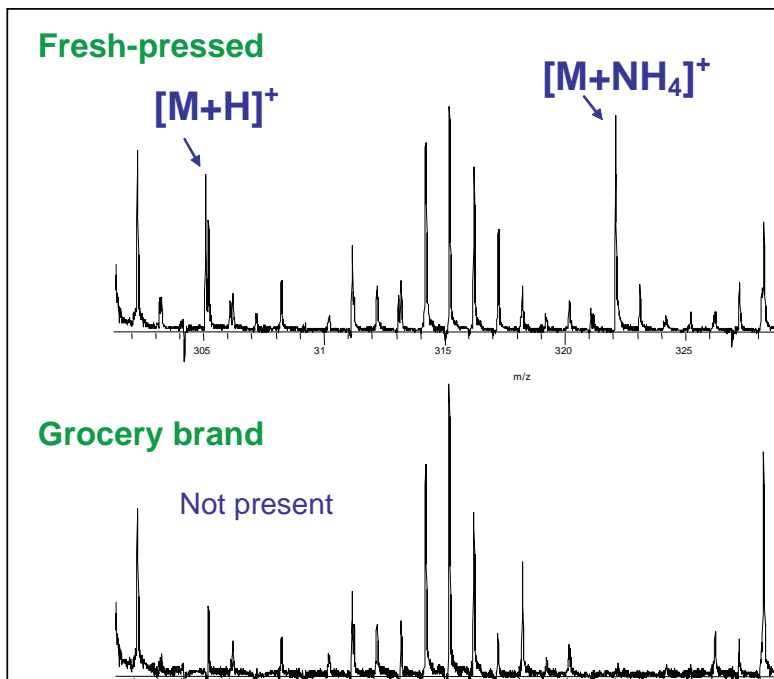


Figure 1. Positive-ion DART mass spectra of two olive oils. Enlarged view of the region where oleocanthal peaks are observed.

The oleocanthal was readily observed in the fresh-pressed oil as $[M+H]^+$ and $[M+NH_4]^+$. The measured masses confirmed the expected composition with excellent mass accuracy.

Conclusion

DART can detect the presence of natural products in cooking oils. Analysis is rapid (within seconds) and no sample preparation is required.

Reference

¹Beauchamp, G.K.; Keast, R. S. J.; Morel, D.; Lin, J.; Pika, J.; Han, Q.; Lee, C.-H.; Smith, A. B.; Breslin, P. A. S. *Nature*, **437**, 45-46 (Sept. 2005). "Phytochemistry: Ibuprofen-like activity in extra-virgin olive oil."

Meas. mass (um)	Diff. (mmu)	Composition	Assignment
305.138977	0.09	C ₁₇ H ₂₁ O ₅	$[M+H]^+$
322.165955	0.50	C ₁₇ H ₂₄ O ₅ N ₁	$[M+NH_4]^+$

This page intentionally left blank for layout purpose.

“No-prep” Analysis of Lipids in Cooking Oils and Detection of Adulterated Olive Oil

Introduction

Dietary fats are categorized according to the level of unsaturation. Oils are a mixture of triglycerides and free fatty acids. Olive oil contains a high concentration of monounsaturated fatty acids, while other oils such as Canola and safflower oil contain larger amounts of polyunsaturated fatty acids. Characterizing the type of lipids present is important for quality control and for detecting adulteration of more expensive oils (e.g. olive oil) with cheaper products. Analysis by HPLC is time-consuming and requires solvents and consumables. DART provides a convenient alternative: no solvents are required and the analysis can be completed in seconds.

Experimental

Analysis was carried out by using a JEOL AccuTOF-DART™ mass spectrometer operated in positive-ion mode at a resolving power of >6000 (FWHM). The

DART source was operated with helium and the gas heater was set to 375°C. Melting point tubes were dipped in oil samples and placed in front of the DART ion source for a few seconds. A cotton swab dipped in dilute ammonium hydroxide was placed nearby to enhance formation of $[M+NH_4]^+$ from triglycerides. A spectrum of PEG 600 was measured between samples to permit exact mass measurements.

Results

Figure 1 shows the DART mass spectrum of a grocery-store olive oil and Figure 2 shows a comparison of mass spectra for different cooking oils. Free fatty acids (Figure 3), squalene and di- and triglycerides (Figure 4) are detected as $[M+NH_4]^+$. The relatively high abundance of free fatty acids in Figure 1 (bottom) is a result of thermal decomposition and is only observed at higher gas temperatures for large amounts of (neat) oil. However, the abundant peaks for the free

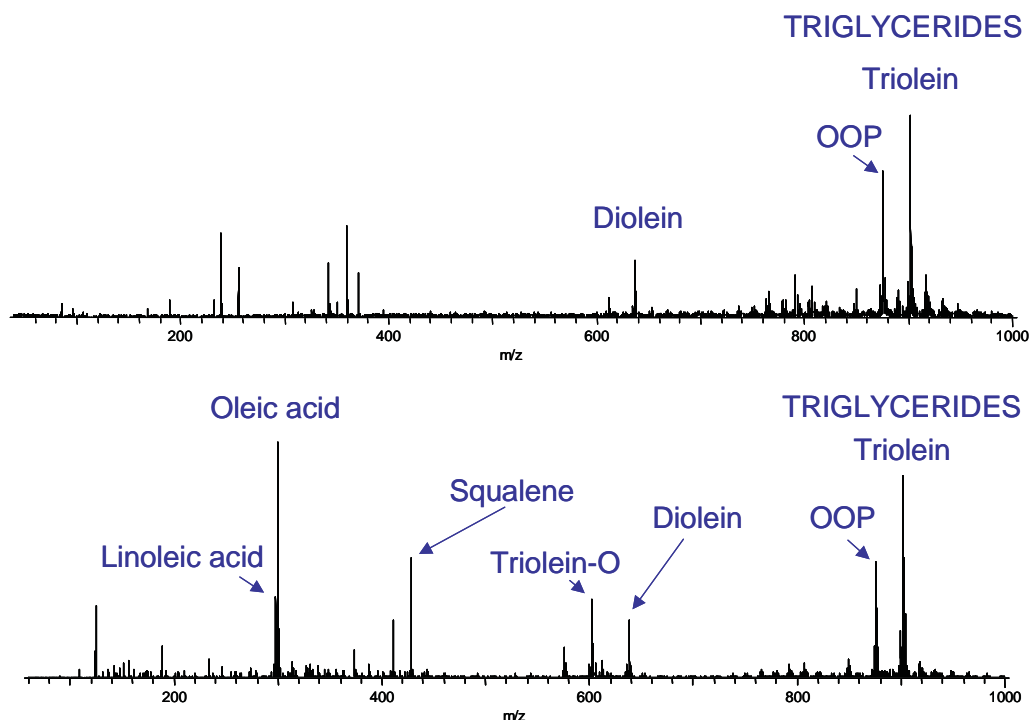


Figure 1. Medium-quality grocery store olive oil. Top: dilute solution of olive oil in hexane, bottom: neat oil (DART at 375°C).

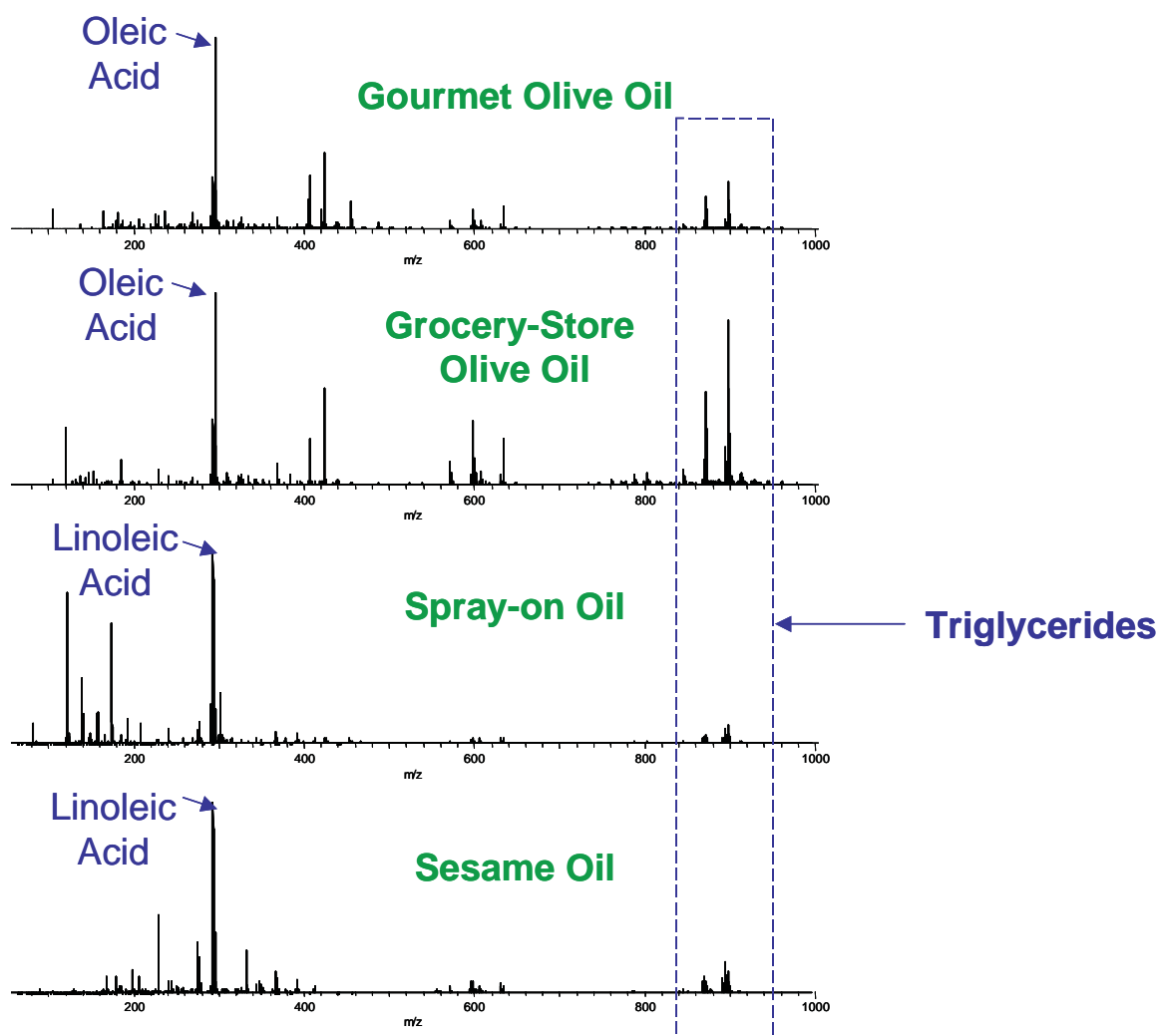


Figure 2. Comparison of cooking oils

fatty acids under these conditions make it easy to see differences in the overall fatty acid content of the oil.

Of the C_{18} fatty acids, oleic acid (O) comprises 55-85% of olive oil¹, while the Omega-6 fatty acid linoleic acid (L) is present at about 9% and the Omega-3 fatty acid linolenic acid (Ln) is present at less than 1.5%. Other fatty acids including the C_{16} palmitic acid (P) are also detected.

The triglycerides are readily detected (Figure 4) and their elemental compositions confirmed by exact mass measurements (Table 1) and isotope pattern matching. Triolein (OOO) is the major component in olive oil,

while increasing unsaturation is observed for the Canola/safflower oil blend and the sesame oil.

Elemental compositions were confirmed for the triglyceride $[M+NH_4]^+$ peaks by exact mass measurements and isotope pattern matching. Examples for triolein (OOO) and OOP are shown in Table 1. Figure 5 shows the DART mass spectrum of an olive oil sample to which 50% of the Canola/safflower oil blend has been added. In comparison with the unadulterated olive oil (Figures 3 and 4), the adulterated oil is easily recognized by the higher degree of unsaturation and the relatively higher abundance of linoleic and linolenic acids.

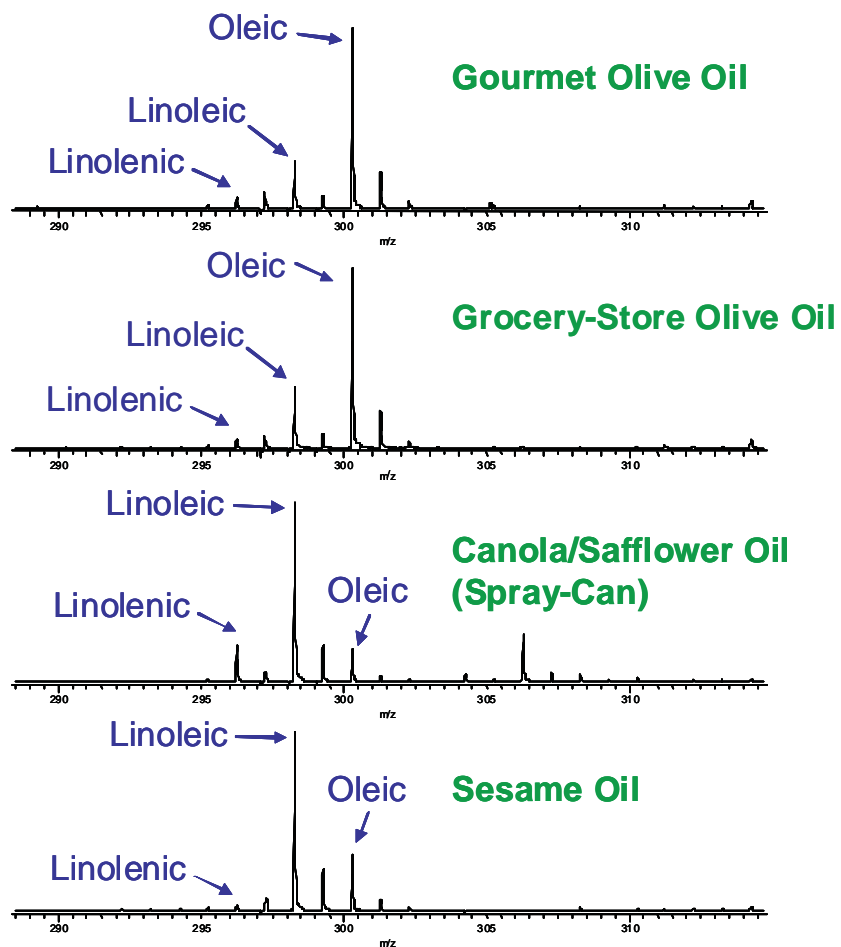


Figure 3. Enlarged view of free fatty acid region

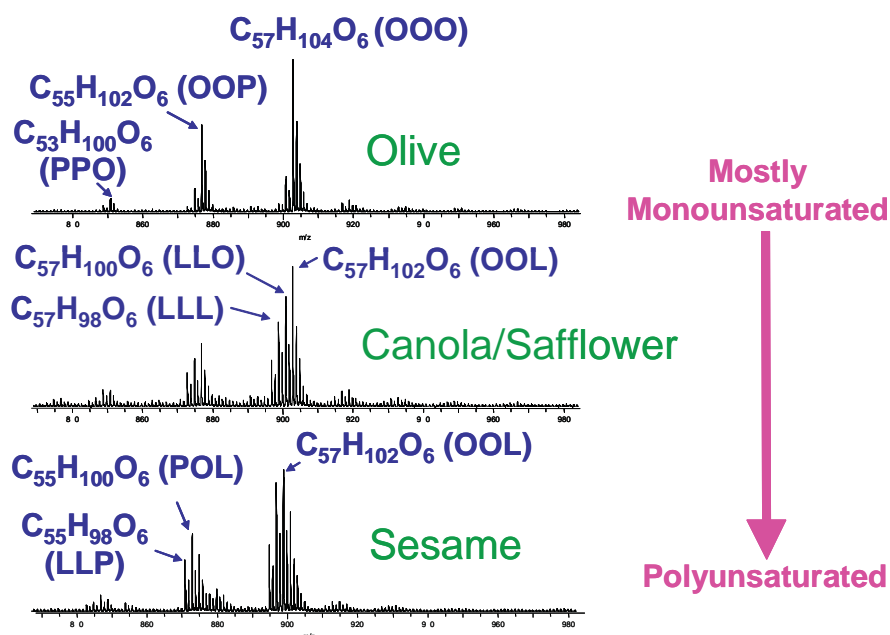


Figure 4. Enlarged view of triglycerides in cooking oils

Meas. mass (μm)	Abund. (%)	Difference (mmu)	Unsaturation	Compositions
876.801270	25.14	-0.75	3.5	C ₅₅ H ₁₀₆ O ₆ N ₁ (OOP)
902.816040	35.62	-1.61	4.5	C ₅₇ H ₁₀₈ O ₆ N ₁ (OOO)

Table 1. Elemental compositions from exact mass measurements

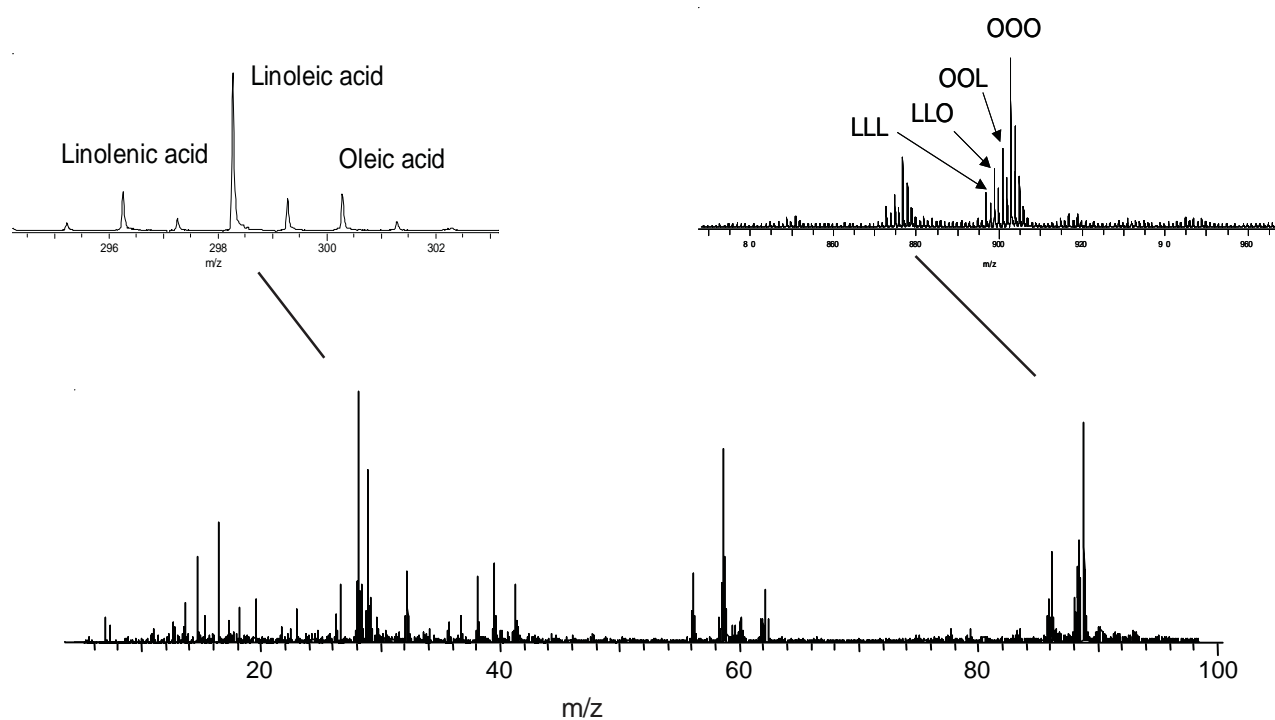


Figure 5. DART mass spectrum of adulterated olive oil

Conclusion

DART can characterize lipids such as fatty acids and mono-, di-, and triglycerides in cooking oils and detect adulterated olive oil within seconds and with no sample preparation.

Reference

1. <http://www.oliveoilsource.com/olivechemistry.htm>

Flavones and Flavor Components in Two Basil Leaf Chemotypes

The chemical composition of herbs and spices can vary dramatically between different species and different growing conditions. Herbs grown under different conditions that have different essential oil compositions are referred to as chemotypes.

Basil is an herb that has widely varying chemotypes^{1,2}. The difference between basil leaves from two different sources was easily observed by using DART. A leaf from a basil plant purchased at a grocery store was compared with a leaf from a Vietnamese restaurant. A small particle from each leaf was analyzed placed in front of the DART source. Mass spectra were obtained within seconds. Elemental compositions were confirmed by exact masses and accurate isotopic abundance measurements.

The resulting mass spectra (Figure 1) show dramatic differences between the two leaves. The basil leaf from the Vietnamese restaurant has a pleasing licorice-like flavor and a fragrant licorice-and-lemon aroma whereas the grocery store basil has a very mild clove flavor and a weak aroma. Both leaves contain terpenes and sesquiterpenes. The mass spectrum of the restaurant basil leaf (top figure) shows an abundant estragole (methyl chavicol, or *p*-allyl anisole) peak and a smaller citral peak. The grocery-store basil shows a weak eugenol peak. Furthermore, the restaurant basil leaf shows an abundance of hydroxymethoxyflavones. Flavones and related compounds are of interest because of possible antioxidant activity or other health benefits^{3,4}. The grocery store basil shows only weak peaks for these compounds.

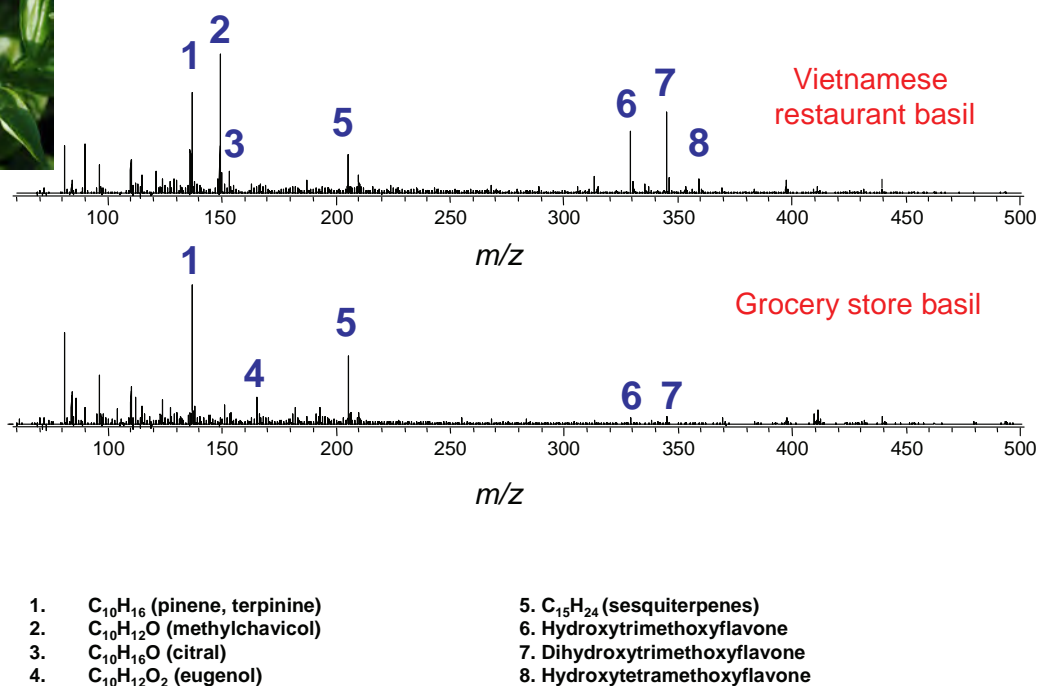


Figure 1. DART analysis of two different basil leaves.

Conclusion

DART can rapidly detect flavor components and antioxidants in herbs and spices and can be used to discriminate between different chemotypes.

References

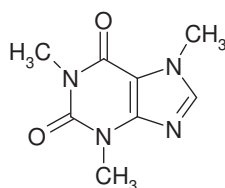
- <http://www.plantphysiol.org/cgi/content/full/136/3/3724>
- <http://www.hort.purdue.edu/newcrop/CropFactSheets/basil.html>
- <http://www.hort.purdue.edu/newcrop/ncnu02/pdf/juliani.pdf>
- <http://lpi.oregonstate.edu/infocenter/phytochemicals/flavonoids/index.html>

This page intentionally left blank for layout purpose.

Direct analysis of caffeine in soft drinks and coffee and tea infusions

Caffeine (Figure 1), a xanthine alkaloid acting as psychoactive stimulant and mild diuretic in human, is an integral part of diet of many people. It is often found in natural products such as tea, coffee and cocoa beans, cola nuts and many others. Analysis of caffeine in various foods and beverages is an important task for analytical laboratories, as its content is considered in assessment of product quality (coffee, cocoa beans and tea). Due to its physiological effect, the amount of caffeine is regulated in selected foods in EU. Maximum limits are set for some soft drinks to which caffeine is added. HPLC methods employing UV detection are commonly used for its control. While for soft drinks and coffee/tea infusions, the sample preparation is not too much time demanding, LC separation of sample components becomes a limiting step in laboratory throughput. Employing AccuTOF-DART system offers straightforward examination of caffeine content in tens of samples per hour, thanks to omitting separation step. Isotope dilution is used for target analyte quantification.

Figure 1 Structure of caffeine (1,3,7-trimethylxanthine, CAS Number: 58-08-2).



Experimental

Samples

The samples were prepared for analysis in following way:

- (i) Soft drinks (ice tea, cola drink, energy drink) were decarbonized by sonication.
- (ii) Soluble coffee 2 g were diluted in 100 mL of boiling water.
- (iii) Ground coffee beans and tea leaves (5 g) were extracted with 100 mL of boiling water under shaking (1 min).

All liquid samples were diluted 50 times and 5 μ l of aqueous solution containing 5 μ g of isotope labeled internal standard ($^{13}\text{C}_3$ -caffeine) were added to 1 mL of each diluted sample.

DART-TOFMS measurements

The DART ion source was operated in positive ion mode with helium as the ionizing medium at a flow rate of 2.7 L/min. The gas beam was heated to 300°C, discharge needle voltage set to 3000 V, perforated and grid electrode voltages were +150 V and +250 V, respectively. Accurate mass spectra were acquired in a range of m/z 50–500 employing 0.2 s recording interval; the peaks voltage value was set to 1000 V. A solution containing a mixture of poly(ethylene glycol) PEG 600 and 200 was introduced at the end of each sample analysis to compensate any mass drift.

The examined samples were introduced automatically with the use of an AutoDart sampler and Dip-it™ tips. Following steps were involved: (i) sampling tip immersed into the sample; (ii) placing of tip in front of the DART gun exit close to the ion source – mass spectrometer axis; (iii) sampling tip disposed. Five replicate measurements were carried out on examined samples.

Results

As shown in Figure 3, both caffeine and isotope labeled internal standard were detected as $[M+H]^+$ ions. The differences between exact and measured masses were as low as -0.7 mmu and -0.6 mmu, respectively.

In Figure 4 calibration plot of caffeine is shown. Each data point is an average of five repeated analyses measured over a period of five days, good linearity was obtained ($R^2 = 0.9989$). Table 1 summarizes the results of analyses obtained by analyses of the above samples. The repeatability of measurements was less than 8% (RSD) within an experimental series for all examined matrices. Good agreement with data obtained by reference HPLC/UV method was obtained.

Conclusions

DART-TOFMS technique was demonstrated to be suitable for accurate determination of caffeine in various beverages including coffee and tea infusions. The requirements on sample preparation are minimal: only dilution, sonication and internal standard addition are needed. The results of preliminary experiments have shown the potential of DART-TOFMS to detect also other regulated compounds in soft drinks (artificial sweeteners, acidulants, preservation agents, etc.).

Figure 3 Positive DART spectrum: diluted coffee infusion.

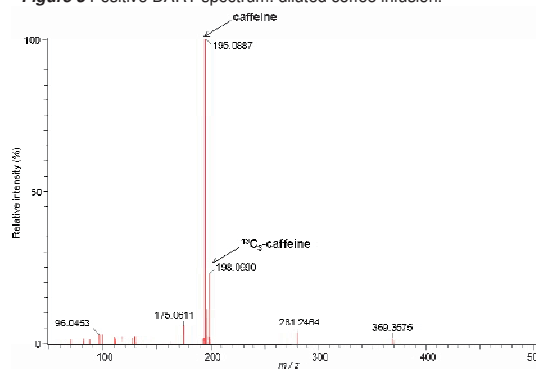


Figure 4 Calibration curve.

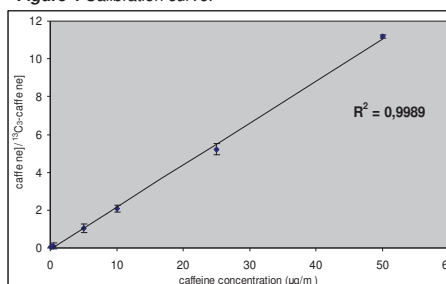


Table 1 Caffeine concentrations in examined samples.

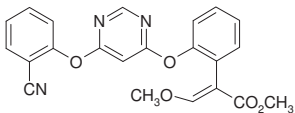
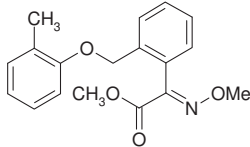
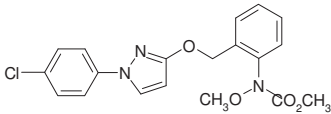
Sample	Caffeine concentration (µg/ml) ^a	RSD (%) ^b
Coffee infusion	825	7.9
Black tea infusion	103	4.2
Green tea infusion	71	3.1
Ice tea	44	5.6
Cola drink	95	4.5
Energy drink	230	3.5

^a calculated to undiluted beverage, ^b n = 5

Rapid screening of strobilurins in crude solid materials (wheat grains) using DART-TOFMS

Direct control of solid materials for pesticide residues is a challenging task enabling fast contamination screening. In our study, we investigated direct analysis of strobilurin fungicides in milled wheat grains. Strobilurins, systemic pesticides originated from natural fungicidal derivatives, play an important role in control of various plant pathogens.^{1,2,3} Because of their unique protective properties, significant yield enhancements and longer retention of green leaf tissue, strobilurins have been widely used in agriculture since their introduction on the market in 1992.³ As other pesticides, these compounds are involved in control and monitoring surveys undertaken by regulation authorities.⁴ Some characteristics of strobilurins are shown in Table 1.

Table 1 Strobilurins: physico-chemical characteristics.

Compound	Structure	log Kow	water solubility (mg l ⁻¹)	molecular weight
Azoxystrobin		2.5	6.0	403.4
Kresoxim methyl		3.4	2.0	313.4
Pyraclostrobin		4.0	4.6	387.8

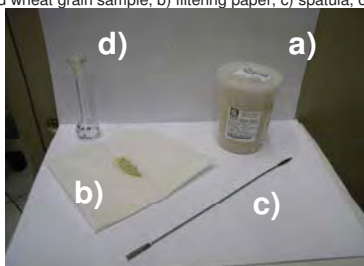
AccuTOF-DART system was used for examination of milled wheat grains containing incurred residues of azoxystrobin, kresoxim methyl and pyraclostrobin.

The DART ion source was operated in positive ion mode with helium as the ionizing medium at flow a rate of 2.7 L/min. The gas beam was heated to 130 °C and the distance between the exit of the DART gun and inlet of the mass spectrometer was 12 mm. The discharge needle voltage of the DART source was set to positive

potential of 2400 V, perforated and grid electrode voltages were +150 V and +250 V, respectively. Accurate mass spectra were acquired in a range of m/z 100–500, spectra recording interval was 0.2 s; the peaks voltage value was set to 850 V. A mixture solution of poly(ethylene glycol) PEG 600 and 200 was used for calibration. The same calibrant was also introduced at the end of each sample analysis to perform mass drift compensation. The mass resolution of the mass spectrometer was typically 6000 ± 500 (FWHM).

Samples were introduced manually with the use of in-hand made filtering paper envelopes containing approximately 1 g of homogenous sample. The sample was spread across the edge of the envelope (see Figure 1) and placed into the DART gas stream to ionize target analytes and detect the respective peaks.

Figure 1 The only items needed for fast analysis of strobilurins in milled wheat grain are: a) incurred wheat grain sample, b) filtering paper, c) spatula, d) PEG solution.



In Figures 2, 3 and 4 a positive-ion DART mass spectrum of directly analyzed wheat grains samples showing the tested strobilurins as $[M+H]^+$. The ion identity was confirmed by elemental composition calculations as documented in Table 2 and also shown in respective Figures.

Figure 2 a) Mass spectrum of wheat grains containing incurred residues of azoxystrobin. b) Estimation of an element composition from exact mass measurement. The highlighted column stands for target analyte.

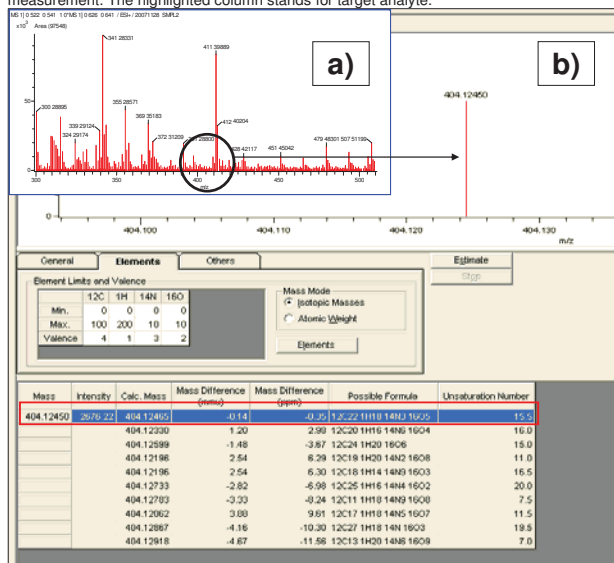


Figure 3 a) Mass spectrum of wheat grains containing incurred residues of pyraclostrobin. b) Estimated element composition from exact mass measurement. The highlighted column stands for target analyte.

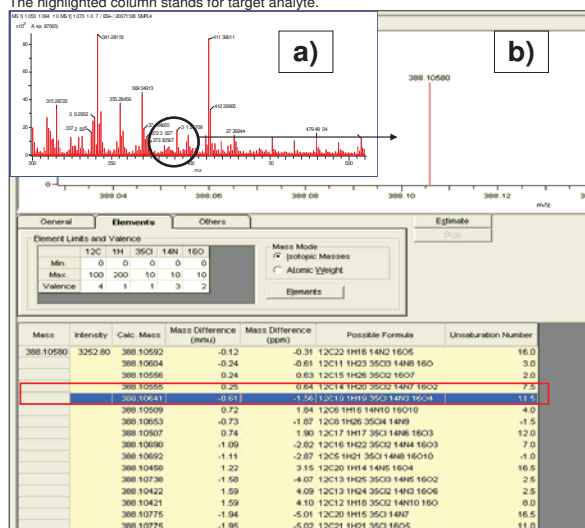


Figure 4 a) Mass spectrum of wheat grains containing incurred residues of kresoxim-methyl. b) Estimated element composition from exact mass measurement. The highlighted column stands for target analyte.

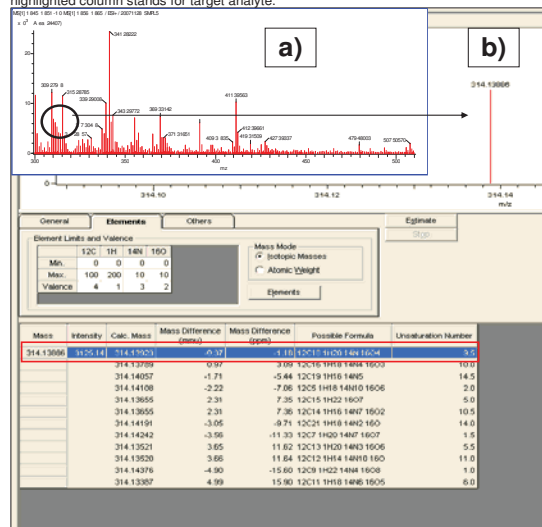


Table 2 Strobilurins identified by exact mass after direct analysis of wheat grains containing incurred residues at different concentration levels.

Compound	Exact mass (mu)	Measured mass (mu)	Difference (mmu)	Elemental composition	Concentration (ppb)
	$[M+H]^+$	$[M+H]^+$			
Azoxystrobin	404.12465	404.12450	-0.14	$C_{22}H_{18}N_3O$	445
Kresoxim methyl	314.13923	314.13886	-0.37	$C_{21}H_{23}N_3O_4$	45
Pyraclostrobin	388.19641	388.10580	-0.61	$C_{19}H_{18}ClN_3O_4$	202

The quantification was performed using DART-TOF MS analysis of ethyl acetate extracts of wheat grains (prochloraz was used as internal standard).⁵

In this study, DART-TOFMS system has been demonstrated as a suitable tool for rapid screening of strobilurin fungicides, time and money consuming sample preparation and purification steps can be omitted. The exact mass measurements provide high degree of confirmation, enabled by elemental composition calculation of target analytes.

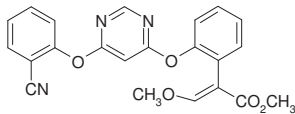
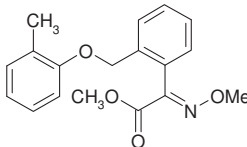
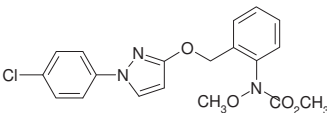
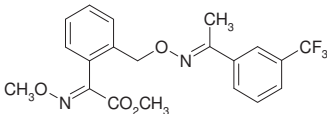
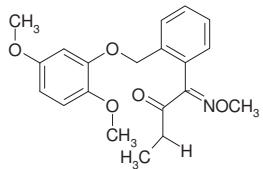
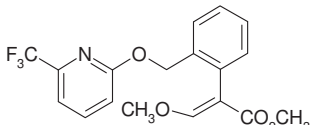
References

- Oerke, E.C., Dehne, H.W., Schonbeck, F., Weber, A., 1994. Crop Protection and Crop Production. Elsevier, Amsterdam, 808p
- Bartlett, D.W., Clough, J.M., Godwin, J.R., Hall, A.A., Hamer, M., Parr-Dobrzanski, B., 2002. Review: the strobilurin fungicides. *Pest Manage. Sci.* 58, 649–662.
- Sauter, H., Steglich, W., Anke, T., 1999. Strobilurins: evolution of a new class of active substances. *Angew. Chem., Int. Ed.* 111, 1416–1438.
- http://ec.europa.eu/food/plant/protection/resources/mrl_pesticide.pdf
- JEOL application report: Analysis of strobilurins in wheat grains using DART-TOFMS, 2008.

Analysis of strobilurins in wheat grains using DART-TOFMS

Strobilurins, systemic pesticides originated from natural fungicidal derivatives, play an important role in control of various plant pathogens.^{1,2,3} Because of their unique protective properties, significant yield enhancements and longer retention of green leaf tissue, strobilurins have been widely used in agriculture since their introduction on the market in 1992.³ As other pesticides, these compounds are involved in control and monitoring surveys undertaken by regulation authorities.⁴ Some characteristics of strobilurins are shown in Table 1.

Table 1 Strobilurins: structure and MRLs in wheat.

Compound	CAS number	Structure	MRL (mg/kg) in wheat		
			UK	Codex	EU
Azoxystrobin	131860-33-8		0.3	none	0.3
Kresoxim methyl	143390-89-0		0.05	0.05	0.05
Pyraclostrobin	175013-18-0		0.2	none	none
Trifloxystrobin	141517-21-7		0.02 ^a	none	none
Dimoxystrobin	149961-52-4		0.05 ^b	none	none
Picoxystrobin	117428-22-5		0.05 ^b	none	0.05 ^a

^a proposed MRL, ^b temporary MRL

The AccuTOF-DART system equipped with an AutoDart HTC PAL autosampler was used for the analysis of strobilurin residues (listed in Table 1) in wheat grain extracts. Crude extracts were prepared by shaking 12.5 g of sample with 50 mL of ethyl acetate and 5 mL of Na₂SO₄, the suspension was then filtered and the volume was made up to 25 mL by rota vapour. Within the validation, extracts spiked with strobilurins in the range from 12 to 1200 ng/g were analyzed. For quantitative analysis, prochloraz was used as an internal standard (samples were spiked with this internal standard at a level of 250 ng/g).

The DART ion source was operated in positive ion mode with helium as the ionizing medium at a flow rate of 2.7 L/min. The gas beam was heated to 300 °C, and the optimal distance between the exit of the DART gun and inlet of the mass spectrometer was 12 mm. The discharge needle voltage set to positive potential of 3000 V, perforated and grid electrode voltages were +150 V and +250 V, respectively. Accurate mass spectra were acquired in a range of *m/z* 100–500 employing 0.2 s recording interval; the peaks voltage value was set to 1000 V. A solution containing a mixture of poly(ethylene glycol) PEG 600 and 200 was used for mass calibration. The same calibrant was introduced at the end of each sample analysis to compensate any mass drift. The mass resolution of the mass spectrometer was typically 6000 ± 500 (FWHM).

The examined samples were introduced automatically with the use of an AutoDart sampler and Dip-it™ tips. A sampling tip was immersed into the sample and then placed in front of the DART gun exit close to the source – mass spectrometer axis. Each sample was examined in six repeated runs. The TIC chromatogram of spiked wheat sample is shown in Figure 1. Due to the variability of absolute responses, the use of internal standard is obviously essential for quantitative measurements.

Figure 1 TIC chromatogram: “on-line” 6 repeated injections of spiked wheat extract followed by PEG mixture.

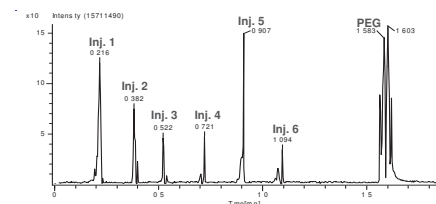


Figure 2 shows a positive-ion DART mass spectrum of crude ethyl acetate wheat extract spiked with strobilurins. Under these experimental conditions, both strobilurins and internal standard were detected as [M+H]⁺. In Table 2, measured and exact masses are compared, the differences ranged from -1.95 to 2.51 mmu.

Figure 2 Strobilurins (240 ng/g) and prochloraz (250 ng/g) in wheat extract.

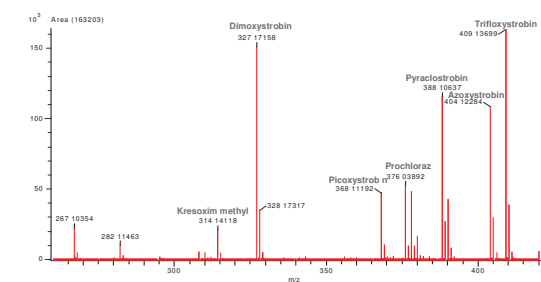


Table 2 Strobilurins identified in wheat extract by exact mass

Compound	Exact mass (mu)	Measured mass (mu)	Difference (mmu)	Elemental composition
	[M+H] ⁺	[M+H] ⁺		[M+H] ⁺
Azoxystrobin	404.12465	404.12284	1.81	C ₂₂ H ₁₈ N ₂ O ₅
Kresoxim methyl	314.13923	314.14118	-1.95	C ₁₈ H ₂₀ NO ₄
Pyraclostrobin	388.19641	388.10637	0.04	C ₁₉ H ₁₉ ClN ₃ O ₄
Trifloxystrobin	409.13752	409.13699	2.51	C ₂₀ H ₂₀ F ₂ N ₂ O ₄
Dimoxystrobin	327.17087	327.17158	-0.71	C ₁₉ H ₁₈ N ₂ O ₃
Picoxystrobin	368.11097	368.11192	-0.95	C ₁₈ H ₁₇ F ₂ NO ₄
Prochloraz	376.03864	376.03892	-0.28	C ₁₅ H ₁₆ Cl ₂ N ₂ O ₂

As Figure 3 shows, acceptable linearity was obtained for the analytes in the range from 12 to 1200 ppb.

The repeatability of measurements at a spiking level of 60 ng/g was in the range 8–15% (*n* = 6), limits of quantification (LOQs) ranged from 12 to 30 ng/g depending on the particular analyte. To prove the trueness of generated data, wheat grains with incurred strobilurin residues (reference material) were employed. Table 3 documents good agreement between the data obtained by DART-TOFMS and accredited LC-MS/MS method.

Figure 3 Calibration plots of strobilurins (analyte to internal std. intensity ratio plotted versus analyte concentration).

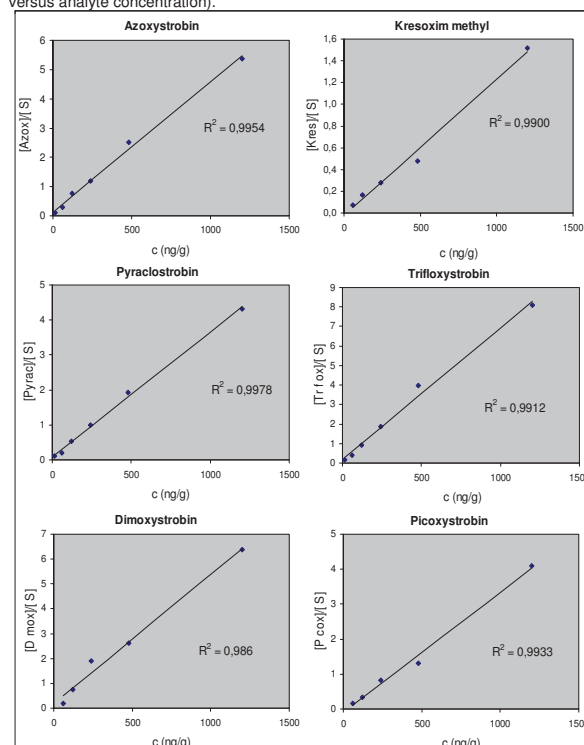


Table 3 Comparison of DART-TOFMS and LC-MS/MS method: analysis of wheat grain reference material.

Analyte	Concentration (ppb)	
	DART-TOFMS	LC-MS/MS
Azoxystrobin	445	429
Kresoxim methyl	45	52
Pyraclostrobin	202	170

Compared to conventional LC-MS/MS method, DART-TOFMS allowed significant decrease of analysis time, thus, enabled increase of sample throughput.

Although the detection limits are somewhat higher employing this new strategy as compared to the LC-MS/MS method, the DART-TOFMS enables convenient control of MRLs set for strobilurins residues in wheat grains which are in the range from 0.05 to 0.3 mg/kg.

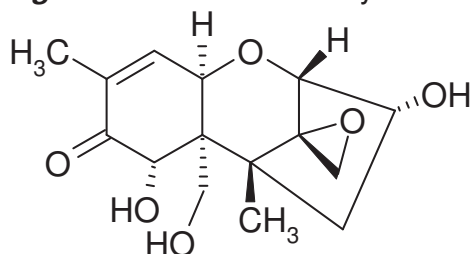
References

- Oerke, E.C., Dehne, H.W., Schonbeck, F., Weber, A., 1994. Crop Protection and Crop Production. Elsevier, Amsterdam, 808p
- Bartlett, D.W., Clough, J.M., Godwin, J.R., Hall, A.A., Hamer, M., Parr-Dobrzanski, B., 2002. Review: the strobilurin fungicides. *Pest Manage. Sci.* 58, 649–662.
- Sauter, H., Steglich, W., Anke, T., 1999. Strobilurins: evolution of a newclass of active substances. *Angew. Chem., Int. Ed.* 111, 1416–1438.
- http://ec.europa.eu/food/plant/protection/resources/mrl_pesticide.pdf

Analysis of deoxynivalenol in beer

Mycotoxins, toxic secondary metabolites of several fungal species, represent food safety issue of high concern. Deoxynivalenol (Figure 1), the most abundant trichothecene mycotoxin, can be found world-wide as a contaminant of wheat, barley, maize and other cereals.^{1,2} The transmission of deoxynivalenol from barley into beer has been reported in several studies.^{3,4} Therefore, its levels should be controlled.

Figure 1 Structure of deoxynivalenol, trichothecene B *Fusarium* toxin.



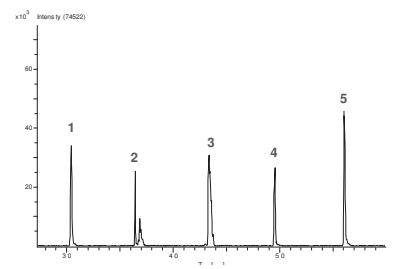
The AccuTOF-LC time-of-flight mass spectrometer equipped with a DART ion source and AutoDart HTC PAL autosampler, was used for examination of beer in this study. Donprep[®] immunoaffinity columns (R-Biopharm) was employed for selective isolation of target analyte from the sample. Briefly, 10 mL of beer with added internal standard (¹³C₁₅-deoxynivalenol, 500 ng/ml) were passed through the cartridge, which was then washed with 5 mL of water. Deoxynivalenol was subsequently eluted with 4.5 mL of methanol. Calibration standards containing deoxynivalenol in the range from 100 to 1500 ng/mL and fixed amount of internal standard (500 ng/mL) were prepared for quantification.

Introduction of the sample ($n = 5$) into the gas beam was carried out automatically with the use of autosampler. Beer extract was placed in the sampling hole, Dip-it[™] sampler stick was immersed into the sample and introduced in front of the DART ion source (Figure 2). After each sample analysis, PEG mixture solution was injected for mass drift compensation. TIC chromatogram of beer sample analysis is shown in Figure 3.

Figure 2 Sample introduction.



Figure 3 Repeated injections of beer sample.



To enhance negative ionization of target analytes, vial containing methylene chloride was placed beneath DART gun exit – MS orifice axis. After sample introduction, both deoxynivalenol and $^{13}\text{C}_{15}$ -deoxynivalenol were immediately detected as $[\text{M}+\text{Cl}]$ (see Figure 4) under parameters setting shown in Table 1. Good mass accuracy was obtained (see Table 2).

Table 1 Optimized DART ion source parameters

Parameter	Setting
Polarity	negative
Helium flow rate	2.7 L/min
Discharge needle voltage	3000 V
Perforated electrode voltage	-150 V
Grid electrode voltage	-250 V
Gas beam temperature	300°C

Figure 4 Positive DART spectrum: deoxynivalenol and internal standard in beer extract.

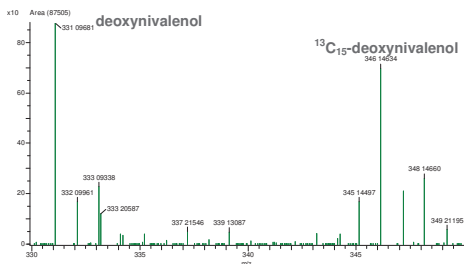
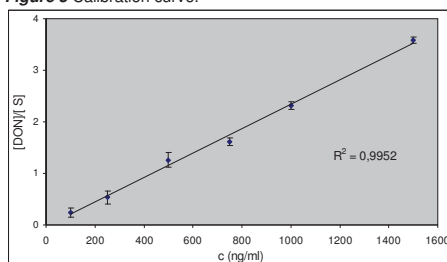


Table 2 Comparison of exact and measured masses.

Compound	Exact mass (mu)	Measured mass (mu)	Diference (mmu)	Elemental composition [M+Cl]
Deoxynivalenol	331.09484	331.09681	-1.97	$\text{C}_{15}\text{H}_{20}\text{O}_5\text{Cl}$
$^{13}\text{C}_{15}$ -Deoxynivalenol	346.14516	346.14634	-1.18	$^{13}\text{C}_{15}\text{H}_{20}\text{O}_5\text{Cl}$

In Figure 5, calibration plot of deoxynivalenol is shown; analyte to internal standard ratio was linear in selected concentration range. Deoxynivalenol concentration determined with the use of DART-TOFMS in particular beer sample was 166 $\mu\text{g}/\text{L}$ and repeatability of the method, estimated from five repetitive analyses, was 3%. In addition, accredited LC-MS/MS method was used for sample examination to confirm the trueness of results obtained by DART-TOFMS. The difference between deoxynivalenol obtained by respective methods was as low as 14 $\mu\text{g}/\text{mL}$.

Figure 5 Calibration curve.



In conclusion, AccuTOF-DART has been demonstrated as a suitable to screen for deoxynivalenol in beer samples purified by simple procedure employing immunoaffinity columns.

References

- Hussein, H. S.; Brasel, J. M.: Toxicity, metabolism, and impact of mycotoxins on humans and animals, *Toxicology*, 167, 2001, 101-134.
- Wiedenbörner, M.: Encyklopedia of food mycotoxins, Springer, Berlin.
- Scott, P. M.: Mycotoxins transmitted into beer from contaminated grains during brewing, *Food Chemical Contaminants*, 79, 1996, 875-882.
- Papadoulou-Bouraoui, A.; Vrabcheva, T.; Valzacchi, S.; Stroka, J.; Anklam, E.: Screening survey of deoxynivalenol in beer from the European market by an enzyme-linked immunosorbent assay, *Food Additives and Contaminants*, 21, 2004, 607-617.

Using Solid Phase Microextraction with AccuTOF-DART™ for Fragrance Analysis

Introduction

Solid phase microextraction (SPME) is a well established sampling technique that is often used to isolate volatile organic components in gaseous mixtures. Once the compounds have been collected, the SPME fibers are typically placed into a heated GC inlet which thermally desorbs these components into a GC-MS system for analysis. Normally, this analysis can take between 10 and 30 minutes to complete depending on the complexity of the samples. In this work, the Direct Analysis in Real Time (DART™) heated gas stream is used to desorb and directly introduce a SPME sample into a high-resolution mass spectrometer. This methodology produces comparable information to the traditional GC-MS technique but streamlines the results into only a few seconds of analysis time.

Experimental

A Supelco DVB/Carboxen/PDMS StableFlex SPME fiber was placed in an enclosed plastic bag with a banana for 10 minutes during each analysis. For direct analysis of the SPME fiber, the JEOL AccuTOF-DART™ system was set to the following parameters: needle voltage 3500V, discharge electrode 150V, grid electrode 250V, helium temperature 200 degrees C, and helium flowrate 2.3 L/

min. A JEOL GC-Mate II high resolution sector bench top system equipped with a DB5-HT (0.25mm × 30m) was used for the GC-MS portion of the analysis. The GC-Mate II was set to the following parameters: inlet temperature 250 degrees C, split ratio 30, and helium flowrate 1.2 mL/min. The GC oven was set for the following temperature profile: 40 degrees C held for 2 min, ramp from 40 to 260 degrees C at 20 degrees C/min, 260 degrees C held for 2 min.

Results and Conditions

Figure 1 shows a typical AccuTOF-DART™ mass spectrum obtained for a banana headspace sample. At first glance, this spectrum might appear complex, but using the JEOL-provided ChemSW *Search from List Software*, all of the [M+H]⁺, [M+NH₄]⁺, and [2M+H]⁺ for each alcohol, acetate, and butyrate were identified, summed together, and normalized in a matter of seconds. Additionally, these results were directly comparable to the data obtained for the traditional GC-MS analysis done using the GC-Mate II. Figure 2 shows a side-by-side comparison of these data sets. This work clearly demonstrates that the AccuTOF-DART™ can be used with SPME to quickly produce results that are comparable to traditional analysis techniques.

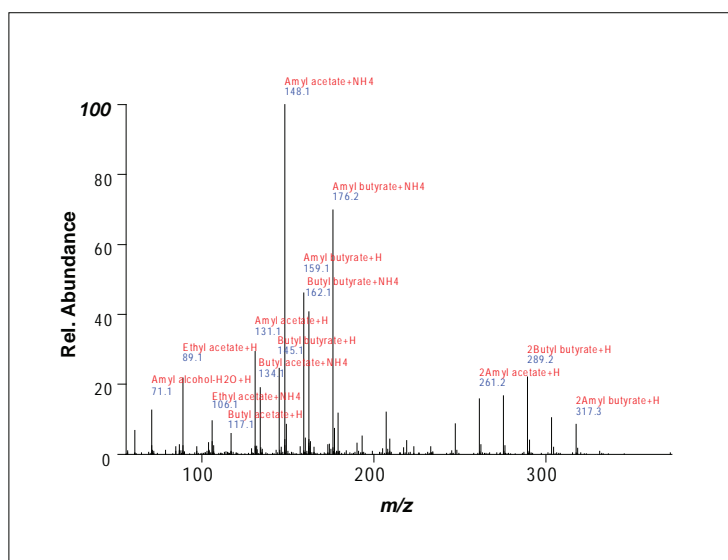


Figure 1. AccuTOF-DART mass spectrum for banana fragrance from SPME fiber.

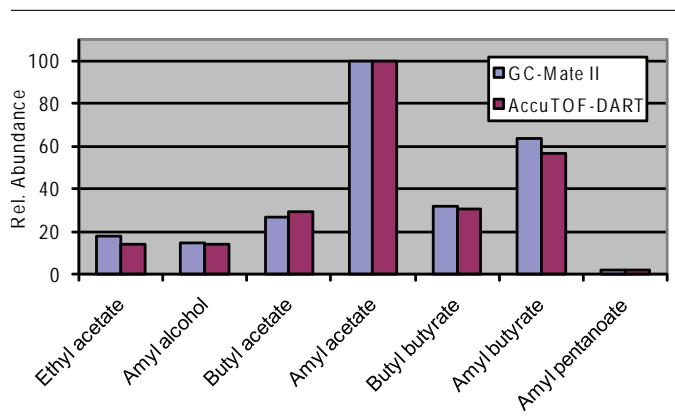


Figure 2. Comparison of relative abundances observed for compound using GC-MS and DART-MS analysis.

This page intentionally left blank for layout purpose.

Chemical Analysis of Fingerprints

Fingerprints contain a great deal of chemical information that is not often exploited for forensic analysis. DART can detect and identify the chemical components of fingerprints, often providing information about what substances a subject has been handling.

An example is shown here for DART analysis of a single fingerprint made on a glass vial after touching an aspirin/oxycodone tablet. The aspirin and oxycodone are readily detected, along with minoxidil (hair-loss

treatment), fatty acids, urea, lactic acid, squalene, cholestadiene, and the common plasticizer BEHP bis(ethylhexylphthalate). The amino acids A, F, G, I/L, S, P, T, and V are also detected with relative abundances between 0.5% and 18%. Other lipids can be detected at higher masses (not shown). Oxycodone is readily separated at the AccuTOF's high resolving power from an unassigned interference at m/z 316.

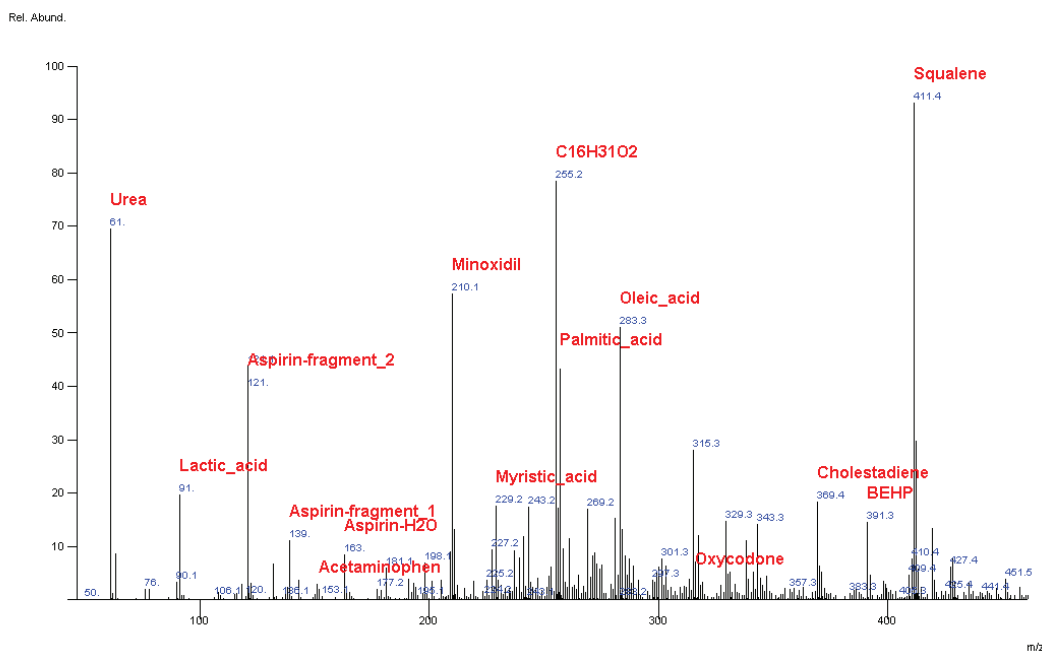


Figure 1. Fingerprint on a glass vial after touching Oxycodone tablet.

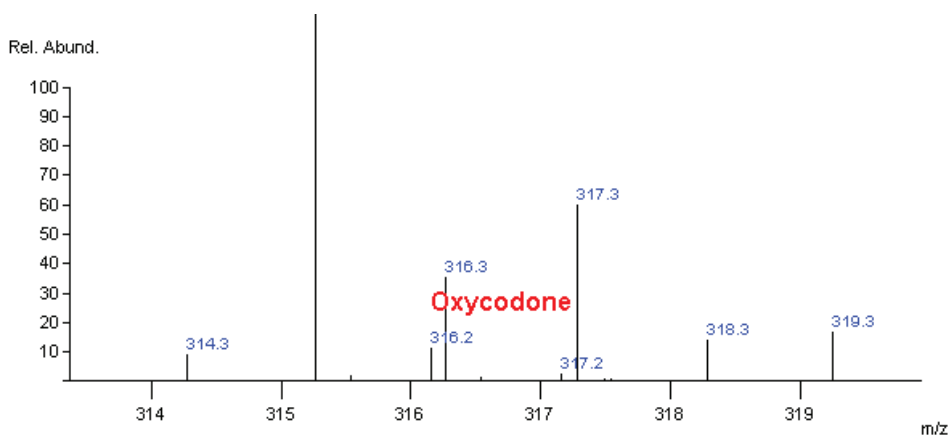


Figure 2. Enlarged view of region near m/z 316, showing that oxycodone is resolved from interference at the same integer m/z .

Name	Meas.	Calc.	Diff(u)	Abund.
Oxycodone	316.1554	316.1549	0.0005	2.3573
Aspirin-H ₂ O	163.0398	163.0395	0.0003	8.9676
Aspirin-fragment_1	139.0401	139.0395	0.0006	11.9823
Aspirin-fragment_2	121.0286	121.0290	-0.0004	42.4559
Minoxidil	210.1355	210.1355	0.0000	61.6484
Urea	61.0413	61.0402	0.0011	74.7234
Palmitic_acid	257.2477	257.2480	-0.0003	46.4336
C ₁₆ H ₃₁ O ₂	255.2324	255.2324	0.0000	84.2178
Squalene	411.3996	411.3991	0.0005	100.0000
Cholestadiene	369.3525	369.3521	0.0004	19.7204
Lactic_acid	91.0400	91.0395	0.0005	21.1630
BEHP	391.2854	391.2849	0.0005	15.6784
Oleic_acid	283.2637	283.2637	0.0000	54.9441
Myristic_acid	229.2162	229.2168	-0.0006	18.8792

Table 1. Compounds detected within 0.002 u of compounds in a list of common drugs and components in human sweat.

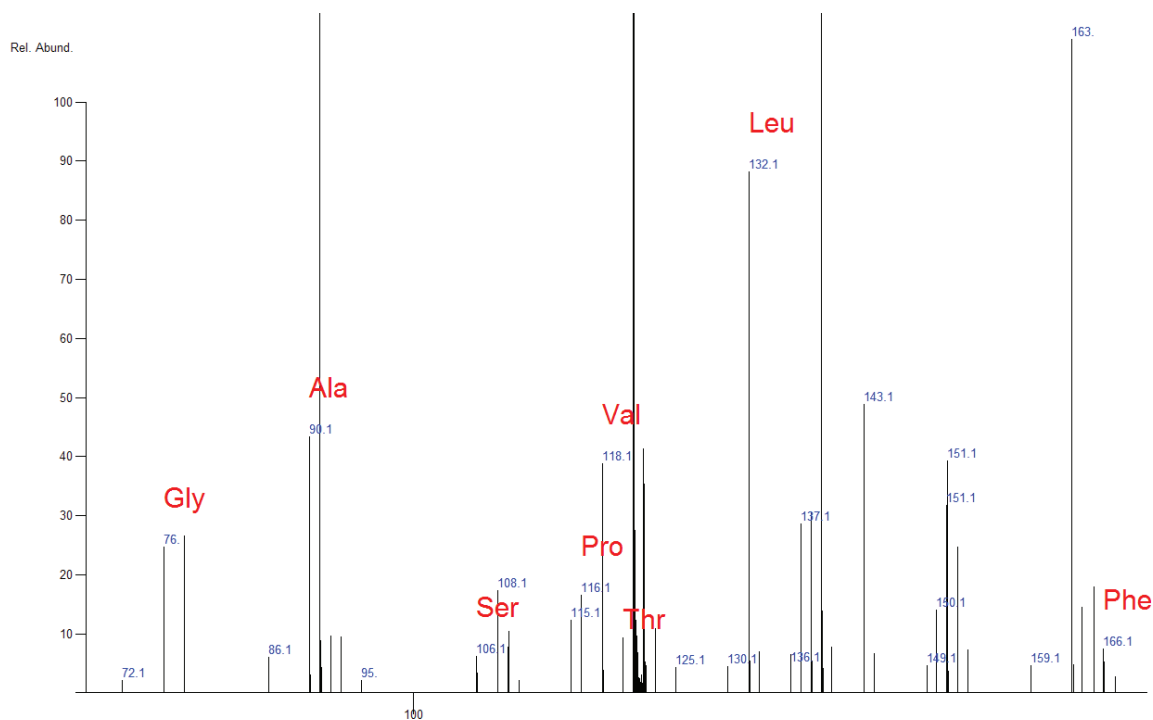


Figure 3. Amino acids A, F, G, I/L, S, P, T, and V detected with relative abundances between 0.5% and 18%

Conclusion

DART can identify compounds in fingerprints, often making it possible to determine what substances a subject has been handling.



Instantaneous Detection of Illicit Drugs on Currency

The widespread presence of illicit drugs on currency is an indication of the extent of the worldwide substance abuse problem. Remarkably, cocaine can be found on virtually all one-dollar bills in the United States — the upper limit for the general background level of cocaine is estimated to be 13 ng per bill¹.

The Direct Analysis in Real Time (DART™) ion source, combined with the AccuTOF™ mass spectrometer can be used to sample drugs on currency within seconds. No sample preparation (extraction, wipes, etc.) or chromatography is required. The bill is placed in front of the DART and the presence of drugs can be detected immediately. Only a small portion of the bill is sampled at any given time. This allows the analyst to view the distribution of drugs on the surface of a bill, and allows the bill to be retained for reexamination at a later time.

Over the past few years, we have used DART to examine paper currency from the United States and other countries. Cocaine was found at various levels on almost all US one-dollar bills. Cocaine was detected in significant amounts on a Venezuelan 50 Bolivares bill and in large amounts on a Spanish 2000 peseta bill. New currency and larger-denomination US bills were much less likely to show the presence of cocaine and other drugs.



Figure 1 shows the presence of cocaine on a US one-dollar bill. Cocaine is detected as

$C_{17}H_{22}NO_4^+$ ($[M+H]^+$) at m/z 304.15488. The assignment of this peak as cocaine was confirmed by raising the orifice potential to induce fragmentation (not shown). The cocaine fragment ion $C_{10}H_{16}NO_2^+$ is observed at m/z 182.1182. Mass measurements for both $C_{17}H_{22}NO_4^+$ and $C_{10}H_{16}NO_2^+$ were within one millimass unit.



Other drugs detected on dollar bills include methylphenidate (Ritalin, figure 2) and procaine. Procaine is a local anesthetic used by drug dealers as a cocaine adulterant.

Substances commonly detected on US bills include nicotine, diethyltoluamide (DEET bug repellent), sunscreen, dioctylphthalate (plasticizer), triethanolamine (from cosmetics) and glycerol and other polyols. Triethanolamine ($[M+H]^+$, m/z 150.1130) is easily distinguished from the illicit drug methamphetamine ($[M+H]^+$, m/z 150.1283) by its exact mass.

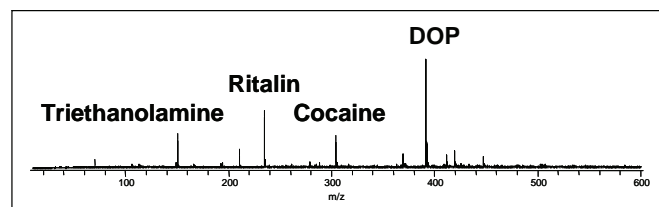
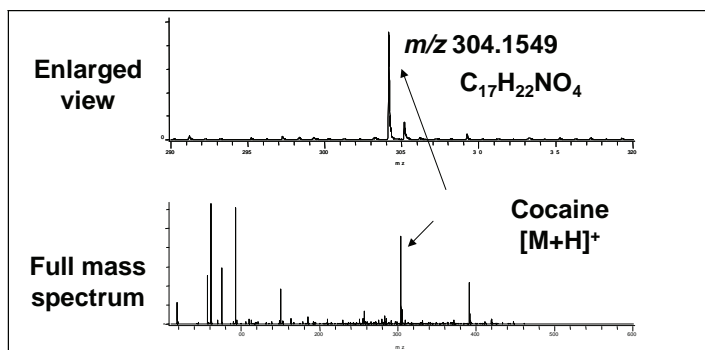


Figure 2. Ritalin and cocaine on a US \$1 bill. All compounds shown were detected as the $[M+H]^+$ and composition assignments were verified by exact mass measurements.

Figure 1. Cocaine on a US \$1 bill.

¹ Paradis, D. RCMP Gas. 1997, 59, 20-22

Instantaneous Detection of the "Date-Rape" Drug -- GHB

Gamma hydroxybutyrate (GHB) is a fast-acting central nervous system depressant¹. Prior to its ban by the FDA in 1990, GHB was sold in bodybuilding formulas. It has been abused as a euphoriant. Because it is colorless and odorless, it can be added to alcoholic drinks of unsuspecting victims. An overdose can result in serious consequences, including respiratory depression and coma. GHB was classified as a Schedule I Controlled Substance in March, 2000.

Detection of GHB is problematic. GC/MS and LC/MS methods are time consuming. A rapid colorimetric assay for GHB has been developed², but this assay suffers from some limitations. For example, ethanol produces the same colorimetric response as GHB.

The AccuTOF[™] mass spectrometer equipped with Direct Analysis in Real Time (DART[™]) can rapidly detect GHB anion ($C_4H_7O_3^-$, m/z 103.0395) on surfaces, in urine, and in ethanol. No solvent extraction, wipes, or chromatography are required. Examples are shown in the figures below.

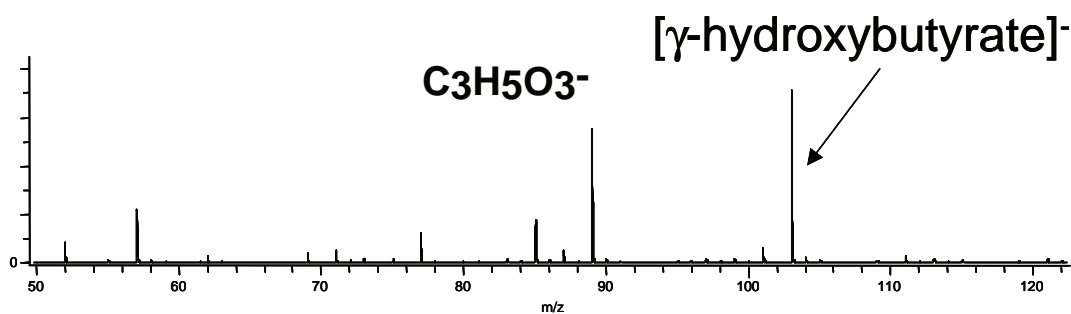


Figure 1. 10 ppm GHB (sodium salt) added to "Bombay Blue Sapphire" Gin.

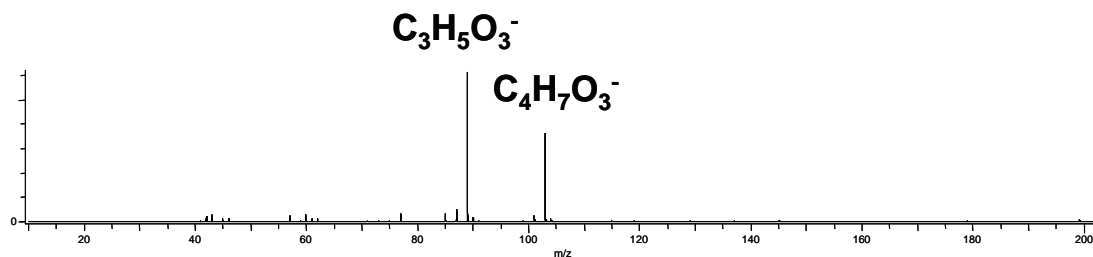


Figure 2. 100 ng of GHB (sodium salt) deposited on the rim of a glass.

¹<http://www.whitehousedrugpolicy.gov/publications/factsht/gamma/>

² Alston WC 2nd, Ng K. Forensic Sci Int. 2002 Apr 18;126(2):114-7. Rapid colorimetric screening test for gamma-hydroxybutyric acid (liquid X) in human urine.

“Laundry Detective”: Identification of a Stain

The AccuTOF-DART™ was recently applied to an unusual analytical problem: finding the cause of oily stains on freshly laundered shirts (Figure 1). No cutting or extraction was required. Stained and unstained regions of the shirt were placed in the DART gas stream and the mass spectra were acquired.

The DART parameters were: helium gas, flow 3-4 LPM, gas heater set to 175 degrees C, positive-ion mode, PEG 600 exact mass reference standard. These conditions did not damage the shirt.

The mass spectrum of the stained region (Figure 2, top) showed a distinctive pattern of saturated fatty acids and their proton-bound dimers, monoglycerides, and triethanolamine. The same components were found in the dryer sheet (Figure 2, bottom). Elemental composition assignments were confirmed by exact mass measurements and computer-aided isotope pattern matching. The assignment of the fatty acids was confirmed by the presence of $[M-H]^-$ peaks in the negative-ion DART spectrum (not shown). Fatty acid esters will not produce $[M-H]^-$ peaks in negative-ion mode. After considering several possible sources of contamination, a matching pattern was found for the bargain-price fabric softener sheet that was placed in the clothes dryer with the shirts. The components causing the stains were released when the dryer sheet was exposed to high temperatures.

Conclusion

AccuTOF-DART was able to determine the nature and cause of oily stains on a shirt without causing any damage to the fabric. Solutions to the problem include lowering the dryer temperature, changing to a different brand of fabric softener, and re-washing the shirts.

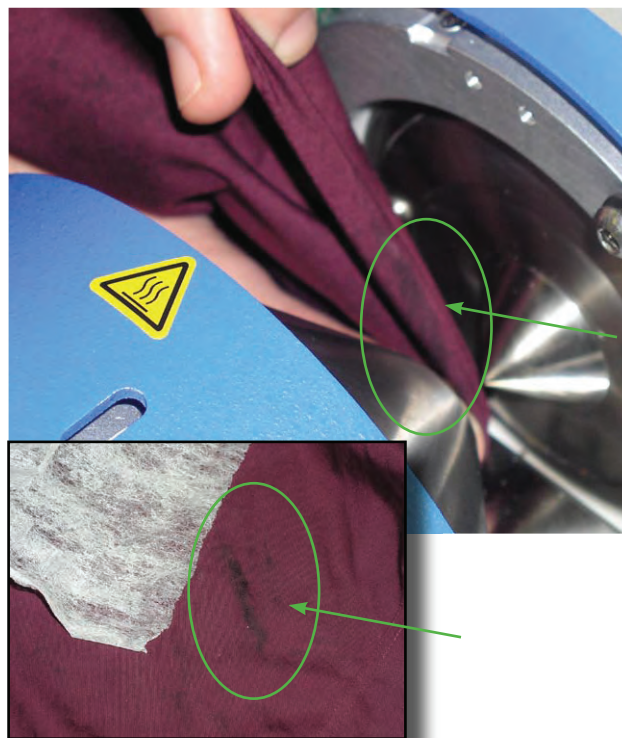


Figure 1. Oily stain on a freshly laundered shirt placed in between DART ion source and AccuTOF mass spectrometer inlet. Inset: stain on shirt circled next to used dryer sheet.

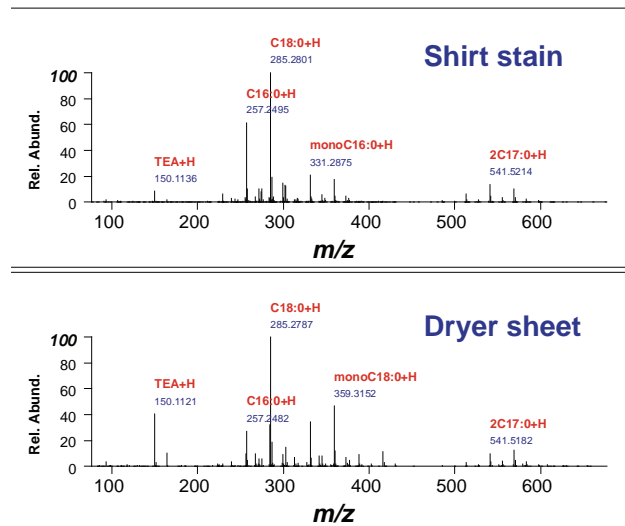


Figure 2. (Top) AccuTOF-DART mass spectrum of stain on shirt. (Bottom) AccuTOF-DART mass spectrum of fabric softener sheet placed in the dryer with the shirts.

This page intentionally left blank for layout purpose.

Analysis of Biological Fluids

The AccuTOF-DART can detect a variety of substances in biological fluids such as urine, blood, and saliva with little or no sample preparation. These substances include drugs, amino acids, lipids, and metabolites.

Urine samples were analyzed by dipping a melting point tube in urine and placing the sample in front of the DART ion source. Figure 1 shows positive-ion DART mass spectra of a urine sample from a subject

taking ranitidine to reduce stomach acid production. The enlarged view in the inset shows the ranitidine metabolites desmethyl ranitidine and ranitidine N-oxide.

Figure 2 shows a negative-ion DART mass spectrum of urine from the same subject. Compounds detected that fall within 0.002 u within the theoretical masses for compounds in a target list include nucleotide bases, caffeine metabolites, uric acid and related compounds, and organic acids.

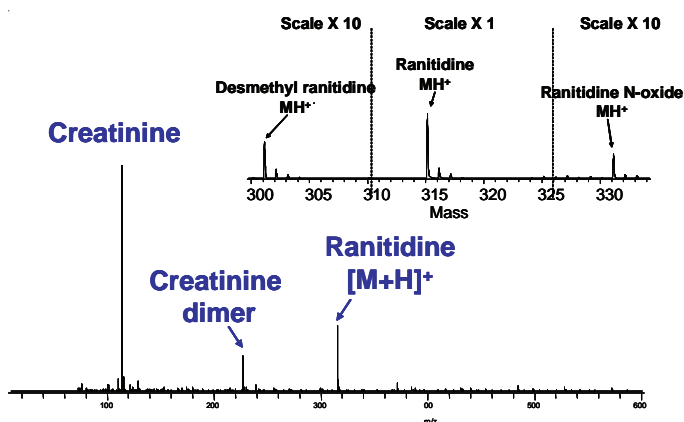


Figure 1. Ranitidine metabolites in human urine.

Name	Meas.	Calc.	Diff(u)	Rel. Abund.
GBL	85.0295	85.0290	0.0006	11.0317
Pyruvic_acid	87.0084	87.0082	0.0002	7.1700
Lactic_acid	89.0236	89.0239	-0.0002	8.3658
Cresol	107.0492	107.0497	-0.0004	0.9294
Creatinine	112.0513	112.0511	0.0002	81.6851
Purine	119.0354	119.0358	-0.0004	31.9510
Dihydro_methyluracil	127.0486	127.0508	-0.0021	23.3773
pGlu	128.0353	128.0348	0.0006	59.2337
Methylmaleic_acid	129.0212	129.0188	0.0024	37.1191
Me_succinate/diMe_malonate	131.0368	131.0358	0.0010	19.3593
Deoxyribose	133.0489	133.0501	-0.0012	28.3521
Hypoxanthine	135.0306	135.0307	-0.0001	100.0000
Methyl_hypoxanthine	149.0454	149.0463	-0.0009	37.5243
Hydroxymethyl_methyl_uracil	155.0453	155.0457	-0.0003	55.5832
Methylxanthine	165.0408	165.0412	-0.0004	32.4341
Hippuric_acid	178.0513	178.0504	0.0009	66.4487
Glucose	179.0552	179.0556	-0.0004	39.7499
Dimethylxanthine	179.0552	179.0569	-0.0017	39.7499
Dimethyluric_acid	195.0527	195.0518	0.0009	23.7577
AAMU (caffeine met.)	197.0667	197.0675	-0.0007	79.6617
Cinnamalidinemalonic_acid	217.0483	217.0501	-0.0017	60.5399
AFMU (caffeine met.)	225.0643	225.0624	0.0019	21.9092
Cytidine	242.0801	242.0777	0.0024	3.4545
Uridine	243.0641	243.0617	0.0024	21.1156
Phenylacetyl_glutamine	263.1033	263.1032	0.0001	48.9665
Ranitidine	313.1321	313.1334	-0.0013	8.7459
Ranitidine+Cl	349.1113	349.1101	0.0011	11.7296

Table I. Compounds identified by exact mass.

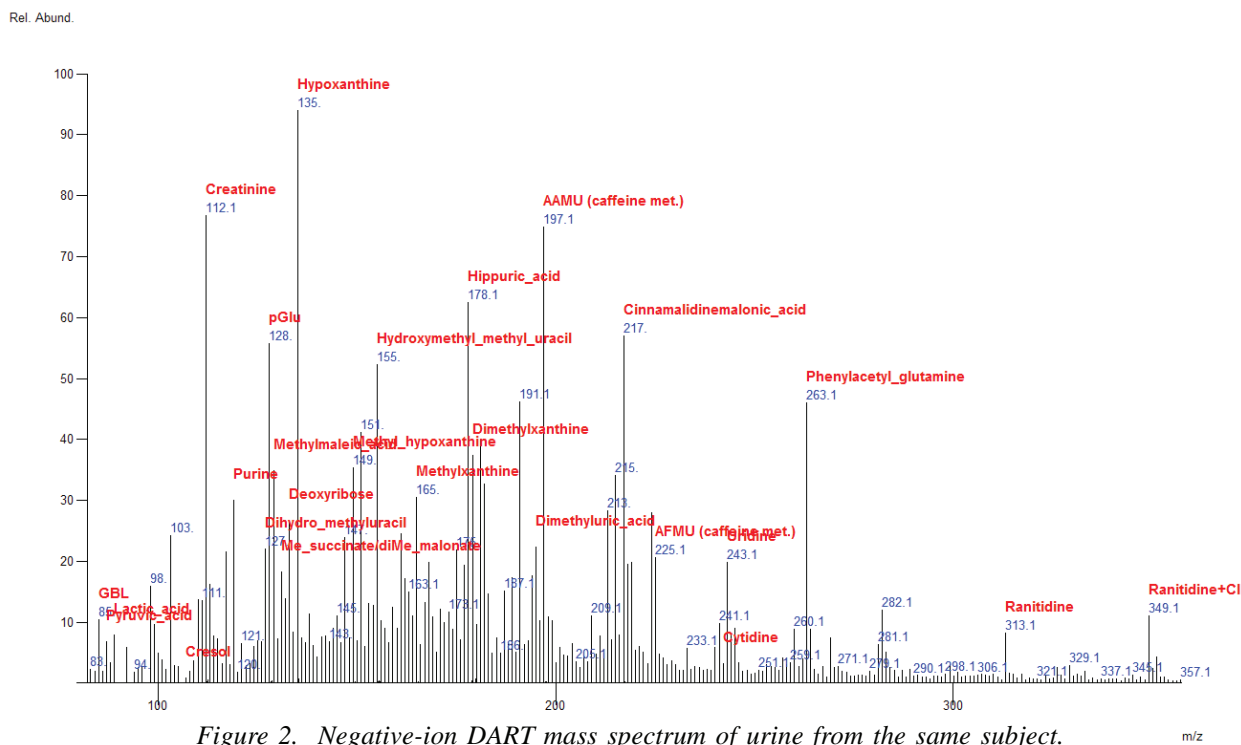


Figure 2. Negative-ion DART mass spectrum of urine from the same subject.

Quantitative analysis is possible. DART response is proportional to sample quantity. However, the absolute response is dependent on the position of the sample in the DART gas stream and on position of the sample relative to the mass spectrometer sampling orifice.

Addition of an internal standard can compensate for variations in ion abundance due to differences in placement of the sample tube in the DART ion source. Figure 3 shows the working curve obtained for urine samples that have been spiked with gamma hydroxy butyrate (GHB) at concentrations ranging from 0 ppm to 800 ppm. Samples were spiked with 50 ppm of a deuterated internal standard (d6-GHB). A melting point tube was dipped into the urine samples and then placed in front of the DART source. Results were obtained within seconds. Five replicates were measured for each concentration over a period of five days. Excellent linearity was observed.

Although some compounds can be detected in whole blood, whole blood is not well suited for analysis with no sample preparation. Minimal sample preparation can reveal compounds that are not readily detected in whole blood. Figure 4 shows amino acids detected in whole blood. Centrifuging the blood sample to remove blood cells makes it possible to detect triglycerides (Figure 5). The addition of acetonitrile to remove blood proteins makes it possible to detect other compounds, such as ranitidine (Figure 6).

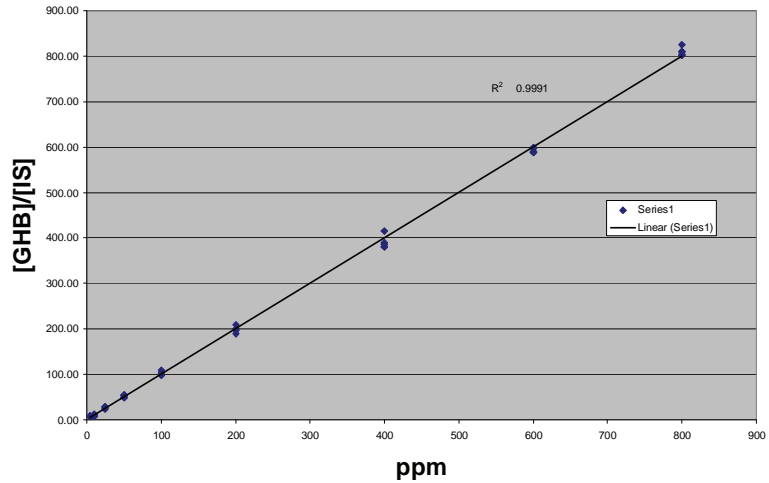


Figure 3. GHB in urine.

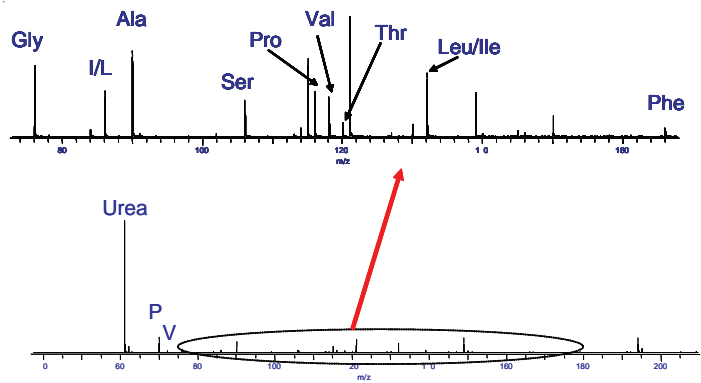


Figure 4. Amino acids in whole human blood.

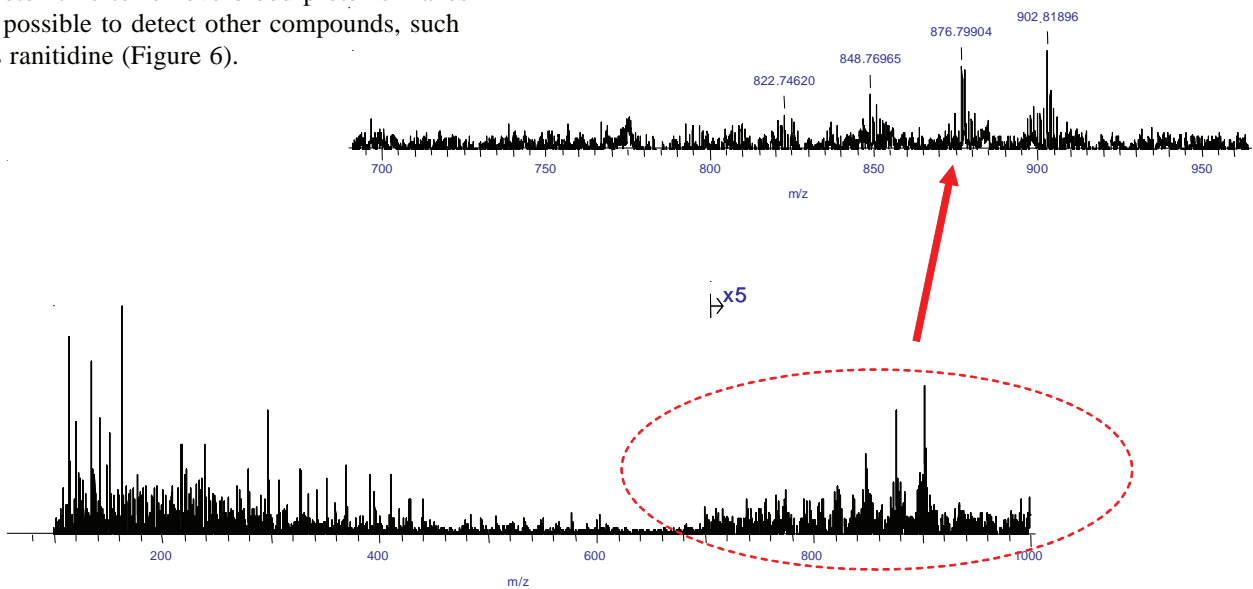


Figure 5. Triglycerides in human blood plasma.

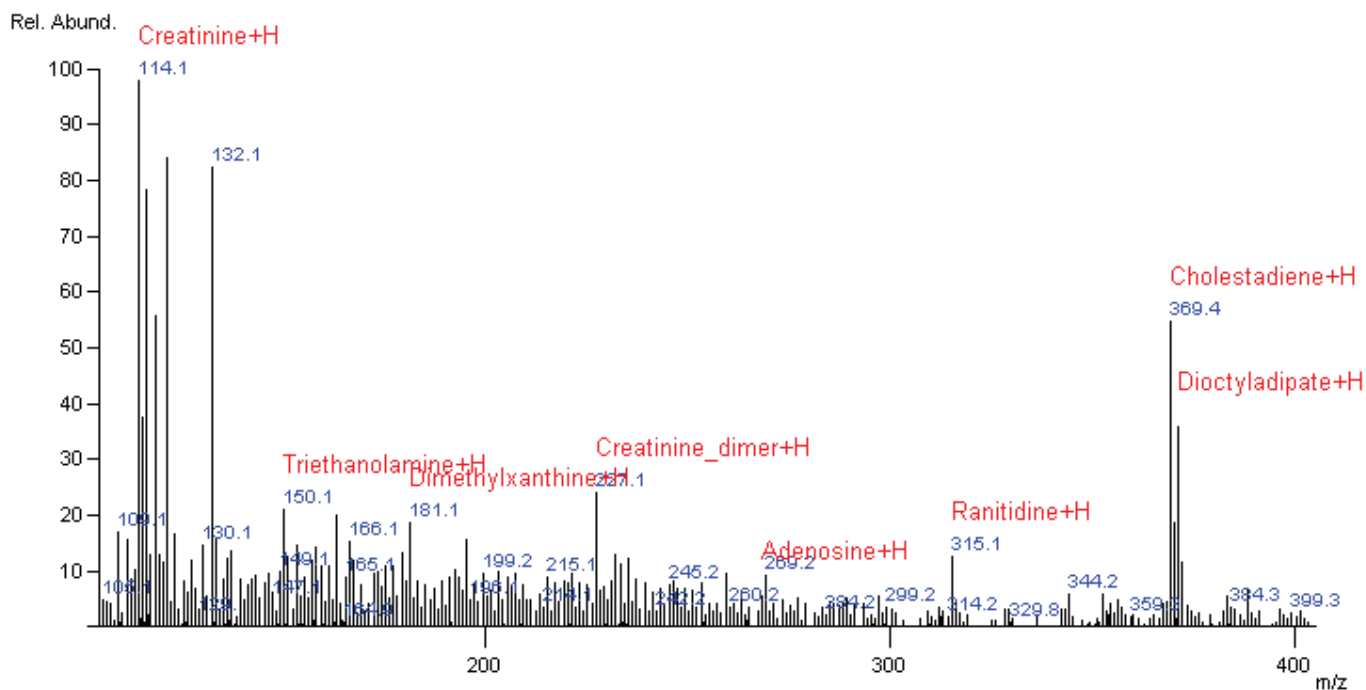


Figure 6. Compounds detected in human plasma after addition of acetonitrile. Amino acids A, P, V, L/I are detected, but not labeled in this figure. Note the presence of caffeine metabolites (dimethylxanthines). Triethanolamine is present in many consumer products and dioctyl adipate is a common plasticizer that may have been extracted from the plastic vial.

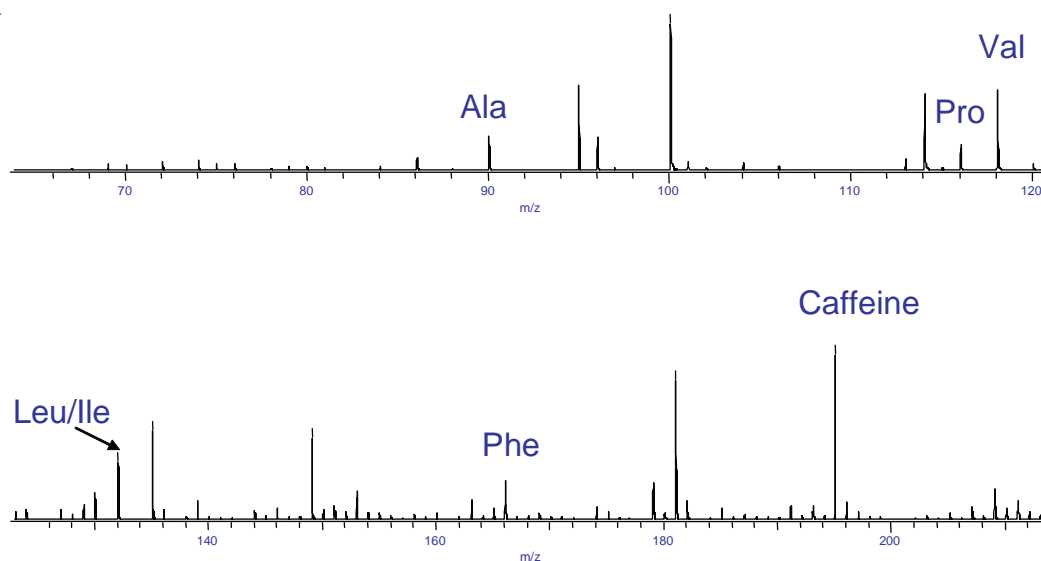


Figure 7. Amino acids and caffeine in saliva.

Analysis of other body fluids has been investigated briefly. Figure 7 shows the detection of amino acids and caffeine in a saliva sample from a coffee drinker.

Detection limits for many compounds with no sample preparation or preconcentration are in the high ppb to low ppm range.

Conclusion

DART can be used to analyze biological fluids. Only a few drops of fluid are required for the analysis.

This page intentionally left blank for layout purpose.



AccuTOF-DART™

Clandestine Methamphetamine Labs: Rapid Impurity Profiling by AccuTOF-DART™

Introduction

Methamphetamine is a Schedule II Controlled Substance that is illegally manufactured in clandestine labs. There are several common synthetic pathways in use. For this study, methamphetamine was synthesized from phenyl-2-propanone by the (1) Leuckart synthesis or (2) Reductive Amination, or from ephedrine or pseudoephedrine by the (3) Nagai, (4) Birch, and (5) Edme syntheses. Each of these reaction sequences resulted in unique impurity profiles¹⁻³ that can be used by law enforcement to track the activities of clan labs, distribution networks, and trafficking patterns. The AccuTOF-DART was used to examine the starting materials, reaction mixtures, and final products from each reaction scheme.

Experimental

A JEOL AccuTOF-DART mass spectrometer was used for all measurements. Samples were deposited on the sealed end of melting point tubes and measured in positive-ion mode with helium DART gas and a gas heater setting of 350°C. Polyethylene glycol (average MW 600) was used as a reference standard for exact mass measurements.

Results

Examples are given of the DART mass spectra measured for methamphetamine synthesized by the Birch (Figure 2) and Nagai (Figure 3) synthetic methods.

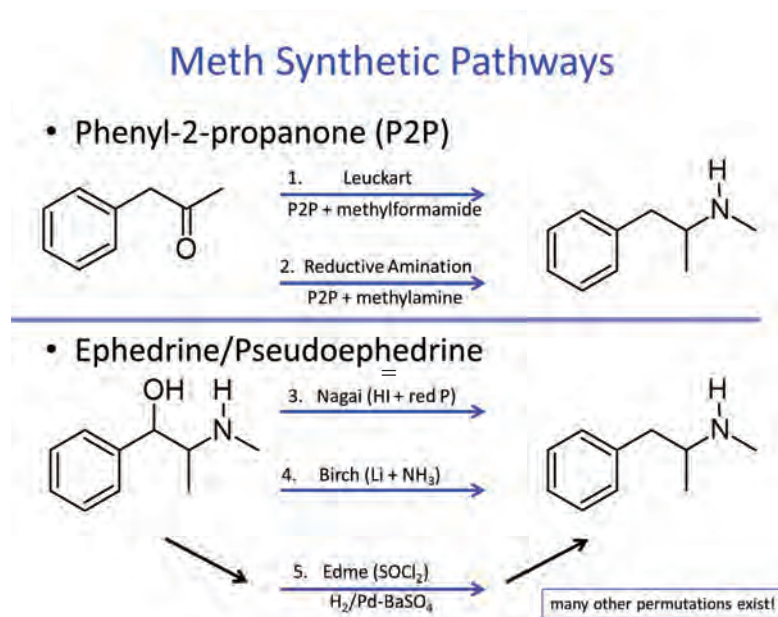


Figure 1. Common synthetic pathways for the illicit manufacture of methamphetamine.

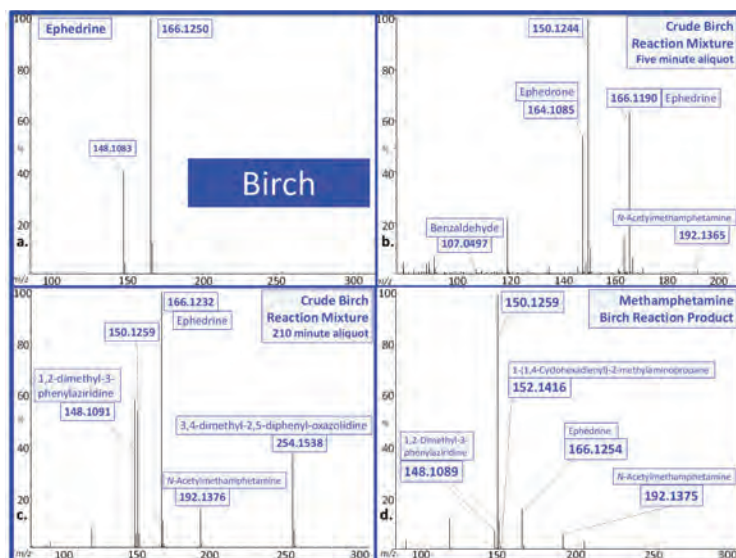


Figure 2. AccuTOF-DART mass spectra for ephedrine, crude reaction mixture at two different reaction times, and the final reaction product of a Birch synthesis.

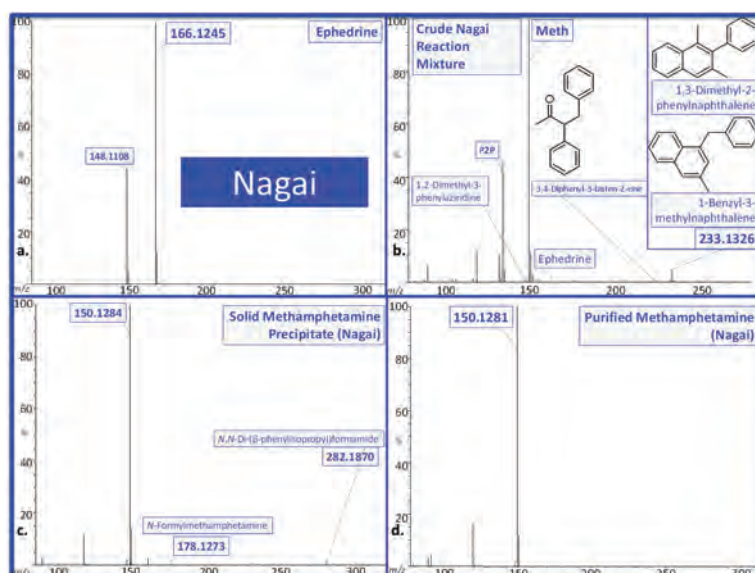


Figure 3. AccuTOF-DART mass spectra for the ephedrine starting material, reaction mixture, methamphetamine precipitate, and purified methamphetamine from a Nagai synthesis.

Conclusion

The AccuTOF-DART can provide rapid impurity profiling that can be used by law enforcement to characterize the starting products, reaction mixtures, and semi-purified final products for methamphetamine manufactured in clandestine laboratories. The results support and complement the alternative GC/MS methods.

Acknowledgement

These data were provided by Prof. Jason Shepard. A more complete discussion of these results for all five reaction methods will be found in a forthcoming publication (reference 4).

References

1. Andersson, K.; Lock, E.; Jalava, K.; Huizer, H.; Jonsson, S.; Kaa, E.; Lopes, A.; Poortman-van der Meer, A.; Sippola, E.; Dujourdy, L.; Dahlén, J., Development of a harmonised method for the profiling of amphetamines VI. *Forensic Science International* 2005 169 (1), 86-99.
2. Dujourdy, L.; Dufey, V.; Besacier, F.; Miano, N.; Marquis, R.; Lock, E.; Aalberg, L.; Dieckmann, S.; Zrcek, F.; Bozenko, J. S., Jr., Drug intelligence based on organic impurities in illicit MA samples. *Forensic Science International* 2008 177 (2), 153-161.
3. Kunalan, V.; Nic Daéid, N.; Kerr, W. J.; Buchanan, H. A. S.; McPherson, A. R., Characterization of Route Specific Impurities Found in Methamphetamine Synthesized by the Leuckart and Reductive Amination Methods. *Analytical Chemistry* 2009, 81 (17), 7342-7348.
4. Shepard, J., manuscript in preparation. 2014.

X-Ray Fluorescence Helps Identify Peaks in DART Mass Spectrum of Electrical Tape - ElementEye JSX-1000S and AccuTOF-DART



LC and Ambient Ionization HRTOF Mass Spectrometer JMS T100LP AccuTOF-DART™

Introduction

The identification of electrical tapes is important for forensic investigation of improvised explosive devices [1]. Pyrolysis mass spectrometry [2] and X-Ray Fluorescence (XRF) [3] are among the methods that are used for the forensic analysis of electrical tapes.

Direct Analysis in Real Time (DART) can be operated with a high gas temperature as an alternative to conventional pyrolysis GC/MS methods [4,5]. A sample of electrical tape analyzed with the AccuTOF-DART™ showed distinctive peaks in the negative-ion DART mass spectrum. No reasonable elemental compositions could be determined by assuming the presence of only the common organic elements: C, H, N, O, P, S, Cl, Si, and Br. X-ray fluorescence (XRF) data obtained with the ElementEye™ indicated the presence of Zn and Sb, allowing us to correctly assign the elemental compositions for the peaks observed in the DART mass spectrum.



X-ray Fluorescence Spectrometer JSX-1000S ElementEye

Experimental

A piece of electrical tape was placed in the DART gas stream with the DART gas heater set to 500°C (pyrolytic DART conditions). A sample of poly(perfluoropropyl ether) was measured in the same data file as a mass reference standard for exact mass measurements. Elemental compositions with isotope matching were determined by using Mass Mountaineer™ software. The XRF spectrum of the sample was measured with the Element Eye by using the Quick and Easy Organic Analysis method and the ElementEye reporting program. The collimator was set to 2 mm and the total analysis time was 60 seconds.

Results and Discussion

The negative-ion DART mass spectrum in Figure 1 shows distinctive peaks with isotope patterns that suggest the presence of multiple halogens (chlorine and/or bromine). This is not unexpected considering that electrical tape can be made of polyvinyl chloride (PVC). However, no reasonable elemental composition assignments could be made by assuming only elements present in common organic polymers. To assign the elemental compositions, we needed additional information about which other elements might be present.

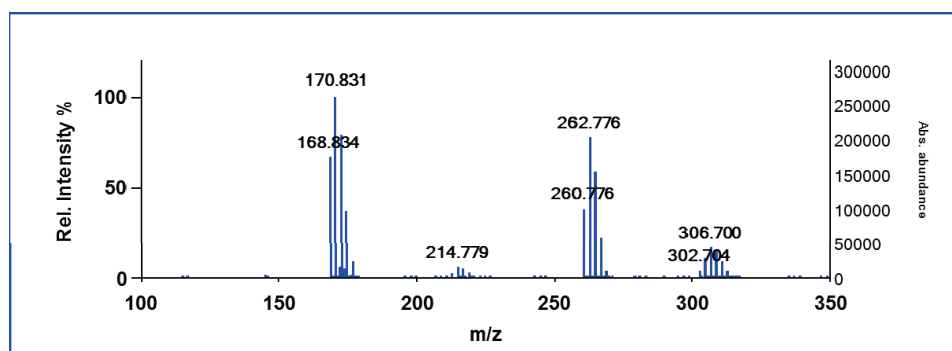


Fig. 1 Negative-ion AccuTOF-DART mass spectrum of a piece of electrical tape.

Among the elements detected in the XRF spectrum (Figure 2, Table 1) are antimony, zinc, chlorine and bromine. Adding these elements to the constraints for the elemental composition calculation for the AccuTOF-DART data allows us to correctly assign the elemental compositions for these peaks (Figure 3). The measured isotope peaks show excellent agreement with the calculated isotope patterns (Figure 4).

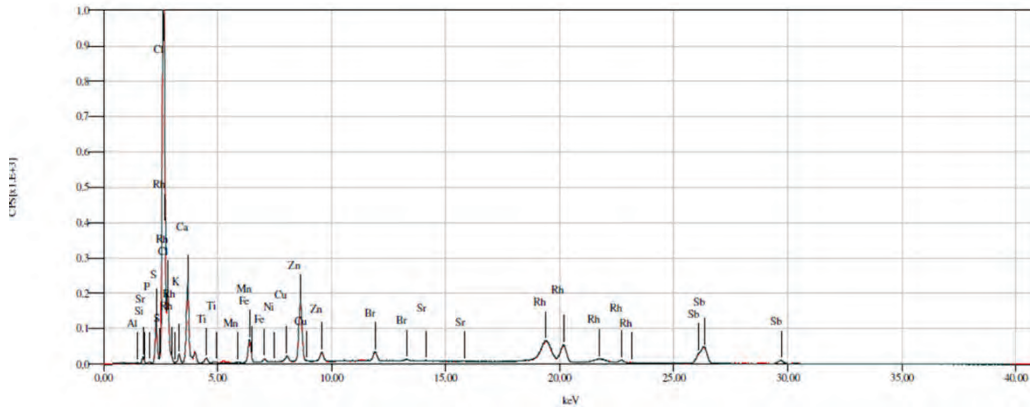


Fig. 2. XRF Spectrum of the electrical tape obtained with ElementEye

Analysis Target	Result	Unit	3sigma
Aluminium(Aluminu	1.01	%	0.30
Iron	0.18	%	0.00
Manganese	0.00	%	0.00
Nickel	0.00	%	0.00
Potassium(Kalium)	0.43	%	0.01
Silicon	1.38	%	0.05
Strontium	0.00	%	0.00
Titanium	0.10	%	0.00
Antimony(Stibium)	1.87	%	0.02
Copper	0.03	%	0.00
Zinc	0.27	%	0.00
Calcium	2.58	%	0.02
Sulfur	1.13	%	0.01
Phosphorus	0.09	%	0.01
Bromine	0.03	%	0.00
Chlorine	19.21	%	0.06

Table 1. Elements detected by the ElementEye

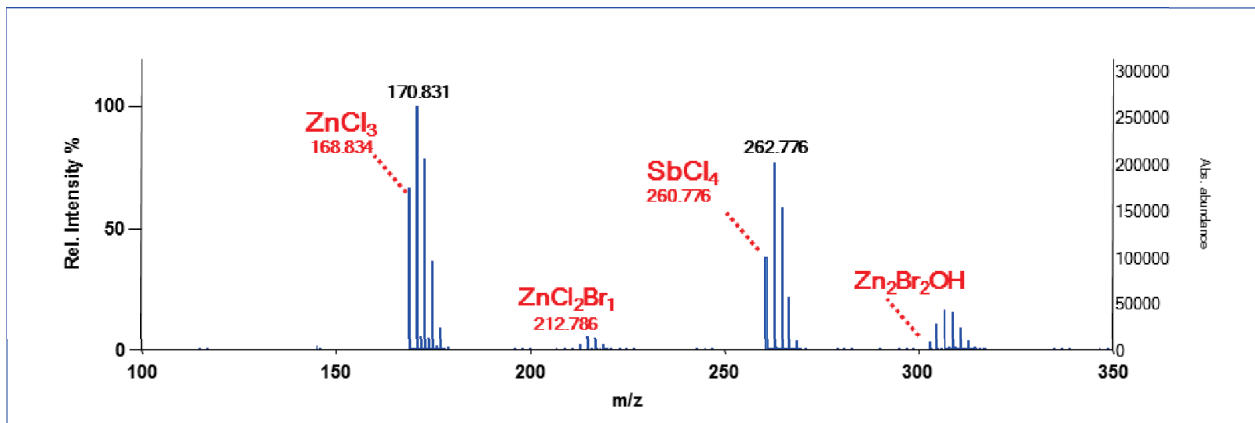


Fig. 3. Elemental composition assignments for the peaks in the mass spectrum from Figure 1 calculated after determining the presence of Zn, Sb, Cl, and Br from the XRF data.

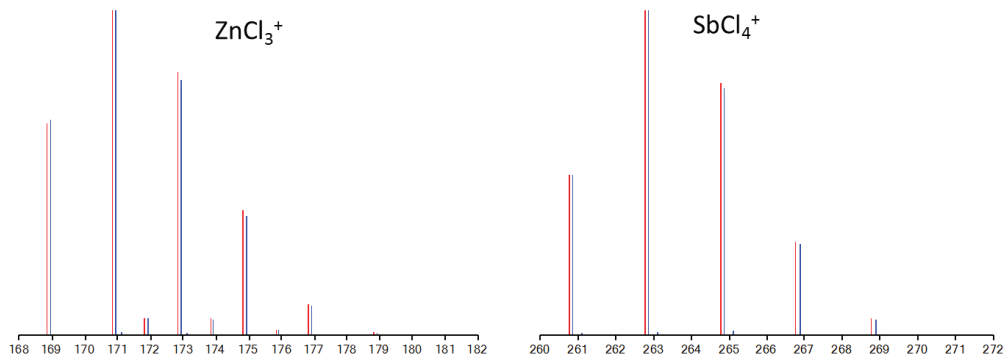


Figure 4. Comparison of calculated (red) and measured (blue) isotope peaks for $ZnCl_3^+$ and $SbCl_4^+$

Conclusion

Elemental composition assignments based on accurate mass and isotope measurements by mass spectrometry require the operator to provide a list of elements that may be present and their limits. If an element is omitted from the list, the correct assignment will not be reported. If too many elements are added to the list, the number of possible compositions becomes uninterpretable. The ElementEye is a rapid and convenient tool that provides complementary elemental information allowing us to assign the unknown peaks in the AccuTOF-DART data for the electrical tape sample.

References

1. Scientific Working Group for Materials Analysis (SWGMA) Daubert Admissibility Package for Tape Evidence. <http://www.swgmat.org/Tape%20Admissibility%20Package.pdf>
2. (SWGMA), S. W. G. f. M. A. Standard Guide for Using Pyrolysis-Gas Chromatography and Pyrolysis-Gas Chromatography/Mass Spectrometry in Forensic Tape Examinations <http://www.swgmat.org/SWG%20tape%20PGC%20guideline.pdf>
3. Keto, R. O., Forensic Examination of Black Polyvinyl Chloride Electrical Tape. <http://swgmat.org/Keto-Characterization%20of%20PVC%20Tapes.pdf>.
4. Loftin, K. B., Development of Novel DART™ TOFMS Analytical Techniques for the Identification of Organic Contamination on Spaceflight-Related Substrates and Aqueous Media. Ph.D. Thesis, University of Central Florida, 2009
5. Lancaster, C.; Espinoza, E., Analysis of select Dalbergia and trade timber using direct analysis in real time and time-of-flight mass spectrometry for CITES enforcement. *Rapid Communications in Mass Spectrometry* **2012**, *26* (9), 1147-1156.

Detection of the Peroxide Explosives TATP and HMTD

Introduction

The explosive peroxide compounds triacetone triperoxide (TATP) and hexamethylenetriperoxide diamine (HMTD) are difficult to detect by conventional mass spectrometry methods. These compounds can be easily detected by the Direct Analysis in Real Time (DART™) ion source.

Experimental

Measurements were made with the AccuTOF-DART mass spectrometer operated in positive-ion mode under standard conditions. Little or no heat was required to observe these compounds. Dilute solutions of standard samples of TATP and HMTD were analyzed by dipping melting point tubes into the liquid and dangling the melting point tubes in the DART ion source. Dilute aqueous ammonium hydroxide on a cotton swab was held in the DART gas stream to enhance detection of TATP as the ammoniated molecule.

Results

TATP is readily detected as $[M+NH_4]^+$ at m/z 240.1447 (Figure 1). A trace fragment at m/z 91.0399 is assigned as the $C_3H_7O_3^+$ fragment. Exact mass measurements allow the assignment of the peak at m/z 223.0968 as $C_{12}H_{15}O_4^+$, which is assigned as monobutyl phthalate $[M+H]^+$. Exact mass measurements avoid a mistaken assignment of this peak as protonated TATP (m/z 223.1182), which is not observed.

HMTD is observed as the protonated molecule at m/z 209.0776. This is major species observed. A few small characteristic fragment ions may also be observed in the HMTD mass spectrum.

Conclusion

Peroxide explosives TATP and HMTD were easily detected by the AccuTOF-DART with no sample preparation. Both compounds were detected at trace levels on a variety of surfaces including fingertips, boarding passes, and cloth. Exact mass measurements confirmed the compositions and avoided mistaken assignment of a contaminant as a target analyte peak.

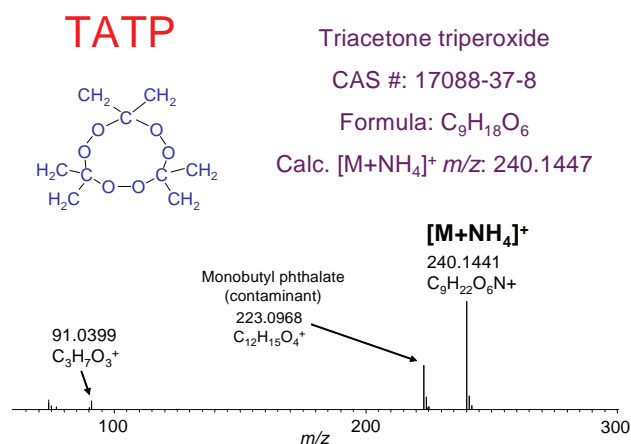


Figure 1. AccuTOF-DART mass spectrum of TATP

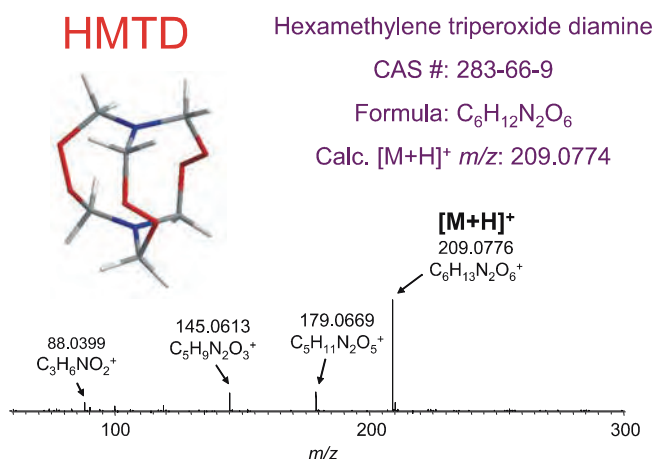


Figure 2. AccuTOF-DART mass spectrum of HMTD

Instantaneous Detection of Explosives on Clothing

The detection of explosives is of vital importance in forensic applications and in preventing criminal or terrorist activity. The analytical detection of explosives on surfaces is normally done by using solvent extractions or wipes and chromatography or chromatography combined with mass spectrometry. This is inefficient because solvent extractions and wipes only result in a partial transfer of material from the surface into the sampling material. Furthermore, the chromatographic analysis can be time-consuming and requires the use of disposable solvents (an environmental concern).

The JEOL AccuTOF™ with Direct Analysis in Real Time (DART™) has demonstrated the capability to detect both volatile and involatile explosives on surfaces such

as plastic, cloth, concrete, glass, cardboard, metal, and more. No wipes or solvent extractions are required. The method is instantaneous, environmentally friendly, and does not require solvents. An example is shown in this application note.

A construction company has been recently conducting blasting to remove boulders near our offices. One of our employees happened to walk through the edge of the plume from the blasting when he arrived for work in the morning. At the end of the day, more than eight hours later, we tested him for exposure to explosives. By placing the employee's necktie in front of the DART we could easily detect nitroglycerin, as shown in Figure 1 (below). It was not necessary to take the tie off to perform the analysis.

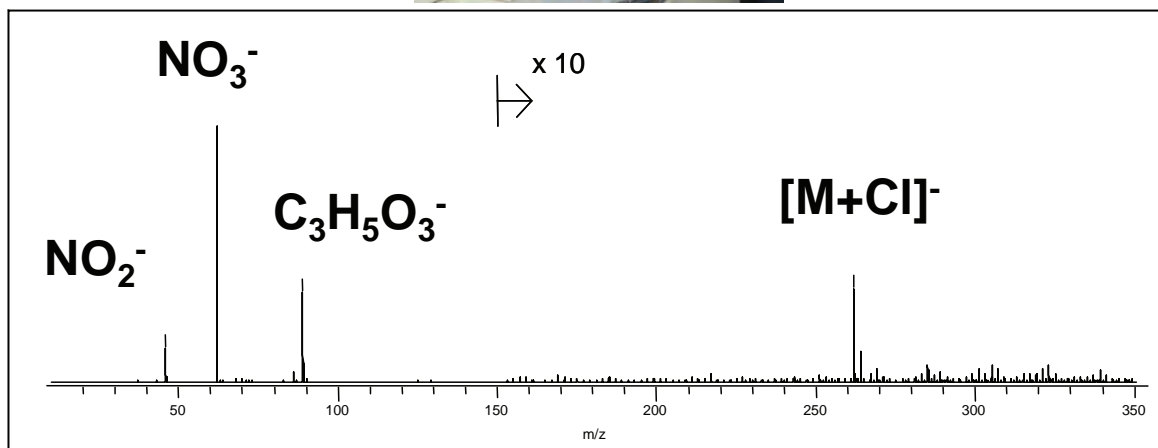
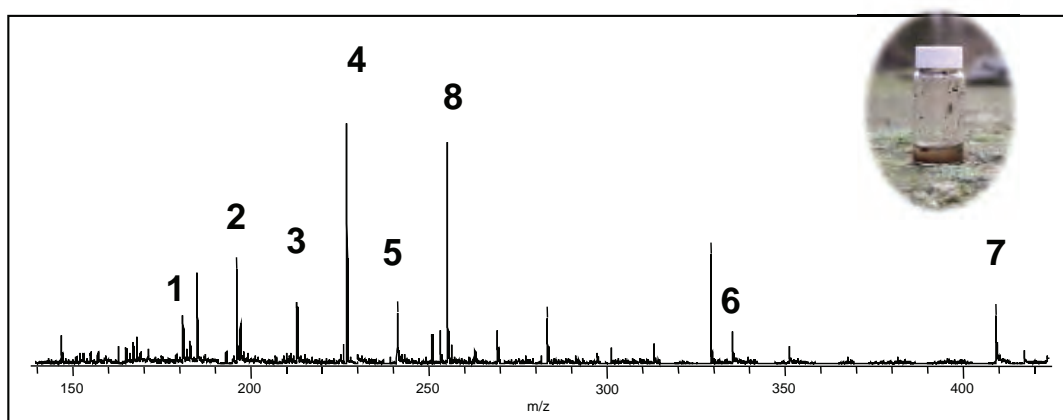


Figure 1. Nitroglycerin detected on an employee's tie after exposure to a plume from blasting. Methylene chloride vapor was placed beneath the DART to enhance the formation of $[\text{M}+\text{Cl}]^-$. All elemental compositions were easily confirmed by exact mass measurements.

Detection of Explosives in Muddy Water

The AccuTOF time-of-flight mass spectrometer equipped with Direct Analysis in Real Time (DART™) has been used to detect a wide variety of explosives in or on a variety of materials ranging from solutions to samples deposited on surfaces ranging from ABS plastic to metal, clothing and cardboard. Detection is rapid, specific, and sensitive. To demonstrate DART's ability to detect explosives in a "messy" sample, we took a sample of muddy water from a frog pond in the woods near our laboratory. The water was spiked with 3 ppm

of an explosives mixture, mixed and allowed to stand. A glass rod was dipped into the spiked water solution and then placed between the DART and the first orifice of the AccuTOF atmospheric pressure interface. An aqueous solution of 0.1% trifluoroacetic acid was placed under the glass rod to permit the formation of trifluoroacetate adducts for HMS and RDX. The results are shown in the figure below. The total time for analysis was 20 to 30 seconds.



Explosives detected in muddy water.

1: dinitrotoluene (DNT) 2: amino-DNT, 3: trinitrobenzene, 4: trinitrotoluene (TNT)
5: tetryl 6: RDX (TFA adduct) 7: HMS (TFA adduct) 8: Palmitate (in pond water).

Some Explosives Analyzed by DART

- Sodium perchlorate
- Nitroglycerin (NG)
- Ethylene glycol dinitrate (EGDN)
- Dinitrotoluene (DNT)
- Amino-dinitrotoluene (DNT)
- Trinitrobenzene
- Hexamethylenetriperoxidediamine (HTMD)
- Triacetone triperoxide (TATP)
- Trimethylenetrinitramine (RDX)
- Tetramethylenetetra nitramine (HMX)
- Picrylmethylnitramine (Tetryl)
- Pentaerythritol tetranitrate (PETN)

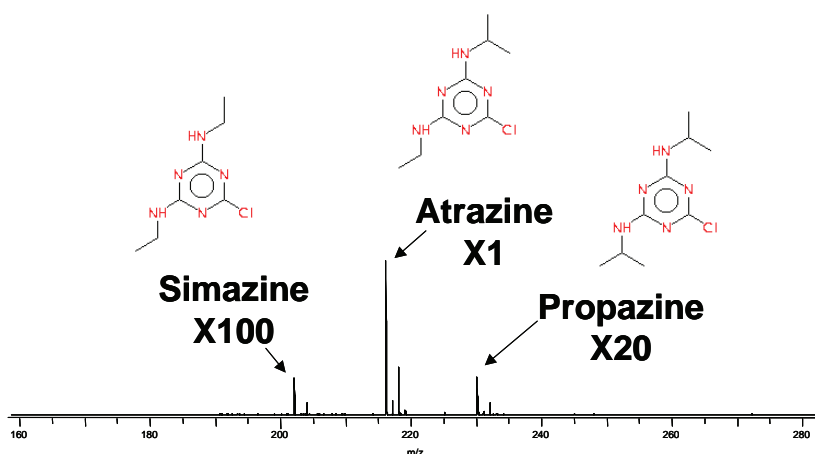
Rapid Detection and Exact Mass Measurements of Trace Components in an Herbicide

Analytical chemists are often asked to identify trace components in manufactured compounds such as drugs, consumer products, and agricultural chemicals. A common approach to the identification of minor components is to use gas or liquid chromatography coupled with high-resolution mass spectrometry. Although this approach is effective, it may be time-consuming and difficult to set up.

The AccuTOF with Direct Analysis in Real Time (DART™) provides a rapid solution. The high dynamic range of both source and detector permit the determination of minor components in the presence of a

major component. The AccuTOF always provides high-resolution data with exact mass measurements and accurate isotope ratios that can provide elemental composition assignments for unknown compounds.

In this example, a few dust particles from a sample of atrazine herbicide containing 1% propazine and 0.2% simazine were deposited on a glass rod and placed in front of the DART. The mass spectrum shown below was measured in seconds. All three components were detected with good signal-to-noise and excellent mass accuracy and isotopic abundances.



Exact Mass Measurements

Compound	[M+H] [±]	Measured	Calculated	Diff. (mmu)
Atrazine	C ₈ H ₁₅ N ₅ Cl	216.10159	216.10160	-0.01
Propazine	C ₉ H ₁₇ N ₅ Cl	230.11760	230.11725	+0.35
Simazine	C ₇ H ₁₃ N ₅ Cl	202.08440	202.08595	+1.60

Rapid Analysis of *p*-Phenylenediamine Antioxidants in Rubber

Introduction

p-Phenylenediamine (PPD) and derivative compounds are commonly used as antioxidants and antiozonants in black rubber. These compounds can cause sensitization leading to contact dermatitis in susceptible individuals. Detection of additives in polymers such as rubber can be important for clinical, forensic, and manufacturing applications. Here we show that DART can be used to identify the presence of these compounds within seconds without requiring

any solvents or sample preparation.

Experimental

Analysis was carried out by using the AccuTOF-DART. A piece of rubber from a mountain bike tire was placed in front of the DART ion source, which was operated with helium in positive-ion mode and a gas heater temperature of 250 degrees C. Signals appeared within seconds after placing the rubber in front of the DART source.

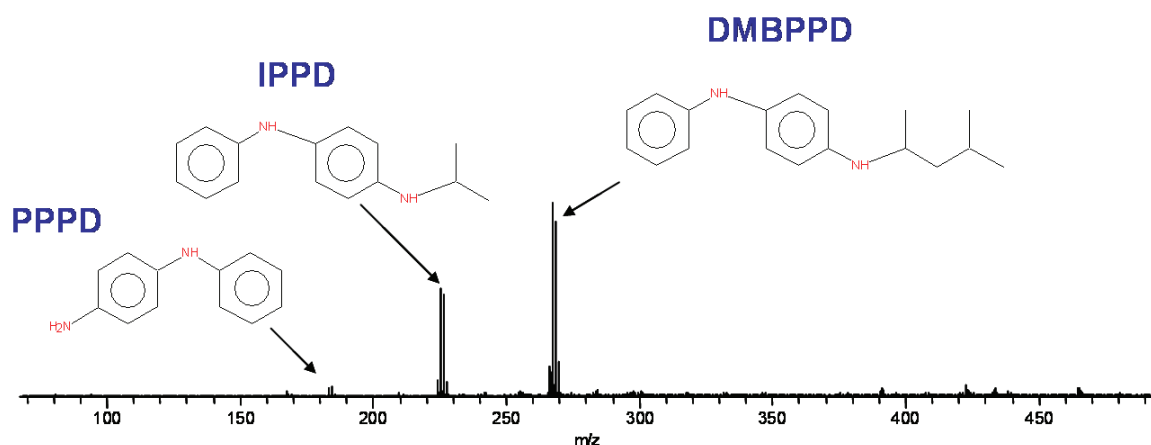


Figure 1. DART mass spectrum of a rubber particle from a mountain bike tire.

Meas. mass u	Abund. %	Diff. mmu	Unsat.	Compositions	
226.147202	0.00	0.20	8.0	C ₁₅ H ₁₈ N ₂	IPPD M ⁺
227.154297	0.00	-0.53	7.5	C ₁₅ H ₁₉ N ₂	IPPD [M+H] ⁺
268.194214	0.00	0.27	8.0	C ₁₈ H ₂₄ N ₂	DMBPPD M ⁺
269.201385	0.00	-0.40	7.5	C ₁₈ H ₂₅ N ₂	DMBPPD [M+H] ⁺

Table 1. Elemental compositions for *p*-phenylenediamine antiozonants in a rubber tire.

Results

Exact mass measurements combined with accurate isotopic abundances provided elemental compositions (Table I) that were searched against the NIST mass spectral database. Three antiozonant compounds were recognized from their exact mass measurements

(see Table 1): N-Phenyl-*p*-phenylenediamine (PPD), N-Isopropyl-N'-phenyl-*p*-phenylenediamine (IPPD), and N-(1,3-Dimethyl butyl)-N'-phenyl-*p*-phenylene diamine (DMBPPD).

Direct Analysis of Adhesives

DART can be used with a heated gas stream to rapidly pyrolyze and identify low-volatility materials such as adhesives and resins, directly on surfaces. Although these materials are not pure compounds, a library of DART mass spectra can be created and searched to identify materials, and exact mass measurements coupled with accurate isotopic abundances can be used to identify unknown components. Examples are shown here for cured and uncured epoxies and acrylate adhesives on metal and glass.

All samples were analyzed by acquiring positive-ion mass spectra with the DART source operated with helium

and a gas heater setting of 450° C (helium temperature ~350° C). All mass spectra were measured over the m/z range 60-1000 at a resolving power of 6000. Following each analysis, a glass rod coated with PEG 600 was placed in front of the DART source to provide a calibration for exact mass measurements. A nominal-mass library of adhesive mass spectra was created by using the software link to the NIST version 2.0 mass spectra database search program. All figures shown here are copied from that library and only integer masses are shown although exact masses were recorded for all peaks.

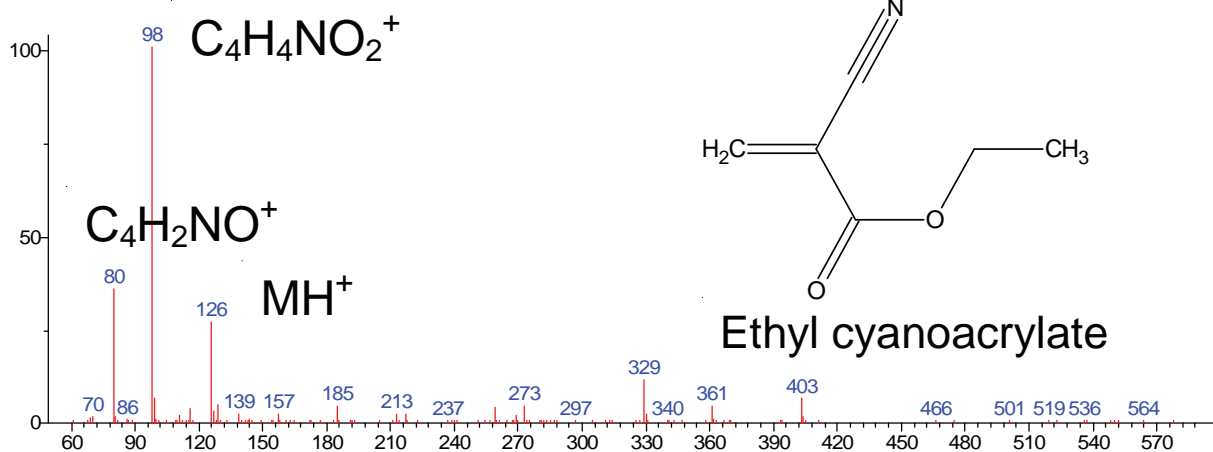


Figure 1. Cyanoacrylate adhesive on metal (Product 1)

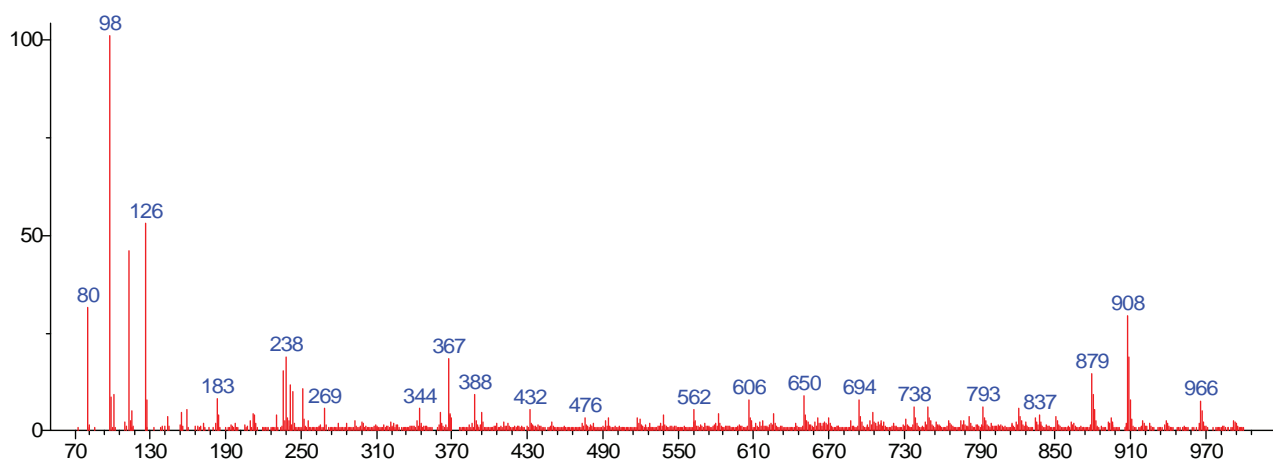


Figure 2. Cyanoacrylate adhesive on metal (Product 2)

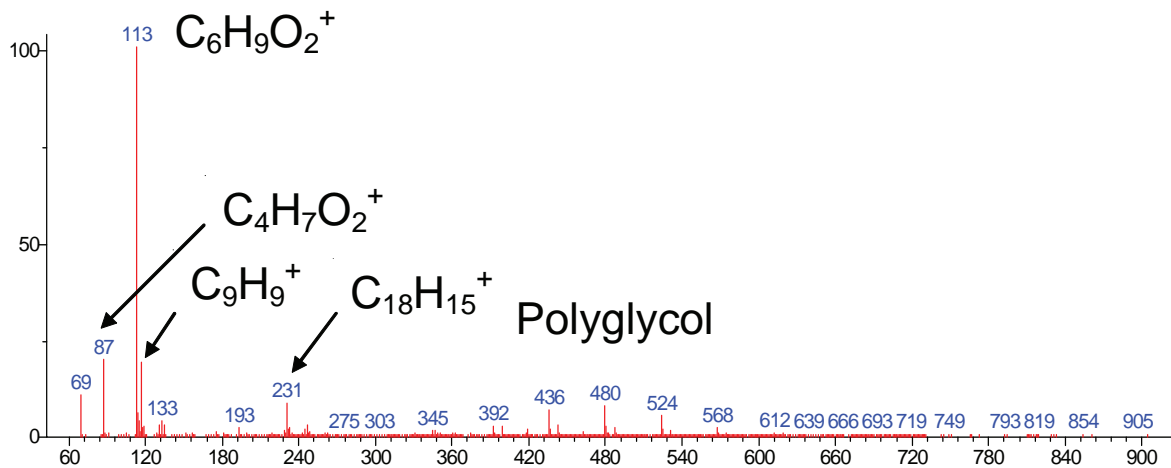


Figure 3. Methacrylate ester adhesive on glass (Product 3)

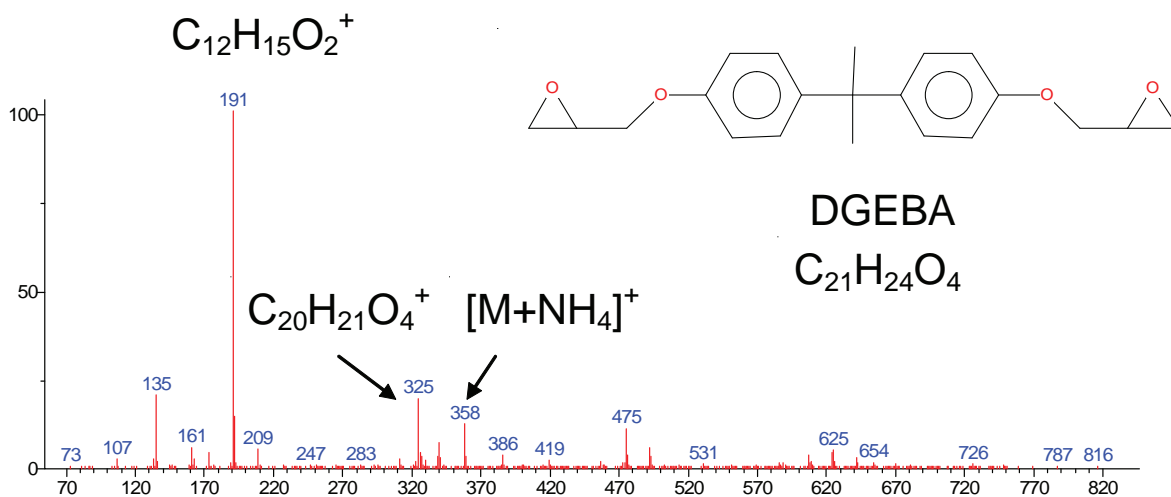


Figure 4. Epoxy resin (black component, uncured)

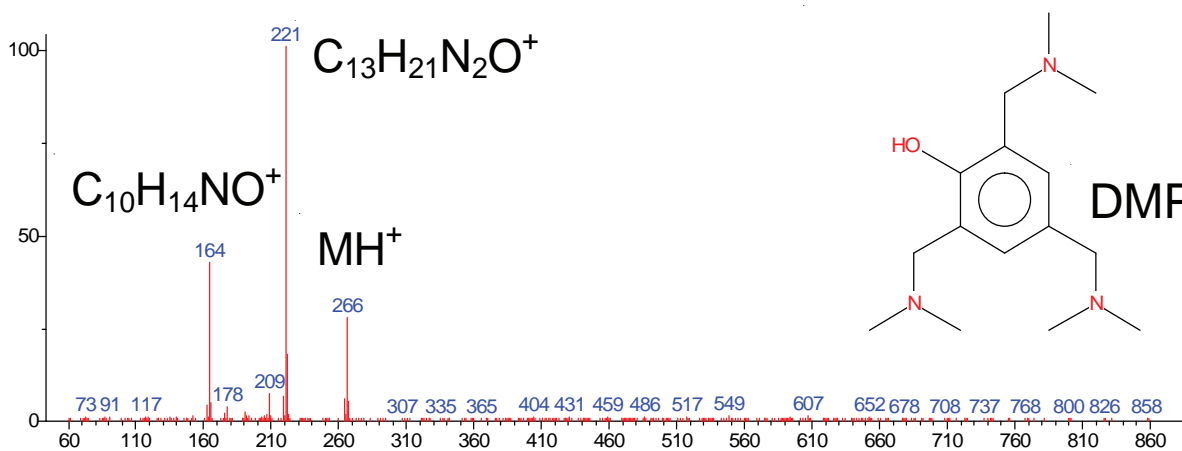


Figure 5. Epoxy hardener (white component)

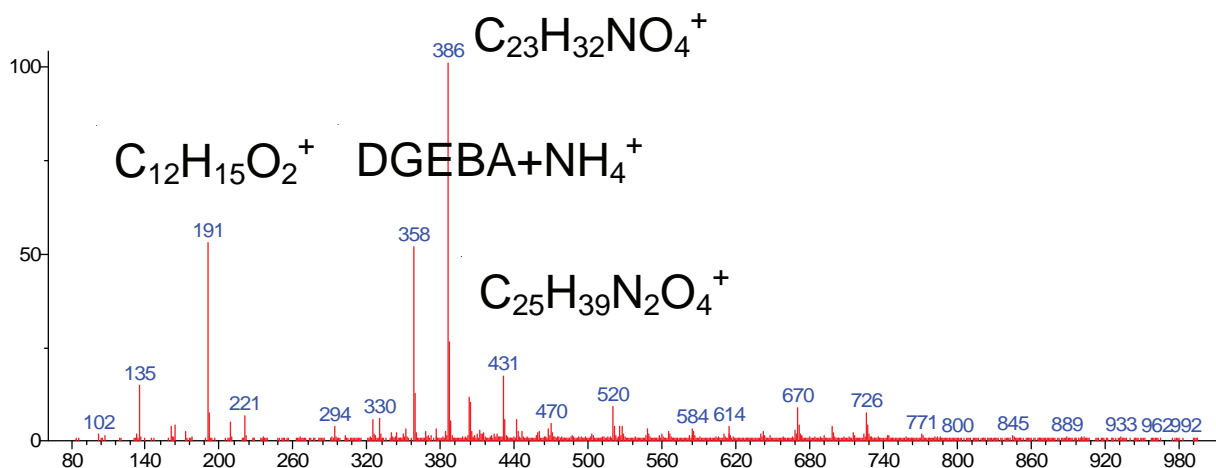


Figure 6. Cured epoxy

Both cyanoacrylate products show ethyl cyanoacrylate (m/z 126.0555) and fragment ions $C_4H_2NO^+$ (m/z 80.0136) and $C_4H_4NO_2^+$ (m/z 98.0242). Product 2 shows an additional peak at measured m/z 113.0602. This differs by only -0.05 u from the calculated m/z for $C_6H_9O_2$, tentatively assigned as $[M+H]^+$ for allyl methacrylate. Product 2 also shows a series of high-mass peaks that differ by 44.0262, indicative of ethylene oxide based polymer subunits. A product described as a “methacrylate ester” (Figure 3) was dominated by the same $C_6H_9O_2^+$ peak (assigned as allyl methacrylate), with methacrylic acid observed as $C_4H_7O_2^+$ at m/z 87.0447 ($+0.1$ mmu error).

Several binary epoxy formulations (separate resin and hardener) were examined. Figures 4 and 5 show the spectrum of two separate uncured components of a fast-curing epoxy and Figure 6 shows the cured epoxy.

The major compound in the uncured epoxy resin (black component) is identified by exact mass as the diglycidyl ether of bisphenol A or DGEBA. This has the composition $C_{21}H_{24}O_4$ with $[M+NH_4]^+$ observed at m/z 358.2018. Fragments are seen at m/z 191.1072

($C_{12}H_{15}O_2^+$) and m/z 325.143982 ($C_{20}H_{21}O_4^+$). The major component in the hardener is identified as tris (2,4,6-dimethylaminomethyl) phenol (“DMP”), a widely used epoxy accelerator, with abundant fragments at nominal m/z 164.1075 ($C_{10}H_{14}NO^+$) and 221.165388 ($C_{13}H_{21}N_2O^+$). Peaks corresponding to DGEBA and the accelerator are evident in the cured epoxy resin.

A variety of other glues, cements, and adhesives were examined. Each showed a characteristic pattern, permitting the identification of the material. Residual solvent, residual monomer, unreacted and partially reacted components were detected together with pyrolysis fragments.

Conclusion

DART can be applied to the direct identification of adhesives and resins on surfaces. Exact mass measurements coupled with accurate isotopic abundances aid in the assignment of components in the adhesive formulations.

This page intentionally left blank for layout purpose.

Identification of Polymers

DART can be used to analyze polymers, cements, resins, and glues by increasing the gas temperature to 450-550° C to induce pyrolysis. This has been applied to a variety of polymers including Nylons, polypropylene and polyethylene, polyethylene terephthalate (PET), polyesters, poly(methyl methacrylate) (PMMA), polycarbonate, phenoxy resin, polystyrene, and cellulose. Examples are shown here for standard samples of Nylon, polystyrene, and cellulose.

The DART source was operated with helium in positive-ion mode. The gas heater was set to 475° C. Resins were cured in an oven for several hours before analysis; some resin samples had been cured for longer periods of time (months or years). Exact masses and accurate isotopic abundances were used to assign elemental compositions for peaks in the mass spectra. Nominal-mass spectra were exported into a library database in NIST format to facilitate identification of unknowns.

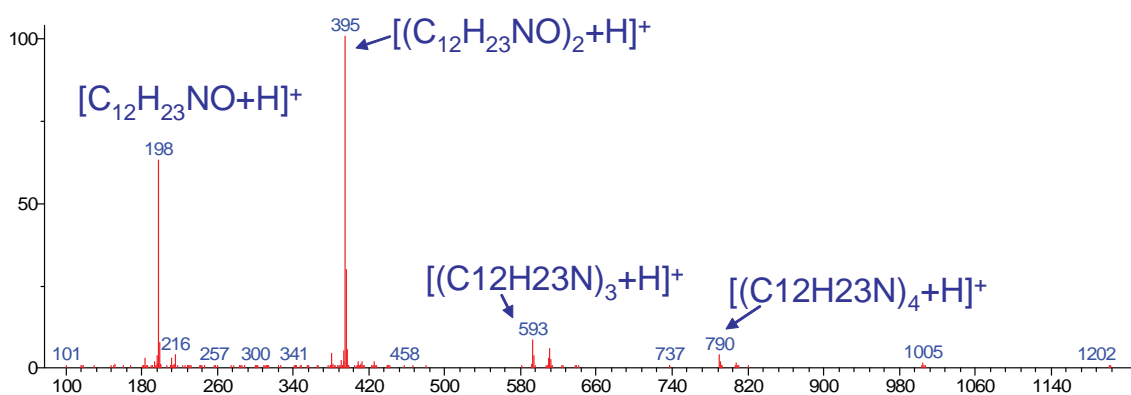


Figure 1. Nylon 12: Poly(lauryl lactam).

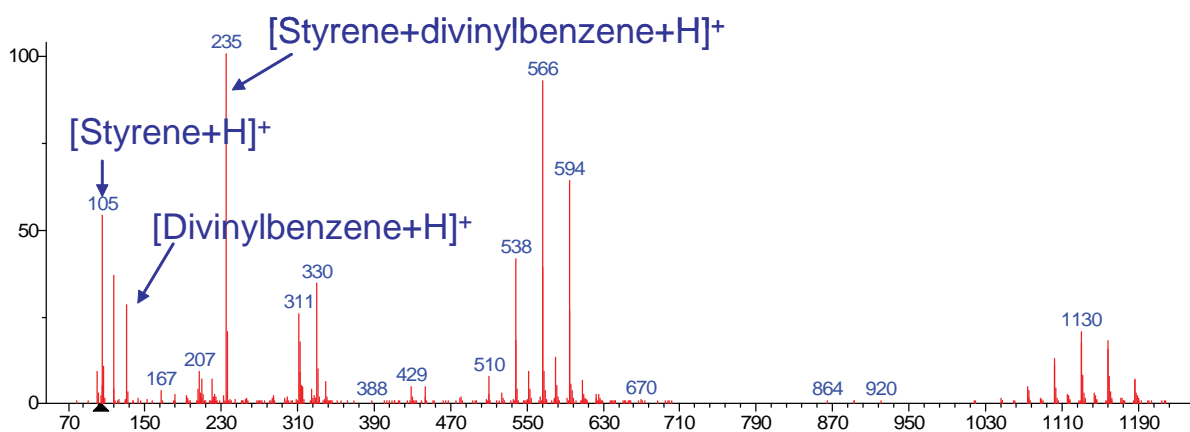


Figure 2. Polystyrene bead, average molecular weight ~ 240,000

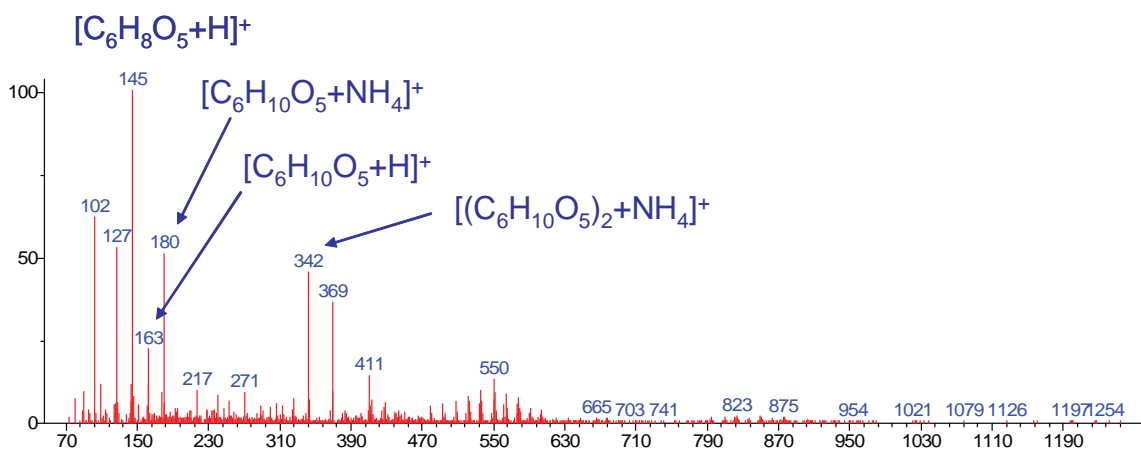


Figure 3. Cotton fibers showing peaks characteristic of cellulose $(C_6H_{10}O_5)_n$. Dilute ammonium hydroxide vapor enhanced $[M+NH_4]^+$ formation.

It should be noted that mass spectra of commercial polymers may be dominated by plasticizers and other additives which can complicate the analysis. Nevertheless, it was possible to identify polyethylene in a milk bottle, poly(ethylene terephthalate) in a soda bottle, and polystyrene in a CD case and a mass spectrometer filament box.

Conclusion

Polymers can be analyzed by DART. Fingerprint mass spectra are produced, and common formulation components can often be identified and confirmed by exact mass measurements.

Rapid Analysis of Glues, Cements, and Resins

DART™ can be used to analyze polymers, cements, resins, and glues by increasing the gas temperature to 450-550° C to induce pyrolysis. This has been applied to a variety of glues and resins, including epoxies, polyimide resins, PVD cement, and cyanoacrylates. Examples are shown here for cured and uncured epoxy resin and cyanoacrylate glues.

The DART was operated with helium in positive-ion mode. The gas heater was set to 475° C. Resins were cured in an oven for several hours before analysis; some resin samples had been cured for longer periods of time (months or years). Exact masses and accurate isotopic abundances were used to assign elemental compositions for peaks in the mass spectra. Nominal-mass spectra were exported into a library database in NIST format to facilitate identification of unknowns.

The black component (Figure 1) of a common binary quick-curing epoxy is found to be bisphenol A diglycidyl ether

ether (DGEPA) and the white component (Figure 2) is the hardener DMP 30. The cured epoxy (Figure 3) shows some peaks common to both of these components, but new peaks are also observed from the polymerized resin.

Two different cyanoacrylate glues were examined. Both showed ethyl cyanoacrylate $[M+H]^+$ (m/z 126) and its fragments $C_4H_2NO^+$ (m/z 80) and $C_4H_4NO_2^+$. Product 1 also contained allyl methacrylate and a polymer component with ethylene oxide (EO) subunits. Product 2 contained the common plasticizers tributyl citrate and tributyl acetylacrylate.

Conclusion

Glues, cements, and resins can be analyzed by DART. Fingerprint mass spectra are produced, and common formulation components can be identified and confirmed by exact mass measurements.

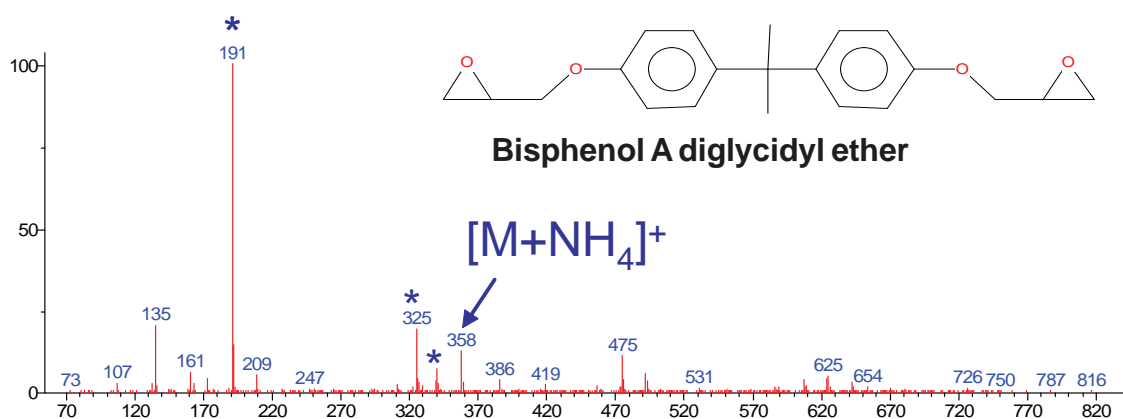


Figure 1. Uncured epoxy resin (black component)

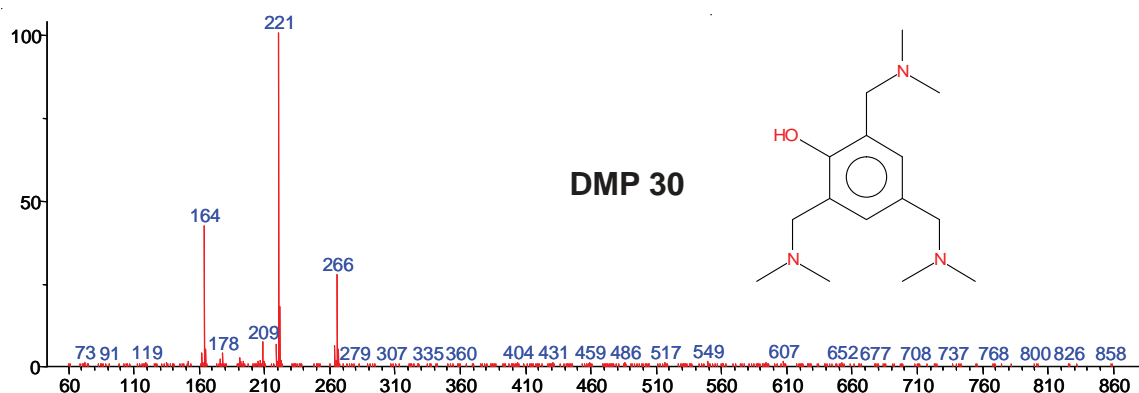


Figure 2. Uncured epoxy resin (white component)

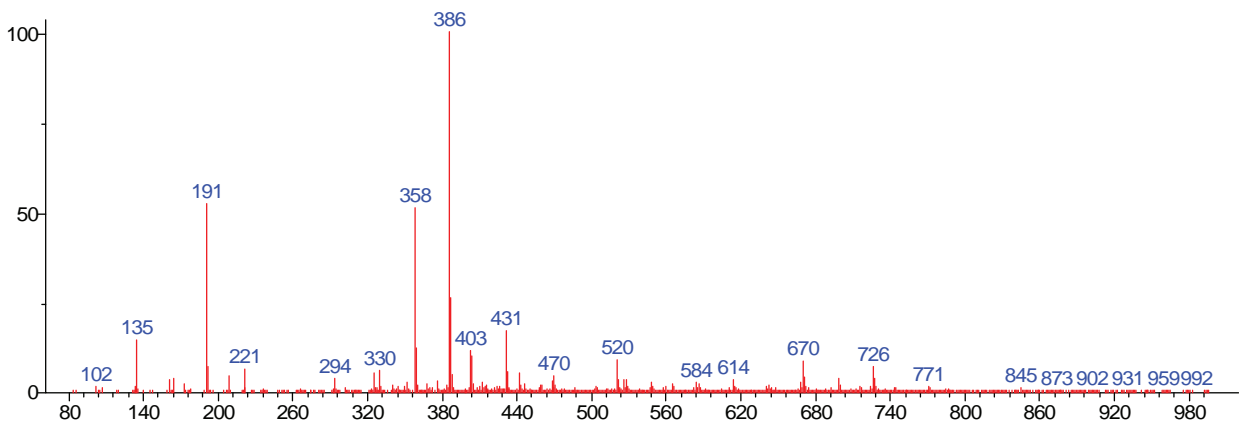


Figure 3. Cured epoxy resin on metal surface

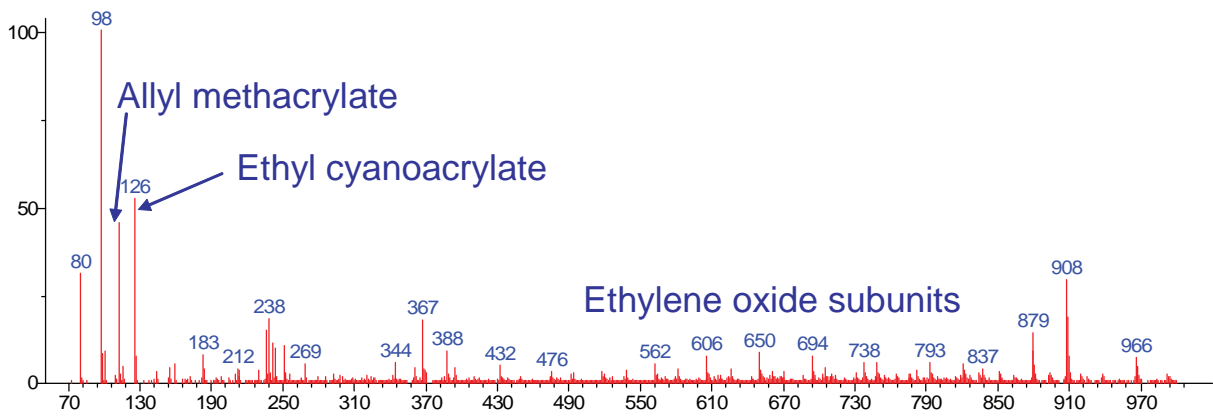


Figure 4. Cured cyanoacrylate glue product 1

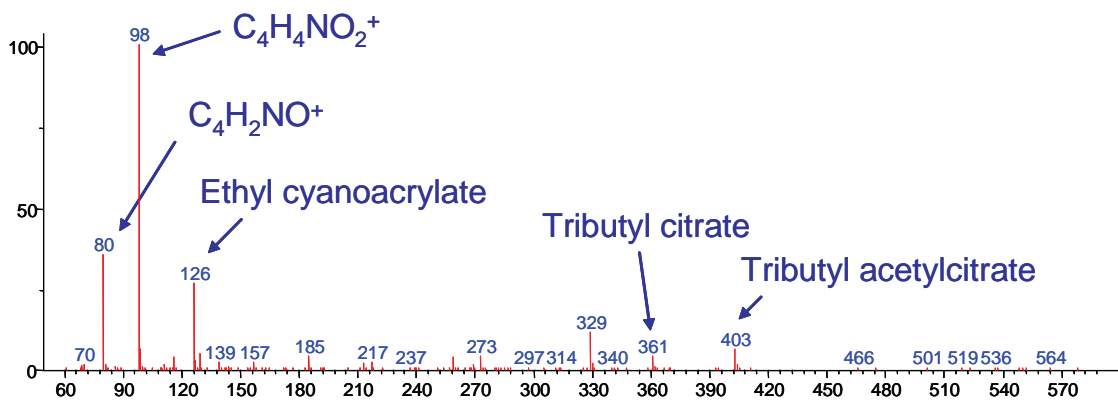


Figure 5. Cured cyanoacrylate glue product 2

~ Application Note for DART ~

Analysis of Organic Contaminant on Metal Surface

DART can ionize organic substance on solid surface in atmospheric pressure. By utilizing this feature, we analyzed organic contaminant adhered to a metal part (Fig. 1).

We wiped of the organic contamination on the metal surface by using ceramic fiber paper and analyzed it by holding up the ceramic fiber paper directly into the DART ion source. Peaks with 74 interval at m/z 371, m/z 445, and m/z 519 are observed (Fig. 2; upper). The elemental compositions of these ions were deduced from their respective accurate masses (Table 1) and they were found to be poly(dimethylsiloxane) series.

One of the candidates for the contamination was silicone vacuum grease. The grease was analyzed separately by DART and the mass spectrum (Fig. 2; lower) was found to contain the same peaks. We concluded that the contamination was from the vacuum grease.



Fig. 1 Organic contamination on metal surface

Conditions

Ionization: DART (+)
Helium gas temperature: 250°C

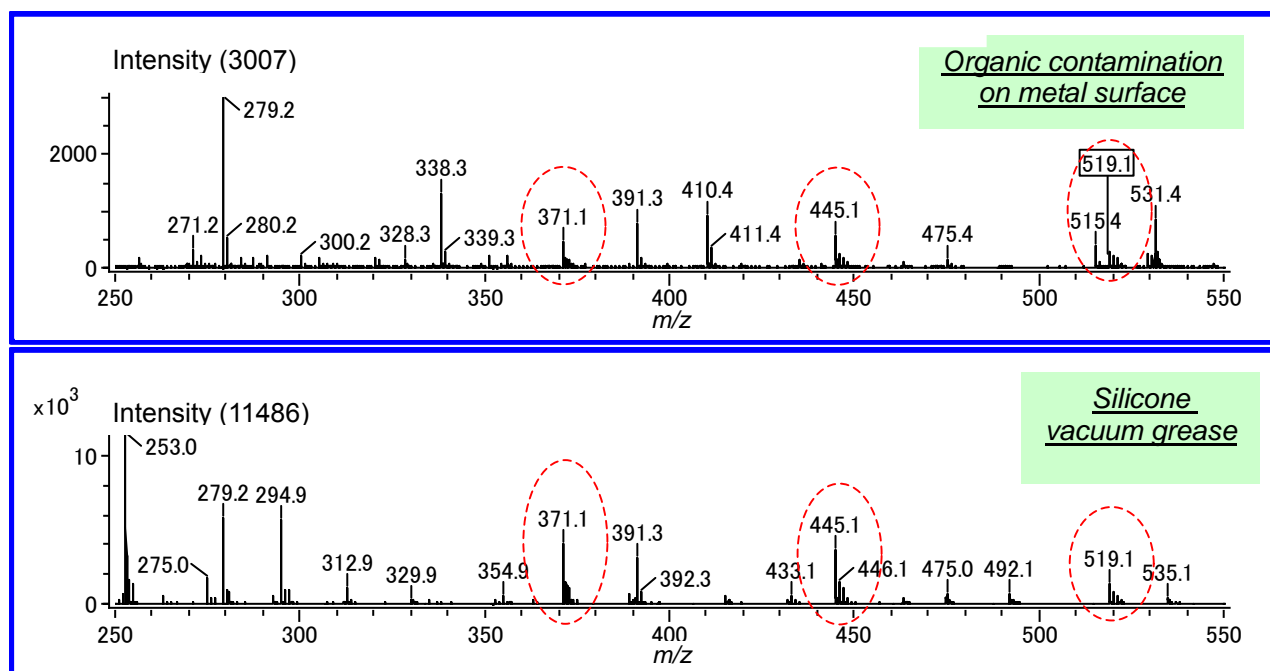


Fig. 2 DART (+) mass spectra

Upper: sample, lower: silicone vacuum grease

Table 1 Estimated elemental compositions of major ions from the sample

Observed m/z	Calculated m/z	Error (ppm)	Estimated composition	Unsaturation
371.10133	371.10178	-1.20	12C10 1H31 16O5 28Si5	0.5
445.12036	445.12057	-0.48	12C12 1H37 16O6 28Si6	0.5
519.13959	519.13936	0.44	12C14 1H43 16O7 28Si7	0.5

~ Application Note for DART ~

Analysis of low polar compound by DART

~ analysis of organic electroluminescence materials ~

Introduction

In MS Tips No. D031 we introduced the example of high polar compound analysis with DART. This application note introduces the example of the analysis of low polar compounds

For the mass spectrometric analysis of organic electroluminescence (EL) materials, which have been one of the typical luminescent materials in LC/MS (APCI, APPI), GC/MS (refer to MS Tips 78 and 87), MALDI-TOFMS, and TOFSIMS have been used.

This time, we have analyzed organic EL materials using DART as follows.

Methods

The samples were adhered to the tip of a glass rod and presented directly to the DART™ ion source.

Sample 4,4'-Bis(carbozoi-9-yl)biphenyl (CBP)
4,4'-Bis(2,2-diphenyl-ethen-1-yl)biphenyl (DPVBi)
(made by Luminescence Technology Corp., Taiwan)

Mass spectrometer JMS-T100TD time-of-flight mass spectrometer

Ionization DART (+)

Helium gas temperature 250 °C

Results and discussion

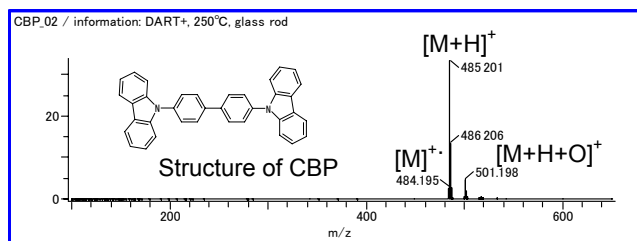


Fig. 1 DART(+) mass spectrum of CBP

Table 1 Estimated composition of CBP

Observed	Calculated	Error (10 ⁻³ u)	Estimated composition	Unsat.
485.20113	485.20177	-0.64	C ₃₆ H ₂₅ N ₂	25.5
501.19760	501.19669	0.92	C ₃₆ H ₂₅ N ₂ O	25.5

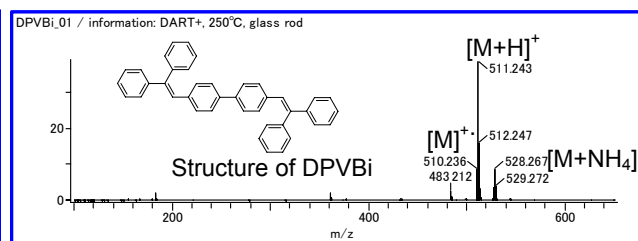


Fig. 2 DART(+) mass spectrum of DPVBi

Table 2 Estimated composition of DPVBi

Observed	Calculated	Error (10 ⁻³ u)	Estimated composition	Unsat.
511.24287	511.24258	0.29	C ₄₀ H ₃₁	25.5
528.26722	528.26912	-1.90	C ₄₀ H ₃₄ N ₁	25.5

In both samples, [M+H]⁺ was detected as base peak. In addition, [M+NH₄]⁺ and [M]⁺ were also detected. With CBP, ion which can be deduced as [M+H+O]⁺ from the accurate mass has also been detected. DART has been proven effective in the analysis of low polar compounds such as organic EL.

Chemical Reaction Monitoring with the AccuTOF-DART™ Mass Spectrometer

Introduction

DART provides a convenient means for monitoring the progress of chemical reactions. Reactants, intermediates, products and byproducts can be detected by simply dipping a glass rod into the reaction pot and then placing the rod in front of the DART ion source. The AccuTOF's ability to measure accurate masses and isotopic abundances makes it possible to confirm or identify the elemental compositions of peaks in the mass spectra. Here we show the use of AccuTOF-DART to monitor the acetylation of 1,2-hexanediol as a function of time.

Experimental

600 μl of 1,5-hexanediol (4.9 mmol) was mixed with 700 μl (12.3 mmol) of glacial acetic acid and one drop of concentrated sulfuric acid in a loosely capped scintillation vial. The reaction was slowly warmed with a heat gun and a fume vent was positioned over the reaction vial and the DART source. Samples were taken periodically for analysis with the AccuTOF-DART by dipping a melting point tube into the reaction mixture and placing the tube in front of the DART ion source for a few seconds. The reaction progress was monitored by plotting the fractional

abundances of the protonated molecules (MH^+) as measured for each component in the mass spectra.

Results

Figure 1 shows the time dependence of the fractional abundances of unreacted 1,5-hexanediol (MH^+ at m/z 119.1072), the reaction intermediate 1,5-hexanediol monoacetate (MH^+ at m/z 161.1178) and the product 1,5-hexanediol diacetate (MH^+ at m/z 203.1283). At 20 minutes, roughly equal amounts of the intermediate monoacetate and the diacetate are present. At 90 minutes, the reaction was incomplete and unchanging because an insufficient excess of acetic acid was present. Adding another 100 μl of acetic acid allowed the reaction to go to completion in 120 minutes.

Conclusion

AccuTOF-DART provides a convenient and rapid means for monitoring the progress of chemical reactions. Reactants, intermediates, and products are readily detected.

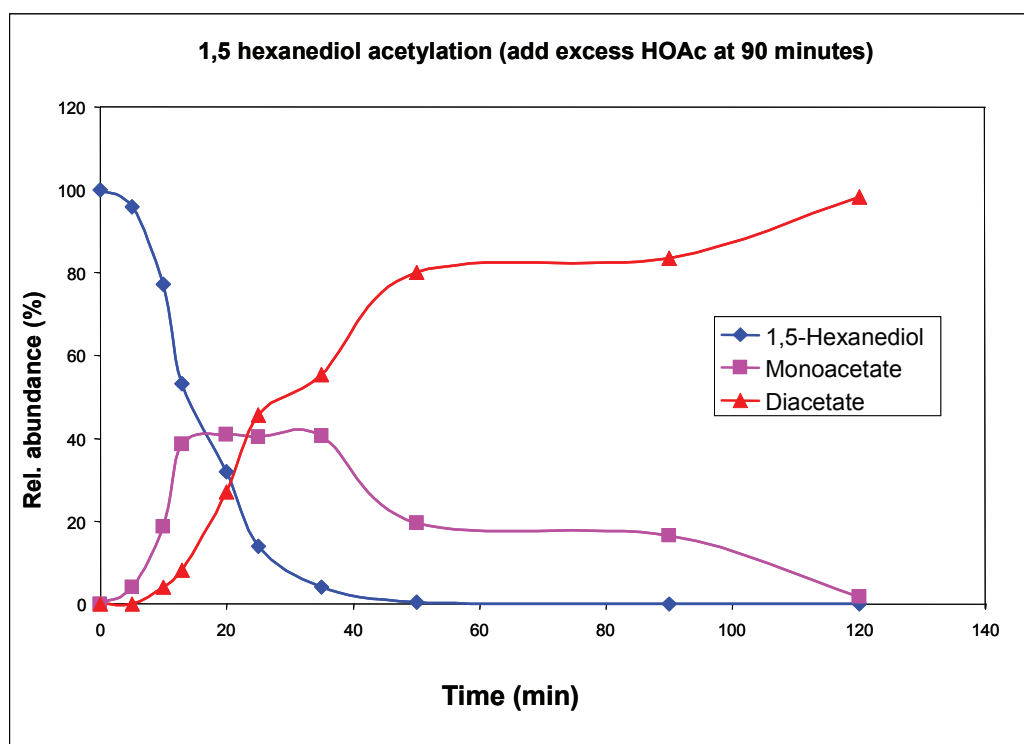


Figure 1. Synthesis of 1,5-hexanediol diacetate monitored by AccuTOF-DART.

This page intentionally left blank for layout purpose.

Direct Analysis of Organometallic Compounds

Summary

Organometallic compounds play an important role in chemistry, as recently recognized by the awarding of the 2005 Nobel Prize in Chemistry to Chauvin, Schrock and Grubbs. Characterization of organometallic compounds by mass spectrometry can sometimes be complicated by problems with solubility and reactivity. Electron ionization can be used for some volatile organometallics. Fast atom bombardment (FAB) and electrospray ionization (ESI) are useful provided suitable solvents can be used. Field desorption (FD) is often effective, but FD emitters can be fragile and the analysis should be carried out by an experienced operator.

DART (Direct Analysis in Real Time) complements these methods and provides an alternative; it is fast and does not require solvents. The sampling area is purged

with an inert gas, reducing the likelihood of undesirable reactions. Further, AccuTOF-DART permits exact mass measurements without requiring the presence of a reference standard during the sample measurement. DART is extremely robust and does not require special operator training.

Mass spectra of several organometallic compounds were obtained by using DART. A few dry particles of each compound were placed in front of the DART source on a melting point tube and mass spectra were obtained within seconds. The best results were obtained by using small quantities of sample; very large quantities can result in ion-molecule reactions between sample ions and sample neutrals, resulting in isotopic patterns characterized by both M^+ and $[M+H]^+$. All labeled assignments were confirmed by exact mass measurements and isotope pattern matching.

Ferrocene: $Fe(C_5H_5)_2$

Ferrocene produces a molecular ion M^+ for low sample quantities (micrograms or less). If a larger quantity is analyzed, ion-molecule reactions result in protonation of the molecule to produce $[M+H]^+$.

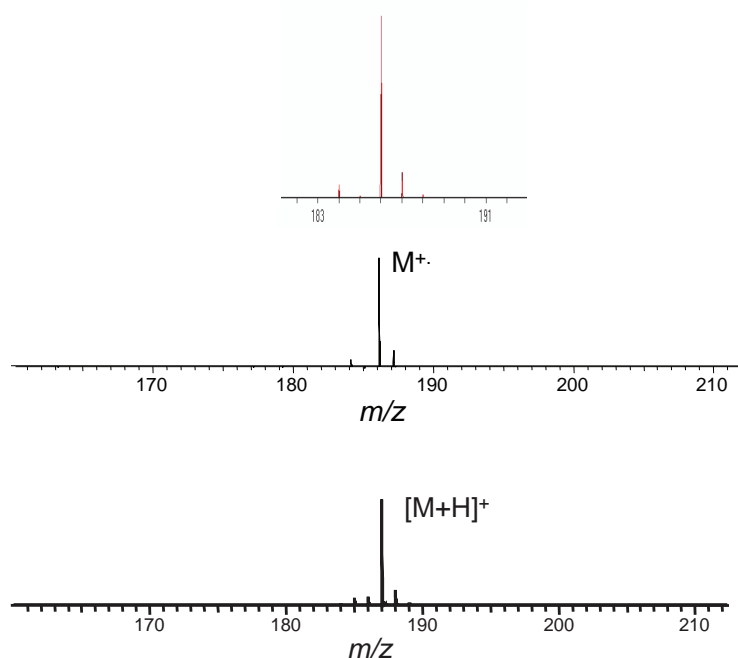


Figure 1. Top: Theoretical isotope pattern for $Fe(C_5H_5)_2^+$. Middle: Mass spectrum obtained by using a very small quantity of ferrocene. Bottom: Mass spectrum obtained by analyzing a large quantity of ferrocene on the melting point tube.

Tungsten hexacarbonyl: $W(CO)_6$

Like ferrocene, tungsten hexacarbonyl produces mass spectra characterized by a molecular ion for low sample concentrations. A protonated molecule is observed if large sample quantities are presented to the DART source.

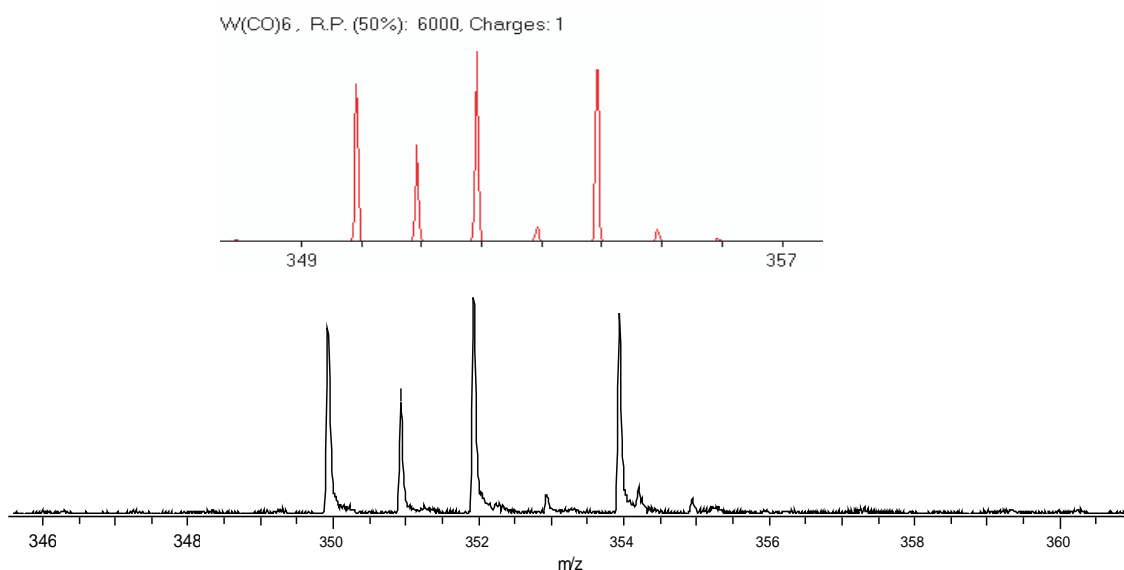


Figure 2. Top: theoretical isotope pattern for $W(CO)_6^+$. Bottom: measured mass spectrum for tungsten carbonyl.

Acetylacetonato rhodium dicarbonyl: $C_5H_8O_2Rh(CO)_2$

This compound readily produces a molecular ion.

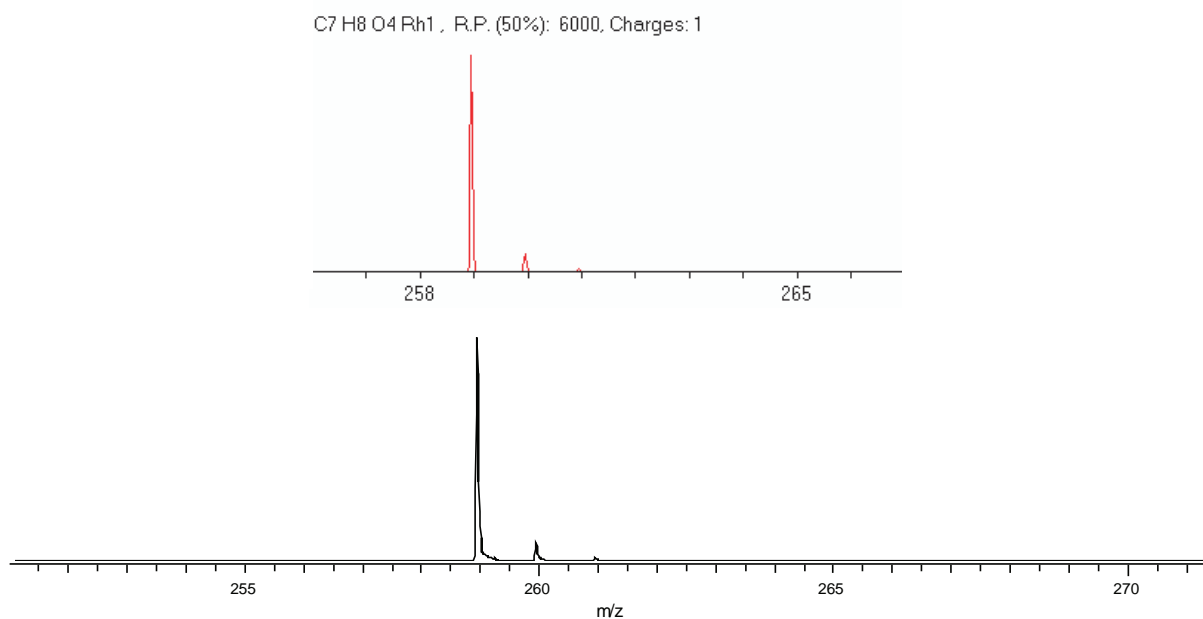


Figure 3. Top: theoretical isotope pattern for $C_5H_8O_2Rh(CO)_2^+$. Bottom: measured mass spectrum.

(1,5-cyclooctadiene) platinum (II) chloride ($C_8H_{12}PtCl_2$)

This compound does not readily protonate. However, it produces an ammonium adduct if vapor from a dilute solution of ammonium hydroxide is present. Chloride loss and a related water adduct are also observed. A dimer ($(C_8H_{12}Pt)_2Cl_3^+$) is also observed at higher mass (not shown).

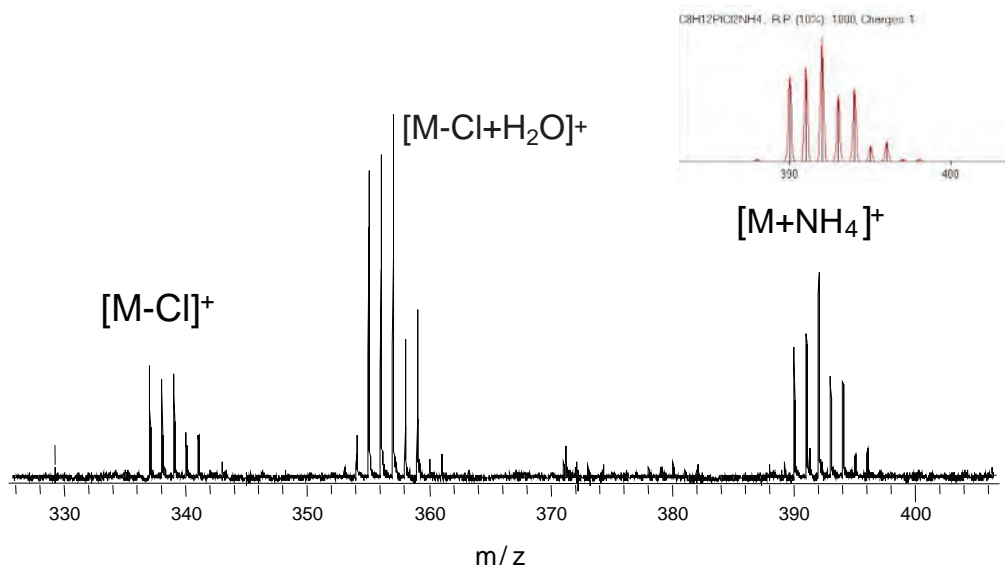


Figure 4. Top inset: theoretical isotope pattern for $[C_8H_{12}PtCl_2+NH_4]^+$. Bottom: measured mass spectrum.

Bis(diphenylphosphoethane) platinum dichloride: $Pt(DPPE)Cl_2$

This compound behaves in a similar manner to (1,5-cyclooctadiene) platinum (II) chloride. An ammonium adduct can be observed, together with a chloride loss and a dimer $[2M-Cl]^+$.

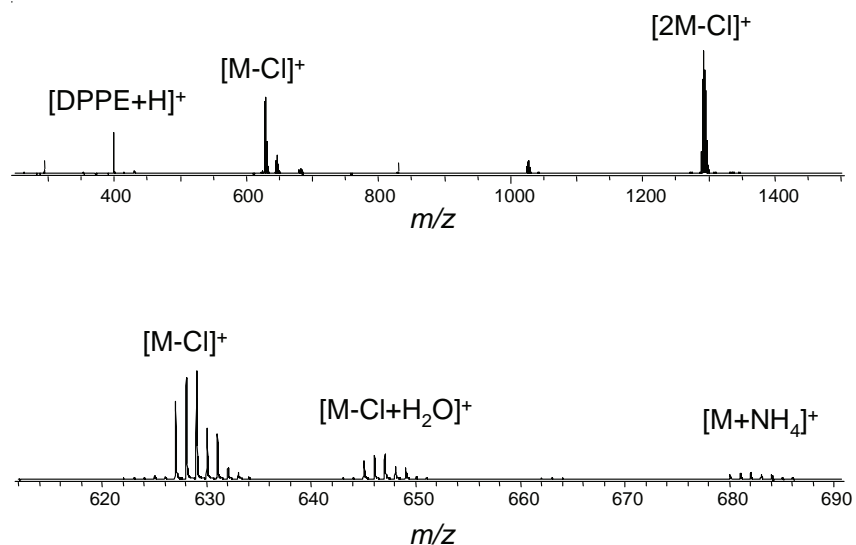


Figure 5. DART mass spectrum of $Pt(DPPE)Cl_2$. Top: mass spectrum for m/z 350 to m/z 1500. Bottom: enlarged view of region near $[M-Cl]^+$.

Conclusion

AccuTOF-DART provides a convenient means for characterizing many organometallic compounds. No solvents are required and excellent agreement between theoretical and observed masses and isotopic abundances are obtained.

~ Application Note for DART ~

Analysis of highly polar compound by DART ~ analysis of ionic liquid ~

Introduction

Direct analysis in real time (DART™) is applicable to a wide variety of samples; from low polar to highly polar compounds.

Ionic liquids have drawn much attention from various engineering fields, such as tribology, because of their unique properties of electrical conductivity, extremely low vapor pressure, low viscosity, low combustibility, etc. The sample was analyzed by dipping a glass rod to the sample and presented it directly to the DART™ ion source.

Methods

Sample	1-ethyl-3-methylimidazolium-bis(trifluoromethylsulfonyl)imide (EMI-TFSI)
Mass spectrometer	JMS-T100TD time-of-flight mass spectrometer
Ionization	DART (+), DART (-)
Helium gas temperature	200 °C

Results and discussion

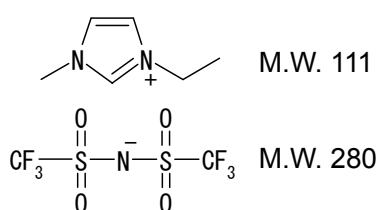


Fig. 1 Structural formulae of EMI-TFSI

As shown in Fig. 2, base peaks were observed at m/z 111 and m/z 280 for DART(+) and DART(-) respectively. The elemental compositions of the cation and anion were confirmed by accurate mass measurements as shown in Table 1.

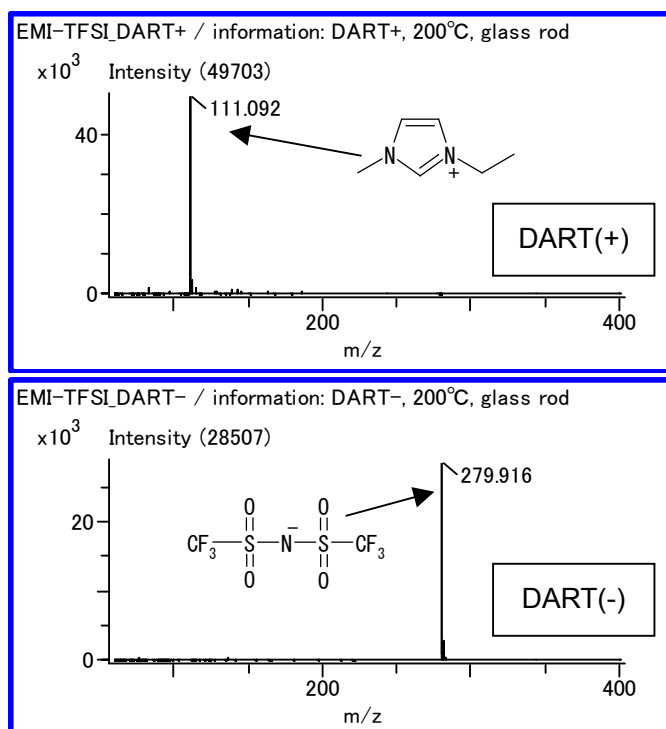


Fig. 2 DART mass spectra (top: DART(+)) bottom: DART(-)

	Measured	Theoretical	Error (10^{-3} u)	Elucidated formula	Unsaturation
Cation	111.09226	111.09222	0.04	$C_6H_{11}N_2$	2.5
Anaion	279.91569	279.91729	-1.60	$C_2F_6NO_4S_2$	2.5

Elemental Compositions from Exact Mass Measurements and Accurate Isotopic Abundances

Introduction

Exact masses have been used for decades to calculate elemental compositions for known and unknown molecules. The traditional approach calculates all possible combinations of user-specified atoms that fall within a given error tolerance of a measured mass. The number of possible combinations increases dramatically with increasing mass and as more atoms are included in the search set. In many cases, it is not possible to determine a unique composition based on mass alone¹.

A common source of error in measuring isotopic abundances with scanning mass spectrometers is

related to fluctuations in ion current during measurement. The AccuTOF family of mass spectrometers overcomes this problem by analyzing all of the isotopes formed at the same instant. Combined with a high-dynamic-range detector, this provides highly accurate isotopic abundances². It has been shown that accurately measured isotopic abundances can be combined with measured exact masses to dramatically reduce the number of possible elemental compositions for an unknown³. It is often possible to deduce a unique elemental composition, facilitating the identification of unknown substances.

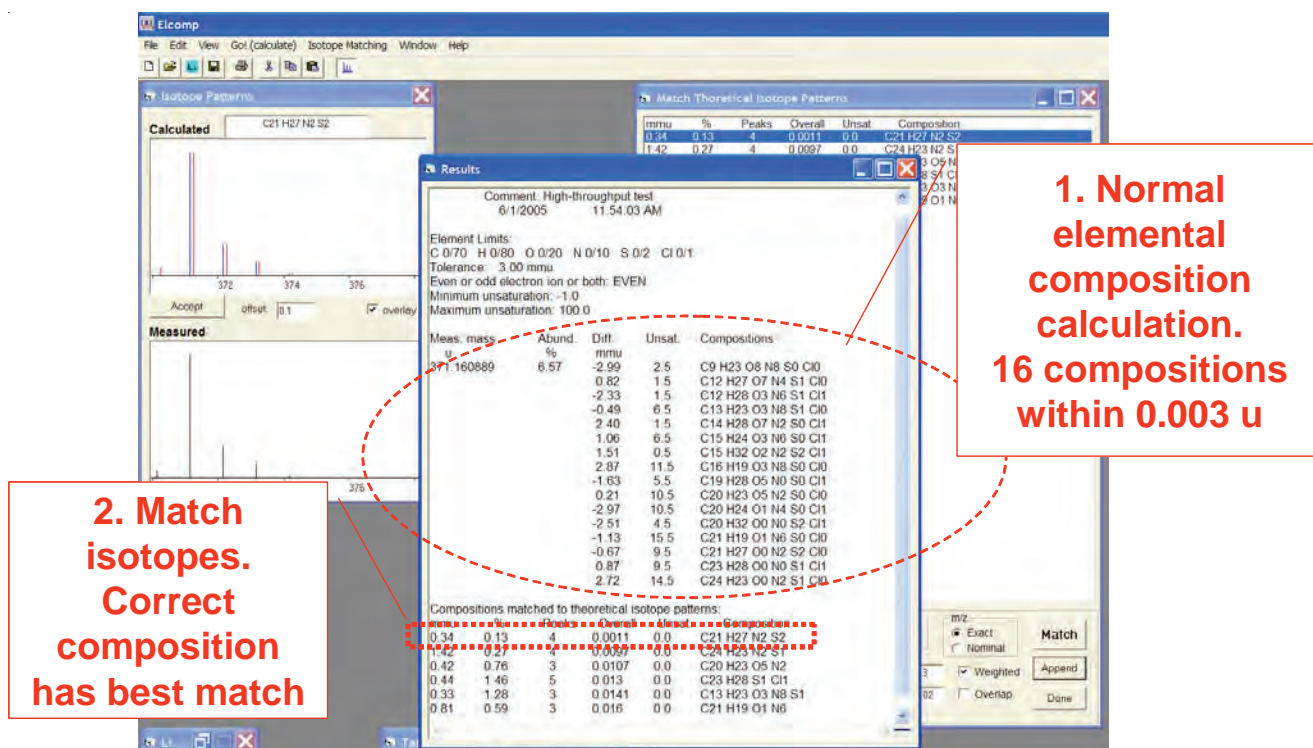


Figure 1. Elemental composition calculation for thioridazine from combined exact mass measurement with isotope matching.

Experimental

Samples in this report were measured with the AccuTOF-DART[™] mass spectrometer. Similar procedures can be used with other members of the AccuTOF mass spectrometer family. Calibrated mass spectra were centroided and saved as JEOL-DX (JCAMP) text files. These text files were processed with the Elemental Composition Workshop from the Mass Spec Tools[™] software suite distributed with AccuTOF mass spectrometers⁴. The program permits automated isotope matching for measured mass spectra and provides a visual comparison between the measured and theoretical isotopic abundances for each hit (Figure 1).

Eleven small drug samples were deposited on melting point tubes and mounted on a support. Samples were passed sequentially in front of the DART source with a measurement time of about 3 seconds per sample. Neat PEG 600 on a melting point tube was also measured to provide an external

mass calibration standard. Elemental compositions were calculated by assuming even-electron ions, a mass measurement error tolerance of 0.003 u, and default tolerances for isotope matching. Elemental limits were set to:

C 0/70 H 0/80 O 0/20 N 0/10 S 0/2 Cl 0/1.

The correct elemental composition was successfully determined for each sample as shown in Table 1. The total number of compositions calculated without isotope matching is shown in column 4 of the table. The correct composition was the number 1 ranked composition from the automated isotope match for all compounds measured. The most dramatic example was reserpine $[M+H]^+$ ($C_{33}H_{41}N_2O_9$) which gave 30 compositions without isotope matching. Isotope matching reduced the number of possible compositions to 11 of which the best match corresponded to the correct composition.

Compound	Composition	Calculated <i>m/z</i>	#Compositions	Rank
Phenolphthalein	C ₂₀ H ₁₅ O ₄	319.097035	18	1
Promazine	C ₁₇ H ₂₁ N ₂ S	285.142544	11	1
Quinine	C ₂₀ H ₂₅ N ₂ O ₂	325.191603	8	1
Nortriptylene	C ₁₉ H ₂₂ N	264.175224	5	1
Thioridazine	C ₂₁ H ₂₇ N ₂ S ₂	371.161565	16	1
Chlorpromazine	C ₁₇ H ₂₀ N ₂ SCl	319.103572	18	1
Doxepin	C ₁₉ H ₂₂ NO	280.170139	5	1
Hydrocortisone	C ₂₁ H ₃₁ O ₅	363.21715	9	1
Reserpine	C ₃₃ H ₄₁ N ₂ O ₉	609.281208	30	1
Caffeine	C ₈ H ₁₁ N ₄ O ₂	195.088201	7	1
Erythromycin	C ₃₇ H ₆₈ NO ₁₃	734.469069	22	1

Table 1. $[M+H]^+$ elemental compositions determined for 11 drugs measured in 0.58 minutes with the AccuTOF-DART. All compositions were correctly identified. The rms mass measurement error was 2.2 ppm.

References

- <http://jeolusa.com/ms/docs/elcomp.html>
- <http://jeolusa.com/ms/docs/phenylalanine.pdf>
- <http://www.epa.gov/nerlesd1/chemistry/ice/pubs.htm>
- JEOL USA, Inc. customers only.
The software is available to all for purchase at <http://www.chemsw.com/13057.htm>

Identifying “Buried” Information in LC/MS Data

It is not always easy to identify minor unknown components in complex LC/MS datasets. The new DART™ ion source screened for components that were not immediately recognized in LC/MS analysis of tea samples.

LC/TOFMS datasets can contain high-resolution, exact-mass data for all ionized components of a complex mixture. Even with concurrent UV detection and chromatographic enhancement software, it is not always easy to identify all of the components that are present in the dataset. Furthermore, suppression effects may mask important information. Here, a new technique known as Direct Analysis in Real Time (DART™) was used to screen tea samples and provide elemental compositions for minor components that were “buried” in LC/MS data collected for tea analysis. DART is a powerful new ionization method that permits direct analysis of solid, liquid, or gas samples at atmospheric pressure and ground potential. DART has been applied to rapid in-situ analysis of a very wide range of materials ranging from drugs to explosives, foods, and beverages.

Experimental Conditions

Drinking-quality green tea was analyzed directly by dipping a glass rod into the liquid and placing the rod between the DART source and the mass spectrometer orifice. Analysis was complete within 30 seconds. Following the tea analysis, a piece of filter paper dipped in PEG 600 was placed in front of the DART to provide reference masses for exact mass measurements. LC/MS conditions were described in a previous application note. (<http://www.lcgc.com/lcgc/article/articleDetail.jsp?id=87195>).

Results and Conclusions

Elemental compositions for several components are given in Table 1 for several compounds identified by DART. Compositions were identified by combined exact-mass measurements and isotope pattern matching for the observed $[M+H]^+$ species. Candidate compositions were proposed by searching the mass spectral database for suitable compounds having the correct elemental composition. Following DART analysis, reconstructed ion mass chromatograms were generated from the LC/MS data for the exact mass of each component.

DART is ideal for screening because the analysis is rapid, suppression is minimal, solvent adducts are not observed, and exact mass measurements are simple and accurate. The presence of several isomers having these candidate compositions was confirmed by the RIC's. The LC/MS data shows well-separated isomers and provides quantitative information about each component.

- | | | |
|----|-------------------|---|
| 1. | $C_6H_4O_2$ | Benzoquinone |
| 2. | $C_4H_4O_2$ | Furanone |
| 3. | $C_5H_4O_2$ | Furfural, pyranone |
| 4. | $C_6H_6O_3$ | Maltol |
| 5. | $C_7H_6O_3$ | Sesamol, dihydroxybenzaldehydes, salicylic acid |
| 6. | $C_{15}H_{10}O_6$ | Kaempferol |
| 7. | $C_{15}H_{10}O_7$ | Quercetin |
| 8. | $C_{15}H_{10}O_8$ | Myricetin |

Table 1. Elemental compositions and some candidate compounds identified by DART in green tea.

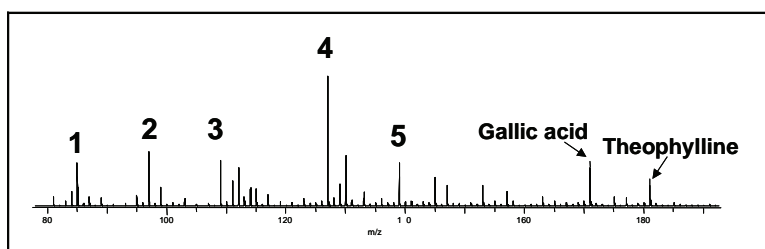


Figure 1. Portion of positive-ion DART mass spectrum for green tea sampled with a glass rod. Larger components such as #6-8, caffeine and catechin were detected but are not shown here.

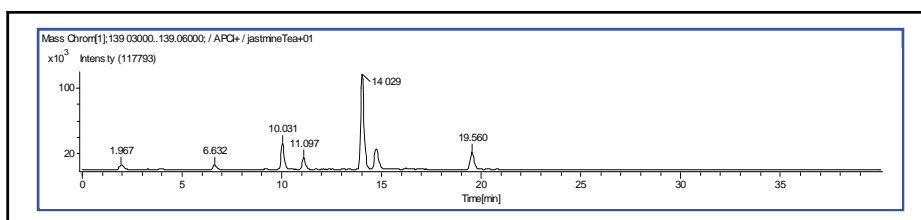


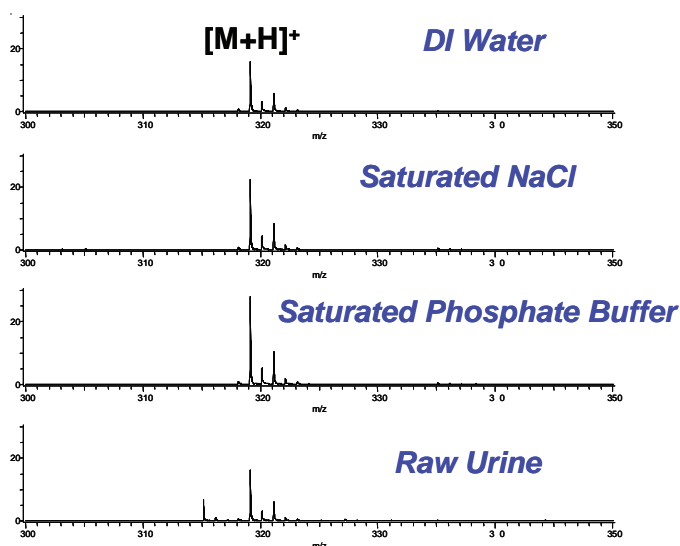
Figure 2. Reconstructed mass chromatogram for m/z 139.0395 ($C_7H_7O_3^+$).

DART Contamination Resistance: Analysis of Compounds in Saturated Salt and Buffer Solutions

DART provides very simple mass spectra that are free of multiple charging and alkali metal cation adducts such as $[M+Na]^+$ and $[M+K]^+$. This facilitates identification of target compounds in mixtures and simplifies assignment of elemental compositions for unknowns. 50 ppm solutions of chlorpromazine were prepared in ultrapure deionized (DI) water, aqueous solutions of saturated sodium chloride and saturated potassium

phosphate buffer, and raw urine. Two microliters of each solution were applied to glass melting point tubes and analyzed by DART.

The mass spectra are shown below. All spectra are characterized by $[M+H]^+$ and there is no evidence of $[M+Na]^+$ or $[M+K]^+$. Sample suppression is not observed at this concentration.



DART analysis of chlorpromazine in various solutions.

Note: Ranitidine (m/z 315) is also present in the urine background.

Conclusion

DART provides simple mass spectra, free of alkali metal cation adducts, even when analytes are present in concentrated salt or buffer solutions.

AccuTOF LC series with DART Bibliography

Updated: August 2015

1. Cody, R.B., J.A. Laramée, and H.D. Durst, *Versatile New Ion Source for the Analysis of Materials in Open Air under Ambient Conditions*. Analytical Chemistry, 2005. **77**(8): p. 2297-2302.
2. Cody, R.B., et al., *Direct Analysis in Real Time (DART™) Mass Spectrometry*. JEOL News, 2005. **40**(1): p. 8-12.
3. Fernández, F.M., et al., *Characterization of Solid Counterfeit Drug Samples by Desorption Electrospray Ionization and Direct-analysis-in-real-time Coupled to Time-of-flight Mass Spectrometry*. ChemMedChem, 2006. **1**(7): p. 702-705.
4. Jones, R.W., R.B. Cody, and J.F. McClelland, *Differentiating Writing Inks Using Direct Analysis in Real Time Mass Spectrometry*. Journal of Forensic Sciences, 2006. **51**(4): p. 915-918.
5. Morlock, G. and W. Schwack, *Determination of isopropylthioxanthone (ITX) in milk, yoghurt and fat by HPTLC-FLD, HPTLC-ESI/MS and HPTLC-DART/MS*. Analytical and Bioanalytical Chemistry, 2006. **385**(3): p. 586-595.
6. Konuma, K., *Guide to Direct Analysis in Real Time (DART) Ionization Source*. Farumarushi, 2007. **43**(9): p. 903-905.
7. Kpegba, K., et al., *Analysis of Self-Assembled Monolayers on Gold Surfaces Using Direct Analysis in Real Time Mass Spectrometry*. Analytical Chemistry, 2007. **79**(14): p. 5479-5483.
8. Kusai, A., *Fundamental and application of the direct analysis in real time mass spectrometry*. Bunseki, 2007. **3**: p. 124-127.
9. Laramée, J.A. and R.B. Cody, *Chemi-ionization and Direct Analysis in Real Time (DART™) Mass Spectrometry*, in *The Encyclopedia of Mass Spectrometry Volume 6: Ionization Methods* M.L. Gross and R.M. Caprioli, Editors. 2007, Elsevier: Amsterdam. p. 377-387.
10. Laramée, J.A., et al., *Forensic Application of DART (Direct Analysis in Real Time) Mass Spectrometry*, in *Forensic Analysis on the Cutting Edge: New Methods for Trace Evidence Analysis*, R.D. Blackledge, Editor. 2007, Wiley-Interscience Hoboken, NJ.
11. Morlock, G. and Y. Ueda, *New coupling of planar chromatography with direct analysis in real time mass spectrometry* Journal of Chromatography A, 2007. **1143**(1-2): p. 243-251
12. Morlock, G. and Y. Ueda, *Coupling Planar Chromatography with Time-of-Flight Mass Spectrometry Using an Open-Air Ion Source*. LCGC: The Peak, 2007: p. 7-13.

13. Pierce, C.Y., et al., *Ambient generation of fatty acid methyl ester ions from bacterial whole cells by direct analysis in real time (DART) mass spectrometry*. Chemical Communications, 2007(8): p. 807 - 809.
14. Ropero-Miller, J.D., et al., *Comparison of the Novel Direct Analysis in Real Time Time-of-Flight Mass Spectrometry (AccuTOF-DART™) and Signature Analysis for the Identification of Constituents of Refined Illicit Cocaine*. Microgram Journal, 2007. 5(1-4): p. 5.
15. Saitoh, K., *Direct analysis for fragrance ingredients using DART-TOFMS*. Aroma Research, 2007. 8(4): p. 366-369.
16. Steiner, R.R., *AccuTOF-DART Mass Spectrometry*. 2007, Virginia Department of Forensic Science Controlled Substances Procedures Manual, Section 31.
17. Vail, T.M., P.R. Jones, and O.D. Sparkman, *Rapid and Unambiguous Identification of Melamine in Contaminated Pet Food Based on Mass Spectrometry with Four Degrees of Confirmation*. Journal of Analytical Toxicology, 2007. 31(6): p. 304-312.
18. Alpmann, A. and G. Morlock, *Rapid and sensitive determination of acrylamide in drinking water by planar chromatography and fluorescence detection after derivatization with dansulfinic acid*. Journal of Separation Science, 2008. 31(1): p. 71-77.
19. Ayers, S., et al., *Pharmacokinetic analysis of anti-allergy and anti-inflammation bioactives in a nettle (Urtica dioica) extract*. Online Journal of Pharmacology and Pharmacokinetics, 2008. 5: p. 6-21.
20. Banerjee, S., et al., *Expression of tropane alkaloids in the hairy root culture of **Atropa acuminata** substantiated by DART mass spectrometric technique*. Biomedical Chromatography, 2008. 22(8): p. 830-834.
21. Banerjee, S., et al., *Analysis of cell cultures of **Taxus wallichiana** using direct analysis in real-time mass spectrometric technique*. Biomedical Chromatography, 2008. 22(3): p. 250-253.
22. Cajka, T., J. Hajslova, and K. Mastovska, *Mass spectrometry and hyphenated instruments in food analysis*, in *Handbook of Food Analysis Instruments*, S. Ötleş, Editor. 2008, CRC Press, Taylor & Francis Group. p. 197-228.
23. Cajka, T., et al., *GC-TOF-MS and DART-TOF-MS: Challenges in the Analysis of Soft Drinks*. LC/GC Europe, 2008. 21(5): p. 250-256.
24. Coates, C.M., et al., *Flammable Solvent Detection Directly from Common Household Materials Yields Differential Results: An Application of Direct Analysis in Real-Time Mass Spectrometry*. Journal of Forensic Identification, 2008. 58(6): p. 624 -631.
25. Fernandez, F.M., M.D. Green, and P.N. Newton, *Prevalence and Detection of Counterfeit Pharmaceuticals: A Mini Review*. Ind. Eng. Chem. Res., 2008. 47(3): p. 585-590.

26. Grange, A.H., *An Inexpensive Autosampler to Maximize Throughput for an Ion Source that Samples Surfaces in Open Air*. Environmental Forensics, 2008. **9**(2): p. 127-136.
27. Grange, A.H., *An Integrated Wipe Sample Transport/Autosampler to Maximize Throughput for a Direct Analysis in Real Time (DART)/Orthogonal Acceleration, Time-of-Flight Mass Spectrometer (oa-TOFMS)*. Environmental Forensics, 2008. **9**(2): p. 137 - 143.
28. Grange, A.H., *An Autosampler and Field Sample Carrier for Maximizing Throughput Using an Open-Air Source for MS*. American Laboratory, 2008. **40**(16): p. 11-13.
29. Grange, A.H. and G.W. Sovocool, *Automated determination of precursor ion, product ion, and neutral loss compositions and deconvolution of composite mass spectra using ion correlation based on exact masses and relative isotopic abundances*. Rapid Communications in Mass Spectrometry, 2008. **22**(15): p. 2375-2390.
30. Hajslova, J., et al. (2008) *Analysis of Deoxynivalenol in Beer*. LCGC: Chromatography Online.
31. Hajslova, J., et al., *DART–TOFMS: A Challenging Approach in Rapid Monitoring of Brominated Flame Retardants in Environmental Matrices*. Organohalogen Compounds, 2008. **70**: p. 922-925.
32. Harris, G.A., L. Nyadong, and F.M. Fernandez, *Recent developments in ambient ionization techniques for analytical mass spectrometry*. Analyst, 2008. **133**: p. 1297-1301.
33. Laramée, J.A., et al., *Detection of Chemical Warfare Agents on Surfaces Relevant to Homeland Security by Direct Analysis in Real-Time Spectrometry*. American Laboratory, 2008. **40**: p. 16-20.
34. Madhusudanan, K.P., et al., *Analysis of hairy root culture of **Rauvolfia serpentina** using direct analysis in real time mass spectrometric technique*. Biomedical Chromatography, 2008. **22**(6): p. 596-600.
35. Newton, P.N., et al., *A Collaborative Epidemiological Investigation into the Criminal Fake Artesunate Trade in South East Asia*. PLoS Medicine, 2008. **5**(2): p. e32.
36. Newton, P.N., et al., *Characterization of “Yaa Chud” Medicine on the Thailand–Myanmar Border: Selecting for Drug-resistant Malaria and Threatening Public Health*. American Journal of Tropical Medicine and Hygiene, 2008. **79**(5): p. 662-669.
37. Roschek Jr., B. and R.S. Alberte, *Pharmacokinetics of Cyanidin and Anti-Influenza Phytonutrients in an Elder Berry Extract Determined by LC-MS and DART TOF-MS*. Online Journal of Pharmacology and Pharmacokinetics, 2008. **4**: p. 1-17.

38. Schurek, J., et al., *Control of Strobilurin Fungicides in Wheat Using Direct Analysis in Real Time Accurate Time-of-Flight and Desorption Electrospray Ionization Linear Ion Trap Mass Spectrometry*. Analytical Chemistry, 2008. **80**(24): p. 9567-9575.
39. Smith, N.J., M.A. Domin, and L.T. Scott, *HRMS Directly From TLC Slides. A Powerful Tool for Rapid Analysis of Organic Mixtures*. Organic Letters, 2008. **10**(16): p. 3493-3496.
40. Stout, P.R. and J.D. Roper-Miller, *Forensic Toxicology Research and Development Evaluation of New and Novel Direct Sample Introduction, Time of Flight Mass Spectrometry (AccuTOF-DART) Instrument for Postmortem Toxicology Screening, Final Report*, in NCJRS Abstract. 2008.
41. Vaclavik, L., et al., *Direct analysis in real time—time-of-flight mass spectrometry: Analysis of pesticide residues and environmental contaminants*. Chemicke Listy, 2008. **102**: p. s324–s327.
42. Yang, X., X. Xu, and H.-F. Ji, *Solvent Effect on the Self-Assembled Structure of an Amphiphilic Perylene Diimide Derivative*. Journal of Physical Chemistry B, 2008. **112**: p. 7196–7202.
43. Yew, J.Y., R.B. Cody, and E.A. Kravitz, *Cuticular hydrocarbon analysis of an awake behaving fly using direct analysis in real-time time-of-flight mass spectrometry*. Proceedings of the National Academy of Sciences, 2008. **105**(20): p. 7135-7140.
44. Bennett, M.J. and R.R. Steiner, *Detection of GHB in various drink matrices via AccuTOF-DART*. Journal of Forensic Science, 2009. **54**(2): p. 370-375.
45. Cody, R.B., *The Observation of Molecular Ions and Analysis of Nonpolar Compounds with the Direct Analysis in Real Time Ion Source*. Analytical Chemistry, 2009. **81**(3): p. 1101-1107.
46. Curtis, M.E., et al., *Determination of the Presence or Absence of Sulfur Materials in Drywall Using Direct Analysis in Real Time in Conjunction with an Accurate-Mass Time-of-Flight Mass Spectrometer*. Journal of the American Society for Mass Spectrometry, 2009. **20**(11): p. 2082-2086.
47. Dane, A.J. and R.B. Cody *Using Solid Phase Microextraction with AccuTOF-DART™ for Fragrance Analysis*, in LC/GC: The Application Notebook. 2009.
48. Grange, A.H., *Rapid Semi-Quantitative Surface Mapping of Airborne-Dispersed Chemicals Using Mass Spectrometry*. Environmental Forensics, 2009. **10**(3): p. 183-195.
49. Harris, G.A. and F.M. Fernandez, *Simulations and Experimental Investigation of Atmospheric Transport in an Ambient Metastable-Induced Chemical Ionization Source*. Analytical Chemistry, 2009. **81**(1): p. 322-329.
50. Jagerdeo, E. and M. Abdel-Rehim, *Screening of Cocaine and Its Metabolites in Human Urine Samples by Direct Analysis in Real-Time Source Coupled to Time-of-Flight Mass Spectrometry After Online Preconcentration Utilizing*

- Microextraction by Packed Sorbent*. Journal of the American Society for Mass Spectrometry, 2009. **20**(5): p. 891-899.
51. Jee, E.H., et al., *Detection of characterising compounds on TLC by DART-MS*. Planta Med, 2009. **75**(09): p. PG38.
 52. Kawamura, M., R. Kikura-Hanajiri, and Y. Goda, *Simple and rapid screening for psychotropic natural products using Direct Analysis in Real Time (DART)-TOFMS*. Yakugaku Zasshi : Journal of the Pharmaceutical Society of Japan, 2009. **129**(6): p. 719-25.
 53. Kim, H.J. and Y.P. Jang, *Direct analysis of curcumin in turmeric by DART-MS*. Phytochemical Analysis, 2009. **published online**.
 54. Konuma, K., *Elementary Guide to Ionization Methods for Mass Spectrometry—Introduction of Direct Analysis in Real Time Mass Spectrometry*. Bunseki, 2009. **9**: p. 464-467.
 55. Laramée, J.A., et al., *Detection of Peroxide and Tetrazine Explosives on Surfaces by Direct Analysis in Real Time Mass Spectrometry*. American Laboratory Online Edition, 2009. **2**(2): p. 1-5.
 56. Laramée, J.A., et al., *Alcohols Can Now Be Analyzed by a Direct Analysis in Real-Time Method: Applications for Chemical Warfare Agent Synthesis*. American Laboratory, 2009. **41**(4): p. 24-27.
 57. Laramée, J.A., et al., *An Improved Protocol for the Analysis of Alcohols by Direct Analysis in Real Time Mass Spectrometry*. American Laboratory, 2009. **41**(7): p. 25-27.
 58. Maleknia, S.D., T.L. Bell, and M.A. Adam, *Eucalypt smoke and wildfires: Temperature dependent emissions of biogenic volatile organic compounds*. International Journal of Mass Spectrometry, 2009. **279**(2-3): p. 126-133.
 59. Maleknia, S.D., et al., *Temperature-dependent release of volatile organic compounds of eucalypts by direct analysis in real time (DART) mass spectrometry*. Rapid Communications in Mass Spectrometry, 2009. **23**(15): p. 2241-2246.
 60. Mayoral, J.G., et al., *NADP+-dependent farnesol dehydrogenase, a corpora allata enzyme involved in juvenile hormone synthesis*. Proceedings of the National Academy of Sciences, 2009. **106**(50): p. 21091-21096.
 61. Nilles, J.M., T.R. Connell, and H.D. Durst, *Quantitation of Chemical Warfare Agents Using the Direct Analysis in Real Time (DART) Technique*. Analytical Chemistry, 2009. **81**(16): p. 6744-6749.
 62. Nyadong, L., et al., *Combining Two-Dimensional Diffusion-Ordered Nuclear Magnetic Resonance Spectroscopy, Imaging Desorption Electrospray Ionization Mass Spectrometry, and Direct Analysis in Real-Time Mass Spectrometry for the Integral Investigation of Counterfeit Pharmaceuticals*. Analytical Chemistry, 2009. **81**(12): p. 4803-4812.

63. Roschek Jr., B., et al., *Pro-Inflammatory Enzymes, Cyclooxygenase 1, Cyclooxygenase 2, and 5-Lipoxygenase, Inhibited by Stabilized Rice Bran Extracts*. *Journal of Medicinal Food*, 2009. **12**(3): p. 615–623.
64. Roschek Jr., B., et al., *Elderberry flavonoids bind to and prevent H1N1 infection in vitro* *Phytochemistry*, 2009. **70**(10): p. 1255-1262.
65. Saka, K., et al., *Identification of active ingredients in dietary supplements using non-destructive mass spectrometry and liquid chromatography–mass spectrometry*. *Forensic Science International*, 2009. **191**(1-3): p. e5-e10.
66. Song, L., et al., *Ionization Mechanism of Negative Ion-Direct Analysis in Real Time: A Comparative Study with Negative Ion-Atmospheric Pressure Photoionization*. *Journal of the American Society for Mass Spectrometry*, 2009. **20**(1): p. 42-50.
67. Song, L., et al., *Ionization Mechanism of Positive-Ion Direct Analysis in Real Time: A Transient Microenvironment Concept*. *Analytical Chemistry*, 2009. **81**(24): p. 10080-10088.
68. Steiner, R.R. and R.L. Larson, *Validation of the Direct Analysis in Real Time (DART) Source for Use in Forensic Drug Screening*. *Journal of Forensic Science*, 2009. **54**(3): p. 617-622.
69. Uchiyama, N., et al., *Identification of a cannabimimetic indole as a designer drug in a herbal product*. *Forensic Toxicology*, 2009. **27**(2): p. 61-66.
70. Vaclavik, L., et al., *Ambient mass spectrometry employing direct analysis in real time (DART) ion source for olive oil quality and authenticity assessment*. *Analytica Chimica Acta*, 2009. **645**(1-2): p. 56-63.
71. Wang, C., Y.-I. Zhou, and D.C. Baker, *Synthesis of a mannose-capped disaccharide with a thiol terminus* *ARKIVOC*, 2009. **xiv**: p. 171-180.
72. Bajpai, V., et al., *Profiling of Piper betle Linn. cultivars by direct analysis in real time mass spectrometric technique*. *Biomedical Chromatography*, 2010. **24**(12): p. 1283-1286.
73. Bevilacqua, V.L.H., et al., *Ricin Activity Assay by Direct Analysis in Real Time Mass Spectrometry Detection of Adenine Release*. *Analytical Chemistry*, 2010. **82**(3): p. 798-800.
74. Block, E., *Garlic and Other Alliums. The Lore and the Science*. 2010, Cambridge, UK: RSC Publishing.
75. Block, E., et al., *Allium chemistry: Use of new instrumental techniques to “see” reactive organosulfur species formed upon crushing garlic and onion*. *Pure and Applied Chemistry*, 2010. **82**(3): p. 535-539.
76. Block, E., et al., *Applications of Direct Analysis in Real Time Mass Spectrometry (DART-MS) in Allium Chemistry. 2-Propenesulfenic and 2-Propenesulfinic Acids, Diallyl Trisulfane S-Oxide, and Other Reactive Sulfur Compounds from Crushed Garlic and Other Alliums*. *Journal of Agricultural and Food Chemistry*, 2010. **58**(8): p. 4617-4625.

77. Cajka, T., et al., *Recognition of beer brand based on multivariate analysis of volatile fingerprint*. Journal of Chromatography A, 2010. **1217**(25): p. 4195-4203.
78. Cajka, T., et al., *Ambient mass spectrometry employing a DART ion source for metabolomic fingerprinting/profiling: A powerful tool for beer origin recognition*. Metabolomics, 2010. **published online: 9 December 2010**.
79. Chernetsova, E.S., et al., *An ultra superfast identification of low-molecular components of pharmaceuticals by DART mass spectrometry*. Journal of Analytical Chemistry, 2010. **65**(14): p. 1537-1539.
80. Chernetsova, E.S., et al., *Capabilities of direct analysis in real time mass spectrometry and gas chromatography-mass spectrometry in the mint oil test*. Mendeleev Communications, 2010. **20**(5): p. 299-300.
81. Chernetsova, E.S., et al., *The use of DART mass spectrometry for express confirmation of empirical formulas of heterocyclic compounds*. Russian Chemical Bulletin, 2010. **59**(10): p. 2014-2015.
82. Cody, R.B. and A.J. Dane, *Direct Analysis in Real Time Ion Source*, in *Encyclopedia of Analytical Chemistry*, R.A. Meyers, Editor. 2010, John Wiley & Sons, Ltd.: Published online: December 15.
83. Curtis, M., et al., *Direct Analysis in Real Time (DART) Mass Spectrometry of Nucleotides and Nucleosides: Elucidation of a Novel Fragment $[C_5H_5O]^+$ and Its In-Source Adducts*. Journal of the American Society for Mass Spectrometry, 2010. **21**(8): p. 1371-1381.
84. Dane, A.J. and R.B. Cody, *Selective ionization of melamine in powdered milk by using argon direct analysis in real time (DART) mass spectrometry*. Analyst, 2010. **135**(4): p. 696-699.
85. Domin, M.A., et al., *Routine analysis and characterization of highly insoluble polycyclic aromatic compounds by direct analysis in real time mass spectrometry (DART)*. Analyst, 2010. **135**(4): p. 700-704.
86. Eberherr, W., et al., *Investigations on the Coupling of High-Performance Liquid Chromatography to Direct Analysis in Real Time Mass Spectrometry*. Analytical Chemistry, 2010. **82**(13): p. 5792-5796.
87. Harris, G.A., et al., *Comparison of the Internal Energy Deposition of Direct Analysis in Real Time and Electrospray Ionization Time-of-Flight Mass Spectrometry*. Journal of the American Society for Mass Spectrometry, 2010. **21**(5): p. 855-863.
88. Haunschmidt, M., et al., *Determination of organic UV filters in water by stir bar sorptive extraction and direct analysis in real-time mass spectrometry*. Analytical and Bioanalytical Chemistry, 2010. **397**(1): p. 269-275.
89. Haunschmidt, M., et al., *Rapid identification of stabilisers in polypropylene using time-of-flight mass spectrometry and DART as ion source*. Analyst, 2010. **135**(1): p. 80-85.

90. Jones, R.W., T. Reinot, and J.F. McClelland, *Molecular Analysis of Primary Vapor and Char Products during Stepwise Pyrolysis of Poplar Biomass*. Energy & Fuels, 2010. **24**(9): p. 5199-5209.
91. Kim, H.J., et al., *Identification of marker compounds in herbal drugs on TLC with DART-MS*. Archives of Pharmacal Research, 2010. **33**(9): p. 1355-1359.
92. Kim, H.J., et al., *Quantitative analysis of major dibenzocyclooctane lignans in schisandrae fructus by online TLC-DART-MS*. Phytochemical Analysis, 2010. **22**(3): p. 258-262.
93. Kubec, R., et al., *Applications of Direct Analysis in Real Time Mass Spectrometry (DART-MS) in Allium Chemistry. (Z)-Butanethial S-Oxide and 1-Butenyl Thiosulfinates and Their S-(E)-1-Butenylcysteine S-Oxide Precursor from Allium sicutum*. Journal of Agricultural and Food Chemistry, 2010. **58**(2): p. 1121-1128.
94. Nilles, J.M., T.R. Connell, and H.D. Durst, *Thermal separation to facilitate Direct Analysis in Real Time (DART) of mixtures*. Analyst, 2010. **135**(5): p. 883-886.
95. Nilles, J.M., et al., *Explosives Detection Using Direct Analysis in Real Time (DART) Mass Spectrometry*. Propellants, Explosives, Pyrotechnics, 2010. **35**(5): p. 446-451.
96. Pérez, J.J., et al., *Transmission-mode direct analysis in real time and desorption electrospray ionization mass spectrometry of insecticide-treated bednets for malaria control*. Analyst, 2010. **135**(4): p. 712-719.
97. Ra, J., et al., *Bambusae Caulis in Taeniam extract reduces ovalbumin-induced airway inflammation and T helper 2 responses in mice*. Journal of Ethnopharmacology, 2010. **128**(1): p. 241-247.
98. Steiner, R.R., *A Rapid Technique for the Confirmation of Iodine and Red Phosphorus Using Direct Analysis in Real Time and Accurate Mass Spectrometry*. Microgram Journal, 2010. **7**(1): p. 3-6.
99. Vaclavik, L., et al., *Rapid determination of melamine and cyanuric acid in milk powder using direct analysis in real time-time-of-flight mass spectrometry*. Journal of Chromatography A, 2010. **1217**(25): p. 4204-4211.
100. Zhou, M., et al., *Rapid Mass Spectrometric Metabolic Profiling of Blood Sera Detects Ovarian Cancer with High Accuracy*. Cancer Epidemiology, Biomarkers & Prevention, 2010.
101. Zhou, M., J.F. McDonald, and F.M. Fernández, *Optimization of a Direct Analysis in Real Time/Time-of-Flight Mass Spectrometry Method for Rapid Serum Metabolomic Fingerprinting*. Journal of the American Society for Mass Spectrometry, 2010. **21**(1): p. 68-75.
102. Adams, J., *Analysis of printing and writing papers by using direct analysis in real time mass spectrometry*. International Journal of Mass Spectrometry, 2011. **301**(1-3): p. 109-126.
103. Beißmann, S., et al., *High-performance liquid chromatography coupled to direct analysis in real time mass spectrometry: Investigations on gradient elution and*

- influence of complex matrices on signal intensities.* Journal of Chromatography A, 2011. **1218**(31): p. 5180-5186.
104. Biniecka, M. and S. Caroli, *Analytical methods for the quantification of volatile aromatic compounds.* TrAC Trends in Analytical Chemistry, 2011. **30**(11): p. 1756-1770.
 105. Block, E., *Challenges and Artifact Concerns in Analysis of Volatile Sulfur Compounds,* in *Volatile Sulfur Compounds in Food, ACS Symposium Series.* 2011, American Chemical Society. p. 35-63.
 106. Block, E., A.J. Dane, and R.B. Cody, *Crushing Garlic and Slicing Onions: Detection of Sulfenic Acids and Other Reactive Organosulfur Intermediates from Garlic and Other Alliums using Direct Analysis in Real-Time Mass Spectrometry (DART-MS).* Phosphorus, Sulfur, and Silicon and the Related Elements, 2011. **186**(5): p. 1085-1093.
 107. Cajka, T., et al., *Ambient mass spectrometry employing a DART ion source for metabolomic fingerprinting/profiling: a powerful tool for beer origin recognition.* Metabolomics, 2011. **7**(4): p. 500-508.
 108. Chernetsova, E.S., et al., *New approach to detecting counterfeit drugs in tablets by DART mass spectrometry.* Pharmaceutical Chemistry Journal, 2011. **45**(5): p. 306-308.
 109. Chernetsova, E.S., et al., *Clarification of the composition of [M+18]⁺ ions in DART mass spectra of polyethylene glycol using high-resolution mass spectrometry.* Journal of Analytical Chemistry, 2011. **66**(13): p. 1348-1351.
 110. Cho, D.S., et al., *Evaluation of direct analysis in real time mass spectrometry for onsite monitoring of batch slurry reactions.* Rapid Communications in Mass Spectrometry, 2011. **25**(23): p. 3575-3580.
 111. Deroo, C.S. and R.A. Armitage, *Direct Identification of Dyes in Textiles by Direct Analysis in Real Time-Time of Flight Mass Spectrometry.* Analytical Chemistry, 2011. **83**(18): p. 6924-6928.
 112. Grange, A.H. and G.W. Sovocool, *Detection of illicit drugs on surfaces using direct analysis in real time (DART) time-of-flight mass spectrometry.* Rapid Communications in Mass Spectrometry, 2011. **25**(9): p. 1271-1281.
 113. Hajslova, J., T. Cajka, and L. Vaclavik, *Challenging applications offered by direct analysis in real time (DART) in food-quality and safety analysis.* TrAC Trends in Analytical Chemistry, 2011. **30**(2): p. 204-218.
 114. Haunschmidt, M., et al., *Identification and semi-quantitative analysis of parabens and UV filters in cosmetic products by direct-analysis-in-real-time mass spectrometry and gas chromatography with mass spectrometric detection.* Analytical Methods, 2011. **3**: p. 99-104.
 115. Howlett, S.E. and R.R. Steiner, *Validation of Thin Layer Chromatography with AccuTOF-DART™ Detection for Forensic Drug Analysis.* Journal of Forensic Sciences, 2011. **56**(5): p. 1261-1267.

116. Kalachova, K., et al., *Simplified and rapid determination of polychlorinated biphenyls, polybrominated diphenyl ethers, and polycyclic aromatic hydrocarbons in fish and shrimps integrated into a single method*. *Analytica Chimica Acta*, 2011. **707**(1-2): p. 84-91.
117. Kawamura, M., R. Kikura-Hanajiri, and Y. Goda, *Simple and Rapid Screening for Methamphetamine and 3,4-Methylene-dioxymethamphetamine (MDMA) and Their Metabolites in Urine Using Direct Analysis in Real Time (DART)-TOFMS*. *Yakugaku Zasshi : Journal of the Pharmaceutical Society of Japan*, 2011. **131**(5): p. 827-833.
118. Kim, H.J., W.S. Baek, and Y.P. Jang, *Identification of ambiguous cubeb fruit by DART-MS-based fingerprinting combined with principal component analysis*. *Food Chemistry*, 2011. **129**(3): p. 1305-1310.
119. Kim, H.J., et al., *Quantitative analysis of major dibenzocyclooctane lignans in ***schisandrae fructus*** by online TLC-DART-MS*. *Phytochemical Analysis*, 2011. **22**(3): p. 258-262.
120. Kim, S.W., et al., *A rapid, simple method for the genetic discrimination of intact ***Arabidopsis thaliana*** mutant seeds using metabolic profiling by direct analysis in real-time mass spectrometry*. *Plant Methods*, 2011. **7**(1): p. 1-10.
121. Kpegba, K., et al., *Epiatzelechin from the Root Bark of *Cassia sieberiana*: Detection by DART Mass Spectrometry, Spectroscopic Characterization, and Antioxidant Properties*. *Journal of Natural Products*, 2011. **74**(3): p. 455-459.
122. Kubec, R., et al., *Precursors and Formation of Pyrithione and Other Pyridyl-Containing Sulfur Compounds in Drumstick Onion, *Allium stipitatum**. *Journal of Agricultural and Food Chemistry*, 2011. **59**(10): p. 5763-5770.
123. Kucerová, P., et al., **Allium* discoloration: the precursor and formation of the red pigment in giant onion (*Allium giganteum* Regel) and some other subgenus *Melanocrommyum* species*. *Journal of Agricultural and Food Chemistry*, 2011. **59**(5): p. 1821-1828.
124. Lee, J.H., et al., *Danshen extract does not alter pharmacokinetics of docetaxel and clopidogrel, reflecting its negligible potential in P-glycoprotein- and cytochrome P4503A-mediated herb–drug interactions*. *International Journal of Pharmaceutics*, 2011. **410**(1-2): p. 68-74.
125. Mess, A., et al., *Qualitative Analysis of Tackifier Resins in Pressure Sensitive Adhesives Using Direct Analysis in Real Time Time-of-Flight Mass Spectrometry*. *Analytical Chemistry*, 2011. **83**(19): p. 7323-7330.
126. Pfaff, A.M. and R.R. Steiner, *Development and validation of AccuTOF-DART™ as a screening method for analysis of bank security device and pepper spray components*. *Forensic Science International*, 2011. **206**(1-3): p. 62-70.
127. Samms, W.C., et al., *Analysis of Alprazolam by DART-TOF Mass Spectrometry in Counterfeit and Routine Drug Identification Cases*. *Journal of Forensic Sciences*, 2011. **56**(4): p. 993-998.

128. Sanchez, L.M., et al., *Versatile Method for the Detection of Covalently Bound Substrates on Solid Supports by DART Mass Spectrometry*. *Organic Letters*, 2011. **13**(15): p. 3770-3773.
129. Vaclavik, L., et al., *Authentication of Animal Fats Using Direct Analysis in Real Time (DART) Ionization-Mass Spectrometry and Chemometric Tools*. *Journal of Agricultural and Food Chemistry*, 2011. **59**(11): p. 5919-5926.
130. Wood, J.L. and R.R. Steiner, *Purification of pharmaceutical preparations using thin-layer chromatography to obtain mass spectra with Direct Analysis in Real Time and accurate mass spectrometry*. *Drug Testing and Analysis*, 2011. **3**(6): p. 345-351.
131. Cody, R.B., et al., *Rapid Classification of White Oak (Quercus alba) and Northern Red Oak (Quercus rubra) by Using Pyrolysis Direct Analysis in Real Time (DART™) and Time-of-Flight Mass Spectrometry*. *Journal of Analytical and Applied Pyrolysis*, 2012. **95**: p. 134-137.
132. Dunham, S.J.B., P.D. Hooker, and R.M. Hyde, *Identification, extraction and quantification of the synthetic cannabinoid JWH-018 from commercially available herbal marijuana alternatives*. *Forensic Science International*, 2012. **223**(1-3): p. 241-244.
133. Grabenauer, M., et al., *Analysis of Synthetic Cannabinoids Using High-Resolution Mass Spectrometry and Mass Defect Filtering: Implications for Nontargeted Screening of Designer Drugs*. *Analytical Chemistry*, 2012. **84**(13): p. 5574-5581.
134. He, X.N., et al., *Mass spectrometry of solid samples in open air using combined laser ionization and ambient metastable ionization*. *Spectrochimica Acta Part B*, 2012. **67**: p. 64-73.
135. Hu, B., et al., *Selective hydrogenation of CO₂ and CO to useful light olefins over octahedral molecular sieve manganese oxide supported iron catalysts*. *Applied Catalysis B: Environmental*, 2012. **132-133**: p. 54-61.
136. Lancaster, C. and E. Espinoza, *Analysis of select Dalbergia and trade timber using direct analysis in real time and time-of-flight mass spectrometry for CITES enforcement*. *Rapid Communications in Mass Spectrometry*, 2012. **26**(9): p. 1147-1156.
137. Lee, S.M., H.-J. Kim, and Y.P. Jang, *Chemometric Classification of Morphologically Similar Umbelliferae Medicinal Herbs by DART-TOF-MS Fingerprint*. *Phytochemical Analysis*, 2012. **23**(5): p. 508-512.
138. Li, Y., *Confined direct analysis in real time ion source and its applications in analysis of volatile organic compounds of Citrus limon (lemon) and Allium cepa (onion)*. *Rapid Communications in Mass Spectrometry*, 2012. **26**(10): p. 1194-1202.
139. Musah, R.A., et al., *Direct Analysis in Real Time Mass Spectrometry for Analysis of Sexual Assault Evidence*. *Rapid Communications in Mass Spectrometry*, 2012. **26**(9): p. 1039-1046.

140. Musah, R.A., et al., *Direct analysis in real time mass spectrometry with collision-induced dissociation for structural analysis of synthetic cannabinoids*. Rapid Communications in Mass Spectrometry, 2012. **26**(19): p. 2335-2342.
141. Musah, R.A., et al., *Rapid identification of synthetic cannabinoids in herbal samples via direct analysis in real time mass spectrometry*. Rapid Communications in Mass Spectrometry, 2012. **26**(9): p. 1109-1114.
142. Novotná, H., et al., *Metabolomic fingerprinting employing DART-TOFMS for authentication of tomatoes and peppers from organic and conventional farming*. Food Additives & Contaminants: Part A, 2012. **29**(9): p. 1335-1346.
143. Singh, S. and S.K. Verma, *Study of the distribution profile of piperidine alkaloids in various parts of Prosopis juliflora by the application of Direct Analysis in Real Time Mass Spectrometry (DART-MS)*. Natural Products and Bioprospecting, 2012. **2**(5): p. 206-209.
144. Singh, V., et al., *Direct Analysis in Real Time by Mass Spectrometric Technique for Determining the Variation in Metabolite Profiles of Cinnamomum tamala Nees and Eberm Genotypes*. The Scientific World Journal, 2012. **2012**: p. 6.
145. Uchiyama, N., et al., *URB-754: A new class of designer drug and 12 synthetic cannabinoids detected in illegal products*. Forensic Science International, 2012. **Publication Date (Web): 9 October 2012**.
146. Bentayeb, K., et al., *Non-visible print set-off of photoinitiators in food packaging: detection by ambient ionisation mass spectrometry*. Food Additives & Contaminants: Part A, 2013. **30**(4): p. 750-759.
147. Cajka, T., et al., *Evaluation of direct analysis in real time ionization-mass spectrometry (DART-MS) in fish metabolomics aimed to assess the response to dietary supplementation*. Talanta, 2013. **115**: p. 263-270.
148. Cajka, T., et al., *Application of direct analysis in real time ionization-mass spectrometry (DART-MS) in chicken meat metabolomics aiming at the retrospective control of feed fraud*. Metabolomics, 2013. **9**(3): p. 545-557.
149. Cody, R.B., *What Is the Opposite of Pandora's Box? Direct Analysis, Ambient Ionization, and a New Generation of Atmospheric Pressure Ion Sources*. Mass Spectrometry, 2013. **2**(Special Issue): p. S0007.
150. Cody, R.B. and A.J. Dane, *Soft Ionization of Saturated Hydrocarbons, Alcohols and Nonpolar Compounds by Negative-Ion Direct Analysis in Real-Time Mass Spectrometry*. Journal of the American Society for Mass Spectrometry, 2013. **24**(3): p. 329-334.
151. Djelal, H., et al., *The use of HPTLC and Direct Analysis in Real Time-Of-Flight Mass Spectrometry (DART-TOF-MS) for rapid analysis of degradation by oxidation and sonication of an azo dye*. Arabian Journal of Chemistry, 2013. **in press/published online**.

152. Dwivedi, P., et al., *Electro-Thermal Vaporization Direct Analysis in Real Time-Mass Spectrometry for Water Contaminant Analysis during Space Missions*. Analytical Chemistry, 2013. **85**(20): p. 9898-9906.
153. Fukuda, E., et al., *Application of mixture analysis to crude materials from natural resources (IV)[1(a-c)]: identification of Glycyrrhiza species by direct analysis in real time mass spectrometry (II)*. Natural Product Communications, 2013. **8**(12): p. 1721-1724.
154. Grange, A.H., *Semi-quantitative analysis of contaminants in soils by direct analysis in real time (DART) mass spectrometry*. Rapid Communications in Mass Spectrometry, 2013. **27**(2): p. 305-318.
155. Hintersteiner, I., R. Hertsens, and C.W. Klampfl, *Direct Analysis in Real Time/Time-of-Flight Mass Spectrometry: Investigations on Parameters for the Coupling with Liquid-Phase Sample Introduction Techniques*. Journal of Liquid Chromatography & Related Technologies, 2013. **37**(13): p. 1862-1872.
156. Houlgrave, S., et al., *The Classification of Inkjet Inks Using AccuTOF™DART™ (Direct Analysis in Real Time) Mass Spectrometry—A Preliminary Study*. Journal of Forensic Sciences, 2013. **58**(3): p. 813-821.
157. Jones, R.W. and J.F. McClelland, *Analysis of writing inks on paper using direct analysis in real time mass spectrometry*. Forensic Science International, 2013. **231**(1-3): p. 73-81.
158. Lesiak, A.D., et al., *Direct Analysis in Real Time Mass Spectrometry (DART-MS) of "Bath Salt" Cathinone Drug Mixtures*. Analyst, 2013. **138**(12): p. 3424-3432.
159. Li, Y., *Applications of a confined DART (direct analysis in real time) ion source for online in vivo analysis of human breath*. Analytical Methods, 2013. **5**(24): p. 6933-6940.
160. Lim, A.Y., et al., *Detection of drugs in latent fingerprints by mass spectrometric methods*. Analytical Methods, 2013. **5**(17): p. 4378-4385.
161. Mess, A., et al., *A novel sampling method for identification of endogenous skin surface compounds by use of DART-MS and MALDI-MS*. Talanta, 2013. **103**: p. 398-402.
162. Park, H.M., et al., *Direct Analysis in Real Time Mass Spectrometry (DART-MS) Analysis of Skin Metabolome Changes in the Ultraviolet B-Induced Mice*. Biomolecules and Therapeutics, 2013. **21**(6): p. 470-475.
163. Rajchl, A., et al., *Rapid determination of 5-hydroxymethylfurfural by DART ionization with time-of-flight mass spectrometry*. Analytical and Bioanalytical Chemistry, 2013. **405**(14): p. 4737-4745.
164. Sisco, E., J. Dake, and C. Bridge, *Screening for trace explosives by AccuTOF™-DART®: An in-depth validation study*. Forensic Science International, 2013. **232**(1-3): p. 160-168.

165. Swider, J.R., *Optimizing Accu Time-of-Flight/Direct Analysis in Real Time for Explosive Residue Analysis*. Journal of Forensic Sciences, 2013. **58**(6): p. 1601-1606.
166. Al-Balaa, D., et al., *DART mass spectrometry for rapid screening and quantitative determination of cholesterol in egg pasta*. Journal of Mass Spectrometry, 2014. **49**(9): p. 911-917.
167. Curtis, M., et al., *Schlieren visualization of fluid dynamics effects in direct analysis in real time mass spectrometry*. Rapid Communications in Mass Spectrometry, 2015. **29**(5): p. 431-439.
168. Cody, R.B., et al., *Identification of bacteria by fatty acid profiling with direct analysis in real time mass spectrometry*. Rapid Communications in Mass Spectrometry, 2015. **29**: in press.
169. Easter, J.L. and R.R. Steiner, *Pharmaceutical identifier confirmation via DART-TOF*. Forensic Science International, 2014. **240**: p. 9-20.
170. Espinoza, E.O., et al., *Distinguishing Wild from Cultivated Agarwood (Aquilaria spp.) Using Direct Analysis in Real Time (DART™) and Time-of-Flight Mass Spectrometry*. Rapid Communications in Mass Spectrometry, 2014. **28**(3): p. 281–289.
171. Fukuda, E., et al., *Identification of the country of growth of Sophora flavescens using direct analysis in real time mass spectrometry (DART-MS)*. Natural Product Communications, 2014. **9**(11): p. 1591-4.
172. Jacobs, A.D. and R.R. Steiner, *Detection of the Duquenois–Levine chromophore in a marijuana sample*. Forensic Science International, 2014. **239**: p. 1-5.
173. Kiguchi, O., et al., *Thin-layer chromatography/direct analysis in real time time-of-flight mass spectrometry and isotope dilution to analyze organophosphorus insecticides in fatty foods*. Journal of Chromatography A, 2014. **1370**: p. 246-254.
174. Kim, H., et al., *DART-TOF-MS based metabolomics study for the discrimination analysis of geographical origin of Angelica gigas roots collected from Korea and China*. Metabolomics, 2014: p. 1-7.
175. Kim, H.J., S.R. Park, and Y.P. Jang, *Extraction-free In situ Derivatisation of Timosaponin AIII Using Direct Analysis in Real Time TOF/MS*. Phytochemical Analysis, 2014. **25**(4): p. 373-377.
176. Lesiak, A.D., et al., *DART-MS for rapid, preliminary screening of urine for DMAA*. Drug Testing and Analysis, 2014. **6**(7-8): p. 788-796.
177. Lesiak, A.D., et al., *Rapid detection by direct analysis in real time-mass spectrometry (DART-MS) of psychoactive plant drugs of abuse: The case of Mitragyna speciosa aka "Kratom"*. Forensic Science International, 2014. **242**: p. 210-218.
178. Lesiak, A.D., et al., *DART-MS as a Preliminary Screening Method for "Herbal Incense": Chemical Analysis of Synthetic Cannabinoids*. Journal of Forensic Science, 2014. **59**(2): p. 337-343.

179. Lesiak, A.D. and J.R.E. Shepard, *Recent advances in forensic drug analysis by DART-MS*. *Bioanalysis*, 2014. **6**(6): p. 819-842.
180. Morlock, G.E., P. Ristivojevic, and E.S. Chernetsova, *Combined multivariate data analysis of high-performance thin-layer chromatography fingerprints and direct analysis in real time mass spectra for profiling of natural products like propolis*. *Journal of Chromatography A*, 2014. **1328**: p. 104-112.
181. Musah, R.A., et al., *DART-MS in-source collision induced dissociation and high mass accuracy for new psychoactive substance determinations*. *Forensic Science International*, 2014. **244**: p. 42-49.
182. Paseiro-Cerrato, R., G.O. Noonan, and T.H. Begley, *Development of a rapid screening method to determine primary aromatic amines in kitchen utensils using direct analysis in real time mass spectrometry (DART-MS)*. *Food Additives & Contaminants: Part A*, 2014. **31**(3): p. 537-545.
183. Prchalová, J., et al., *Characterization of mustard seeds and paste by DART ionization with time-of-flight mass spectrometry*. *Journal of Mass Spectrometry*, 2014. **49**(9): p. 811-818.
184. Sekimoto, K., et al., *Ionization characteristics of amino acids in direct analysis in real time mass spectrometry*. *Analyst*, 2014. **139**(10): p. 2589-2599.
185. Bag, A. and R.R. Chattopadhyay, *Evaluation of Synergistic Antibacterial and Antioxidant Efficacy of Essential Oils of Spices and Herbs in Combination*. *PLoS ONE*, 2015. **10**(7): p. e0131321.
186. Le Pogam, P., et al., *Analysis of the cyanolichen *Lichina pygmaea* metabolites using in situ DART-MS: from detection to thermochemistry of mycosporine serinol*. *Journal of Mass Spectrometry*, 2015. **50**(3): p. 454-462.
187. Lesiak, A.D., et al., *Plant Seed Species Identification from Chemical Fingerprints: A High-Throughput Application of Direct Analysis in Real Time Mass Spectrometry*. *Analytical Chemistry*, 2015. **published online August 3**(Article ASAP).
188. Marino, M.A., et al., *Rapid Identification of Synthetic Cannabinoids in Herbal Incenses with DART-MS and NMR*. *Journal of Forensic Sciences*, 2015. **in press/published online**.
189. Musah, R.A., et al., *A High Throughput Ambient Mass Spectrometric Approach to Species Identification and Classification from Chemical Fingerprint Signatures*. *Scientific Reports*, 2015. **5**: p. 11520_1-16.
190. Singh, A., et al., *Rapid screening and distribution of bioactive compounds in different parts of *Berberis petiolaris* using direct analysis real time mass spectrometry*. *Journal of Pharmaceutical Analysis*, 2015. **in press/published online**.
191. Sisco, E. and T.P. Forbes, *Rapid detection of sugar alcohol precursors and corresponding nitrate ester explosives using direct analysis in real time mass spectrometry*. *Analyst*, 2015. **140**(8): p. 2785-2796.

192. Yew, J.Y. and H. Chung, *Insect pheromones: An overview of function, form, and discovery*. Progress in Lipid Research, 2015. **59**: p. 88-105.
193. Zhou, S., M.W. Forbes, and J.P.D. Abbatt, *Application of Direct Analysis in Real Time-Mass Spectrometry (DART-MS) to the Study of Gas-Phase Surface Heterogeneous Reactions: Focus on Ozone and PAHs*. Analytical Chemistry, 2015. **87**(9): p. 4733-4740.

Certain products in this brochure are controlled under the "Foreign Exchange and Foreign Trade Law" of Japan in compliance with international security export control. JEOL Ltd. must provide the Japanese Government with "End-user's Statement of Assurance" and "End-use Certificate" in order to obtain the export license needed for export from Japan. If the product to be exported is in this category, the end user will be asked to fill in these certificate forms.



JEOL Ltd.

1-2 Musashino 3-chome Akishima Tokyo 196-8558 Japan Sales Division Tel. +81-3-6262-3560 Fax. +81-3-6262-3577
www.jeol.com ISO 9001 • ISO 14001 Certified

• AUSTRALIA & NEW ZEALAND /JEOL(AUSTRALASIA) Pty.Ltd. Suite 1, L2 18 Aquatic Drive - Frenchs Forest NSW 2086 Australia • BELGIUM /JEOL (EUROPE) B.V. Planet II, Gebouw B Leuvensesteenweg 542, B-1930 Zaventem Belgium • CANADA /JEOL CANADA, INC. 3275 1ere Rue, Local #8 St-Hubert, QC J3Y-8Y6, Canada • CHINA /JEOL(BEIJING) CO., LTD. Zhongkeziyuan Building South Tower 2F, Zhongguancun Nanshanje Street No. 6, Haidian District, Beijing, P.R.China • EGYPT /JEOL SERVICE BUREAU 3rd Fl, Nile Center Bldg., Nawal Street, Dokki, (Cairo), Egypt • FRANCE /JEOL (EUROPE) SAS Espace Claude Monet, 1 Allée de Giverny 78290, Croissy-sur-Seine, France • GERMANY /JEOL (GERMANY) GmbH Oskar-Von-Miller-Strasse 1a, 85386 Eching, Germany • GREAT BRITAIN & IRELAND /JEOL (U.K.) LTD. JEOL House, Silver Court, Watchmead, Welwyn Garden City, Herts AL7 1LT, U.K. • ITALY /JEOL (ITALIA) S.p.A. Palazzo Pacinotti - Milano 3 City, Via Ludovico il Moro, 6/A 20080 Basiglio(MI) Italy • KOREA /JEOL KOREA LTD, Dongwoo Bldg, 7F, 1443, Yangjae Daero, Gangdong-Gu, Seoul, 134-814, Korea • MALAYSIA /JEOL(MALAYSIA) SDN.BHD, 508, Block A, Level 5, Kelana Business Center, 97, Jalan SS 7/2, Kelana Jaya, 47301 Petaling Jaya, Selangor, Malaysia • MEXICO /JEOL DE MEXICO S.A. DE C.V. Arkansas 11 Piso 2 Colonia Napoles Delegacion Benito Juarez, C.P. 03810 Mexico D.F., Mexico • SCANDINAVIA, SWEDEN /JEOL (Skandinaviska) AB Hammarbacken 6A, Box 716, 191 27 Sollentuna Sweden • SINGAPORE /JEOL ASIA PTE.LTD. 2 Corporation Road #01-12 Corporation Place Singapore 618494 • TAIWAN /JIE DONG CO., LTD. 7F, 112, Chung Hsiao East Road, Section 1, Taipei, Taiwan 10023 Republic of China • THE NETHERLANDS /JEOL (EUROPE) B.V. Lireweg 4, NL-2153 PH Nieuw-Vennep, The Netherlands • USA /JEOL USA, INC. 11 Dearborn Road, Peabody, MA 01960, U.S.A.